**TECHNISCHE
UNIVERSITÄT
DRESDEN**

Squark Production in the R-Symmetric Supersymmetric Standardmodel

Master-Arbeit
zur Erlangung des Hochschulgrades
Master of Science
im Master-Studiengang Physik

vorgelegt von

Sebastian Liebschner
geboren am 08.05.1990 in Meerane

Institut für Kern- und Teilchenphysik Physik
Fachrichtung Physik
Fakultät Mathematik und Naturwissenschaften
Technische Universität Dresden
2016

Eingereicht am xx. Monat 20xx

1. Gutachter: Prof. Dr. XX
2. Gutachter: Prof. Dr. YY

Summary

Abstract

English: flaws of the SM

motivation: aesthetic: Coleman-Mandula –> Haag-Lopuszanski-Sohnius-Theorem

 Abstract

Deutsch

Contents

1 Introduction

motivation: aesthetic: Coleman-Mandula –> Haag-Lopuszanski-Sohnius-Theorem

plots for exclusion of squarks in specific SUSY scenarios (from Michael) –> R-Symmetry could be possible explanation for that because:

MSSM-Lagrangian –> trafo rules for superfields under R-symm –> forbidden terms in MRSSM (write down Lagrangian for R-symmetric SUSYQCD)

suppression of squark production in MRSSM by less diagrams (m_{gluino}^{-4} suppression at low energies in MRSSM and only m_{gluino}^{-2} suppression in MSSM)

R-charges of all fields (show in diagram!) –> only if R-charges of final / initial particles are zero, a diagram is allowed in R-symm. model

references to build in

- "Matching Squark Pair Production at NLO with Parton Showers" from Gavin, Hangst, Krämer, Mühlleitner,.. for complete treatment of NLO calculation

- "dIRAC gAUGINOS IN susy - sUPPRESSED jETS + <met sIGNALS: a sNOWMASS wHITEPAPER" FROM kRIBS, mARTIN for Squark production at LO, allude to same result

- "Dirac Gaugino Masses and supersoft SUSY breaking" from Fox, Weiner, Nelson for the introduction of the MRSSM

2 The Standard Model

The Standard Model of particle physics is the commonly accepted theory describing the world's fundamental particles and their interactions. It is a gauge quantum field theory and therefore characterized by its invariance under symmetry groups. The Standard Model contains different fields, whose quantized excitations are interpreted as all known particles.
This chapter summarizes the most important aspects of the Standard Model.

2.1 Symmetries and Transformations

Space-time Symmetries

The Standard Model is defined on Minkowski space, whose coordinates are label with x^μ $\mu \in \{0, 1, 2, 4\}$. As a relativistic theory it is invariant under Poincaré transformations, i.e. it is invariant under Lorentz-transformations (with generators $J^{\mu\nu}$) and translations (with generators P^μ) in spacetime. The set of all Poincaré transformations form the Poincaré group, which is a Lie group. Its generators obey the Poincaré-algebra

$$\begin{aligned}
[P^\mu, P^\nu] &= 0, \\
[P^\mu, J^{\nu\rho}] &= i(g^{\mu\nu} P^\rho - g^{\mu\rho} P^\nu), \\
[J^{\mu\nu}, J^{\rho\sigma}] &= i(g^{\nu\rho} J^{\mu\rho} + g^{\mu\sigma} J^{\nu\rho} - g^{\mu\rho} J^{\nu\sigma} - g^{\nu\sigma} J^{\mu\rho}).
\end{aligned} \tag{2.1}$$

The fields of the Standard Model transform in different representations of the Poincaré-group [1].

Gauge Symmetries

In order to describe interactions of matter particles with spin-1 force mediators, gauge theories are used. In the Standard Model matter fields are described by Dirac spinors. The Lagrangian of a free Dirac field reads

$$\mathcal{L}_{\text{Dirac}} = \overline{\Psi}(i\not{\partial} - m)\Psi, \tag{2.2}$$

where m denotes the particle's mass. To include interactions, one imposes a local group symmetry (gauge symmetry) upon this Lagrangian. A spinor transforms under a generic gauge transformation like

$$\Psi(x) \rightarrow U(x)\Psi(x), \tag{2.3}$$

where $U(x)$ is an element of the gauge group in question. Because the gauge group is an unitary matrix Lie group, it can be written in the form $U(x) = \exp(-igT^a\theta^a(x))$. Here, T^a

are the self-adjoint generators of the associated Lie algebra which obey

$$[T^a, T^b] = i f_{abc} T^c, \tag{2.4}$$

with f_{abc} the structure constants of a Lie algebra, g is the coupling constant of the gauge group and $\theta^a(x)$ are local parameters.

As the parameters of the gauge group are local, the derivative in (2.2) spoils gauge invariance. In order to rectify the gauge invariance of the Lagrangian, one introduces a further field for each index a of the generators, the gauge vector $G^{a\mu}$. Defining the transformation of the matrix valued gauge vector $G^\mu := G^{a\mu} T^a$ as

$$G^\mu(x) \to U^{-1}(x) \left(G^\mu(x) + \frac{i}{g} \partial^\mu \right) U(x) \tag{2.5}$$

and introducing the gauge covariant derivative

$$D^\mu = \partial^\mu + ig T^a G^{a\mu}, \tag{2.6}$$

one finds that the expression $D_\mu \Psi(x)$ transforms as

$$D_\mu \Psi(x) \to U(x) D_\mu \Psi(x). \tag{2.7}$$

Therefore, gauge invariance is restored in eq. (2.2) by replacing ∂_μ with D_μ. But if the gauge vector is interpreted as a physical field, there must also be a kinetic term associated with it. Using eq. (2.7) one defines the field strength tensor[1] $F^{a\mu\nu}$, whose matrix valued form

$$F^{\mu\nu} = F^{a\mu\nu} T^a := \frac{1}{ig} [D^\mu, D^\nu] = \partial^\mu G^\nu - \partial^\nu G^\mu - g f_{abc} T^c G^{a\mu} G^{b\nu} \tag{2.8}$$

transforms as $F^{\mu\nu} \to U(x) F^{\mu\nu} U^{-1}(x)$. Using the cyclic property of the trace and the Dynkin index $T(F)$ defined in eq. (10.6) in the appendix, one can write down a gauge invariant kinetic term for the gauge vector:

$$\mathcal{L}_{\text{gauge}} = -\frac{1}{2} \text{Tr} \left(F^{\mu\nu} F_{\mu\nu} \right) = -\frac{T(F)}{2} F^{a\mu\nu} F^a_{\mu\nu}. \tag{2.9}$$

This completes the construction of a Lagrangian which is invariant under non-abelian gauge group transformations. The result is the famous Yang and Mills Lagrangian [3]

$$\mathcal{L}_{\text{Yang−Mills}} = \overline{\Psi}(i\slashed{D} - m)\Psi - \frac{1}{4} F^{a\mu\nu} F^a_{\mu\nu} \tag{2.10}$$

---

[1]An alternative construction of the field strength tensor makes use of the gauge invariant Wilson loop. This gives some insights into the geometry of gauge transformations [2].

This Lagragian gives rise to spin-$\frac{1}{2}$ (matter) particles which interact with spin-1 (force mediator) particles. Furthermore if the gauge group is non-abelian, i.e. $f_{abc} \neq 0$, there are self interactions among the spin-1 particles.

The gauge group of the Standard Model is a direct product of the three gauge groups[2]: $U(1)_Y$, $SU(2)_L$ and $SU(3)_C$. The elements $U(x)$ of those are given in table 2.1.

These gauge groups give rise to 3 forces: the strong force, the weak force and the electromagnetic force.

Gauge Group	Group Element
$U(1)_Y$	$U(x) = \exp\left(-ig_Y \frac{\hat{Y}}{2}\theta_Y(x)\right)$
$SU(2)_L$	$U(x) = \exp\left(-ig_w \vec{\tau} \cdot \vec{\theta}_w(x)\right)$
$SU(3)_C$	$U(x) = \exp\left(-ig_s T^a \cdot \theta_s^a(x)\right)$

Table 2.1: The table lists the explicit element $U(x)$ of the gauge groups $U(1)_Y$, $SU(2)_L$ and $SU(3)_C$ of the Standard Model. The hypercharge operator $\hat{Y}$ gives the eigenvalue of the hypercharge of the field it is applied to (see table 2.3). $\vec{\tau}$ and T^a are the geneators of $SU(2)_L$ and $SU(3)_C$ respectively. In the fundamental representation $\vec{\tau} = \frac{\vec{\sigma}}{2}$ where $\vec{\sigma}$ has the 3 Pauli matrices as components and $T^a = \frac{\lambda^a}{2}$ where λ^a are the 8 Gell-Mann matrices. ε_{abc} and f_{abc} are the structure constants of $SU(2)_L$ and $SU(3)_C$ respectively.

2.2 The Particles of the Standard Model

In the Standard Model different matter particles take part in different interactions, i.e. their corresponding spinor couples to different gauge vectors.

If a spinor couples to a certain gauge vector, it transforms non-trivially (like indicated in table 2.1) under the gauge group which is associated with this gauge vector.[3] This means if a particle couples to a certain force its charge which is associated with this force is non-zero.

The charges of a particle related to a force are defined as the eigenvalues of the generators which correspond to the force.

The Quarks:

Quarks are strongly interacting fermions, which means their spinors transform non trivially under $SU_C(3)$. Because they transform in the fundamental representation of $SU_C(3)$ this means a quark spinor is built up by three spinors each carrying another color. This splitting of the quark spinor in colors is often suppressed for the sake of simplicity. This convention is adopted throughout this thesis.

---

[2]The subscript stands for the associated charge of the groups respectively: Y for hypercharge, L for left handedness (weak Isospin I_3) and C for color

[3]In the Standard Model all matter particles transform in the fundamental (or trivial) representation of gauge groups.

Furthermore, the left handed component of quarks interact weakly, which means that their spinors[4] transform (in the fundamental representation) under $SU(2)_L$ transformations meaning that two left handed quark spinors are assembled within a doublet.

Finally, all quarks carry a hypercharge. In section 2.3 the mechanism of electroweak symmetry breaking is described. This mechanism explains how electromagnetism arises from the groups $SU(2)_L$ and $U(1)_Y$. All quarks interact electromagnetically.

All together, there are six quarks which are listed in table 2.2. They are categorized in 3 generations because their quantum numbers except for their masses reoccur in each generation. The two types of quarks within a generation which have distinct quantum numbers are referred to as up-type and down-type quarks. The up-type-quark and the down-type quark of the same generation built up a doublet.

The Leptons:

Leptons do not interact strongly. They take part in the weak and the electromagnetic interaction, i.e. their spinors transform non-trivially under the fundamental representation of $SU(2)_L$ and $U(1)_Y$. As for the quarks only the left handed components interact weakly and there are six leptons which are classified into three generations (see table 2.2). In each generation is a lepton with a negative electrical charged and an electrically neutral lepton. The latter ones are referred to as neutrinos. Right handed neutrinos have not been observed (yet) and are therefore absent in the Standard Model. The former are called electron, muon and tau. Each left handed leptons with an electric charge is assembled with its neutrino in a doublet.

Particle		1st Generation		2nd Generation		3rd Generation	
u_i	up-type-quark	u	up-quark	c	charm-quark	t	top-quark
d_i	down-type-quark	d	down-quark	s	strange-quark	b	bottom-quark
e_i	charged lepton	e	electron	μ	muon	τ	tau
ν_i	neutrino	ν_e	electron neutrino	ν_μ	muon neutrino	ν_τ	tau neutrino

Table 2.2: The matter particles of the Standard Model. Listed are the symbol and the name of the particles. The labeling of particles has been taken from [4]. The shortcut charged lepton refers to electrically charged leptons.

Quarks and leptons are the matter particles of the Standard Model. They are listed together with their charges for the different forces in table 2.3. There is the color for strong interactions, the third component of the weak isospin I_3 for weak interactions (the eigenvalue of the third generator of the $SU(2)_L$) and the half of the hypercharge $\frac{Y}{2}$ to obtain the electric charge Q via the Gell-Mann–Nishijima formula: $Q = I_3 + \frac{Y}{2}$.

---

[4]The left handed part of a 4-spinor Ψ is projected out by the appropriate projector P_L. This is explained in Appendix 10.3.

Because the left- and right-handed parts of spinors transform differently under the $SU_L(2)$ they are listed separately. All quarks occur with three different colors.

In the last row, the Higgs-boson is listed. Its associated field is responsible for the mass of elementary particles. That is explained in section 2.3.

Particle	Symbol	Color	I_3	$\frac{Y}{2}$	Q
left-handed quarks	$q_{iL} = \begin{pmatrix} u_{iL} \\ d_{iL} \end{pmatrix}$	red, green, blue	$\begin{pmatrix} +\frac{1}{2} \\ -\frac{1}{2} \end{pmatrix}$	$+\frac{1}{6}$	$\begin{pmatrix} +\frac{2}{3} \\ -\frac{1}{3} \end{pmatrix}$
right-handed quarks	u_{iR}	red, green, blue	0	$+\frac{2}{3}$	$+\frac{2}{3}$
	d_{iR}	red, green, blue	0	$-\frac{1}{3}$	$-\frac{1}{3}$
left-handed leptons	$\ell_{iL} = \begin{pmatrix} \nu_{iL} \\ e_{iL} \end{pmatrix}$	-	$\begin{pmatrix} +\frac{1}{2} \\ -\frac{1}{2} \end{pmatrix}$	$-\frac{1}{2}$	$\begin{pmatrix} 0 \\ -1 \end{pmatrix}$
right-handed leptons	e_{iR}	-	0	$+1$	$+1$
Higgs	H	-	$-\frac{1}{2}$	$+\frac{1}{2}$	0

Table 2.3: This table lists all matter particles in the Standard Model and the Higgs particle with their charges for all forces. This is the color, the weak isospin I_3, the half of their hypercharge and their electrical charge. The index $i = 1, 2, 3$ labels the generation of the matter particles and is written out in table 2.2. If there are no colors specified or charges are zero this means that the fields in question transform trivially under the pertaining gauge transformation. In fact, the Higgs particle originates from a $SU(2)_L$-doublet. This is not given here because within a certain gauge only the Higgs particle is a real particle.

The Force Particles

Before EWSB			After EWSB		
group	coupling constant	gauge field	coupling constant	gauge field	Particle
$SU(3)_C$	g_s	G_μ^a	g_s	G_μ^a	Gluon
$SU(2)_L$	g_w	W_μ^b	$g_W = \sqrt{2}g_w,$	$W_\mu^\pm,$	$W^\pm,$
			$g_Z = \sqrt{g_w^2 + g_Y^2}$	Z_μ^0	Z^0 Boson
$U(1)_Y$	g_Y	B_μ	$e = g_Y \cdot c_w$	A_μ	Photon

Table 2.4: The gauge fields and their coupling constants before and after electro weak symmetry breaking (EWSB). The Gluon field is not affected by EWSB. $a = 1, \ldots 8$ and $b = 1, 2, 3$ label the number of gauge fields. c_w is the cosine of the electroweak mixing angle defined in 2.3.

The force particles are described by gauge fields. The gauge field of $SU(3)_C$ is the gluon field. Because the $SU_C(3)$ has eight generators there are eight gluons. Their coupling constant is denoted with g_s.

For the other force particles in the Standard Model - the $W^\pm$ bosons, the Z_0 boson and the photon the situation is slightly more involved. They are obtained as a mixture of the W^b_μ ($b = 1, 2, 3$) and the B_μ field which are the gauge fields of $SU_L(2)_L$ and $U_Y(1)_Y$ respectively. This mixing procedure is explained in section 2.3.

For the moment being the coupling constants and gauge fields before and after this mixing are quoted in table 2.4.

The Lagrangian of the SM is built up by qualitatively different terms. Firstly there are the kinetic and minimal coupling terms of the matter fields

$$\mathcal{L}_{\text{matter}} = \sum_{i=1}^{3} \left(\bar{\ell}_{iL} i \not{D} l_{iL} + \bar{e}_{iR} i \not{D} e_{iR} + \bar{q}_{iL} i \not{D} q_{iL} + \bar{u}_{iR} i \not{D} u_{iR} + \bar{d}_{iR} i \not{D} d_{iR} \right), \tag{2.11}$$

where $i \in \{1, 2, 3\}$ labels the generations of matter. The gauge covariant derivative is given by

$$D_\mu = \partial_\mu + i g_Y \frac{\hat{Y}}{2} + i g_w \vec{\tau} \cdot \vec{W}^\mu + i g_s T^a G^\mu_a, \tag{2.12}$$

where for each field the corresponding representation (fundamental or trivial) of the gauge group is to be inserted (see table 2.3). The hypercharge operator $\hat{Y}$ gives the eigenvalue of the hypercharge of the field it is applied to. These can also be found in table 2.3. The kinetic terms of the gauge fields are given by

$$\mathcal{L}_{\text{gauge}} = -\frac{1}{4} F^{\mu\nu} F_{\mu\nu} - \frac{1}{4} W^{a\mu\nu} W^a_{\mu\nu} - \frac{1}{4} G^{a\mu\nu} G^a_{\mu\nu}. \tag{2.13}$$

2.3 Electroweak Symmetry Breaking

So far, no mass terms like in the Dirac Lagrangian 2.2 have been introduced. The reason for this is that they are not gauge invariant, for left- and right-handed spinors transform differently. The same argument forbids terms like $-\frac{m^2}{2} A^\mu A_\mu$ for a generic gauge boson. Electroweak symmetry breaking (EWSB) ascribes masses to those particles [5–11]. To this end one considers a complex scalar doublet

$$\Phi = \begin{pmatrix} \phi^+ \\ \phi^0 \end{pmatrix}, \tag{2.14}$$

which receives a vacuum expectation value (VEV) $\langle \Phi \rangle = \frac{1}{\sqrt{2}} \begin{pmatrix} 0 \\ v \end{pmatrix}$ by the Higgs potential

$$V(\Phi^\dagger \Phi) = -\mu^2 \Phi^\dagger \Phi + \lambda (\Phi^\dagger \Phi)^2 \tag{2.15}$$

where $\mu^2, \lambda > 0$ and v is given by $v = \sqrt{\frac{\mu^2}{\lambda}}$. The Higgs sector of the Standard Model reads

$$\mathcal{L}_{\text{Higgs}} = (D_\mu \Phi)^\dagger (D^\mu \Phi) - V(\Phi^\dagger \Phi). \tag{2.16}$$

The Higgs doublet couples to the gauge fields of $SU(2)_L$ and $U_Y(1)$ in the fundamental representation. Inserting an expansion[5] around the VEV

$$\Phi = \begin{pmatrix} \phi^+(x) \\ \frac{1}{\sqrt{2}}(v + H(x) + i\sigma(x)) \end{pmatrix} \tag{2.17}$$

one obtains quadratic terms, i.e. mass terms, for the gauge fields in question. In order to obtain mass eigenstates out of B_μ and W_μ^3 and charge eigenstates for Q and I_3 out of W_μ^1 and W_μ^2 one performs the transformation

$$\begin{pmatrix} A_\mu \\ Z_\mu^0 \end{pmatrix} = \begin{pmatrix} \cos\theta_w & \sin\theta_w \\ -\sin\theta_w & \cos\theta_w \end{pmatrix} \begin{pmatrix} B_\mu \\ W_\mu^3 \end{pmatrix}, \qquad W_\mu^\pm = \frac{1}{\sqrt{2}}(W_\mu^1 \mp iW_\mu^2), \tag{2.18}$$

where the electroweak mixing angle is given by $\cos\theta_w = \frac{g_w}{\sqrt{g_w^2 + g_Y^2}}$. These gauge fields acquire masses:

$$m_W = \frac{g_w}{2}v, \qquad\qquad m_Z = \frac{\sqrt{g_w^2 + g_Y^2}}{2}v, \qquad\qquad m_A = 0. \tag{2.19}$$

Apart from the massive bosons $W_\mu^\pm$ and Z_μ^0 one obtains the massless photon A_μ. As the photon is massless it is still associated with a gauge symmetry called $U_{em}(1)$. One therefore often writes EWSB as the breaking of the gauge group $SU(2)_L \times U_Y(1)$ to $U_{em}(1)$.

Matter particles acquire mass via Yukawa coulings to the Higgs doublet. For up-type-quarks one uses that the charge conjugate of Φ: $\Phi^C = i\sigma^2\Phi^*$ also transforms as Φ. The Yukawa Lagrangian is given by

$$\mathcal{L}_{\text{Yukawa}} = -\sum_{i,j=1}^3 \left(y_{ij}^e \overline{\ell}_L \Phi e_R + y_{ij}^d \overline{q}_L \Phi d_R + y_{ij}^u \overline{q}_L \Phi^C u_R \right) + h.c., \tag{2.20}$$

where y^e, y^d, y^u are 3×3 matrices in generation space. The fermion mass matrices are therefore:

$$m_{ij}^e = \frac{y_{ij}^e}{\sqrt{2}}v, \qquad\qquad m_{ij}^d = \frac{y_{ij}^d}{\sqrt{2}}v, \qquad\qquad m_{ij}^u = \frac{y_{ij}^u}{\sqrt{2}}v. \tag{2.21}$$

---

[5]The complex $\phi^+(x)$ and the real $\sigma(x)$ are the fields of the so-called massless Goldstone bosons. These degrees of freedom can be absorbed in the longitudinally polarized degrees of freedom of the arising gauge bosons $W^\pm$ and Z^0. This is referred to as unitary gauge [12]. The real $H(x)$ is the Higgs field, whose excitation is the Higgs boson.

The quark mass matrices are not diagonal, which is the precondition of the violation of CP-invariance.[6] One therefore has to distinguish between interaction and mass eigenstates of the quarks. The corresponding transformation matrix is the well known CKM-matrix [13, 14]. Throughout this thesis, the CKM-matrix is approximated with the unit matrix as it will have no influence upon the results.

The upshot of EWSB are masses for all matter particles except for the neutrinos and masses for the gauge bosons $W^\pm$ and Z^0.

2.4 Quantization

The Quantization of spin-0 and spin-$\frac{1}{2}$ fields yield no complication in the Lagrangian formalism. To quantize spin 1 fields it turns out that the usual gauge invariance needs to be replaced by the so called BRST invariance [15–17]. This results in two extra contributions in the Lagrangian. Firstly there are the gauge fixing terms:

$$\mathcal{L}_{R_\xi} = -\frac{1}{2\xi_A}(\partial^\mu A_\mu)^2 - \frac{1}{\xi_W}|\partial^\mu W_\mu^+ - im_W\xi_W\phi^+|^2 - \frac{1}{2\xi_Z}(\partial^\mu Z_\mu - m_Z\xi_Z\sigma)^2 - \frac{1}{2\xi_G}(\partial^\mu G_\mu^a)^2. \tag{2.22}$$

Here, R_ξ-gauge is chosen, where the parameters ξ_i specify the gauge further. The second and third term are modified with the Goldstone bosons from section 2.3. This is to cancel terms of the form $V_\mu\partial^\mu\phi$ up to a total derivative arising from EWSB which would lead to non-diagonal propagators, where V stands for a gauge boson $W^\pm$ or Z^0 and ϕ for a Goldstone boson. Secondly, there is a ghost Lagrangian

$$\mathcal{L}_{\text{ghost}} = -\bar{c}_a\partial^\mu\left(\partial_\mu c_a + g_s f_{abc} c_b G_{c\mu}\right) + \mathcal{L}_{\text{weak ghosts}}. \tag{2.23}$$

The ghost Lagrangian corresponding to the electroweak sector is not needed within this thesis and due to its lengthy form not quoted here. It can found in [12]. In eq. 2.23 c_a and $\bar{c}_a$ are the Faddeev-Popov ghost and antighosts. This fields do not correspond to physical particles because they violate the spin–statistics theorem, i.e. they anticommute while being spin 0 fields. Ghost fields are an elegant way of accounting for an additional term in the Lagrangian of non-abelian gauge fields which is best seen in the path integral quantization [2].

2.5 Lagrangian of the Standard Model

The complete Lagrangian of the Standard Model reads

$$\mathcal{L}_{\text{SM}} = \mathcal{L}_{\text{matter}} + \mathcal{L}_{\text{gauge}} + \mathcal{L}_{\text{Higgs}} + \mathcal{L}_{\text{Yukawa}} + \mathcal{L}_{R_\xi} + \mathcal{L}_{\text{ghost}} \tag{2.24}$$

---

[6]The actual CP-violating term is in the coupling term of quarks to the W-bosons.

with the corresponding parts of the previous chapters. For further reading and the electroweak Lagrangian given completely in terms of physical fields, see [12].

3 The Minimal Supersymmetric Standard Model

Even though the Standard Model is a very well working machinery which has been tested to an impressive accuracy it is not the ultimate theory of nature. This is not only because of its incompleteness regarding gravity but also because of its missing incorporation of dark matter. This is that astrophysical observations [18] indicate that only 4.9% of the universe's mass energy consist of ordinary matter while the majority is represented by 26.8% of dark matter and 68.3% of dark energy. Another puzzle is the hierarchy problem which questions the large difference between the Higgs boson mass and its quantum correction, see [19]. Finally, the gauge groups of the Standard Model cannot be unified to a theoretically appealing single gauge group at some high energy scale for the three gauge couplings do not meet at any renormalization scale [19]. There are many other problems which are not mentioned here [4]. Supersymmetry provides a possible extension of the Standard Model. It constitutes a mathematically very aesthetic solution of the above mentioned problems[7]. This section explains briefly the mechanism of supersymmetry and the minimal supersymmetric extension of the Standard Model (MSSM).

3.1 Supersymmetry as an Extention of the Poincaré Symmetry

As already seen in the previous chapter symmetries are of vital importance when studying particle physics. Coleman and Mandula [20] found that for any reasonable quantum field theory space-time and internal symmetries, i.e. gauge symmetries "cannot by combined in any but the trivial way" [21]. Ergo the symmetry groups of the Standard Model are the most general ones.

This statement was corrected by the Haag-Lopuszanski-Sohnius theorem [22] which weakened the condition of the quantum field theory by allowing also for anticommuting symmetry generators. This is, by introducing the generators Q_α and $\overline{Q}^{\dot{\alpha}}$ with $\alpha, \dot{\alpha} \in \{1, 2\}$, the Poincare-algebra eq. (2.1) can be nontrivially extended to the so called superalgebra (see appendix (10.3) for the definition of the σ-matrices):

$$\{Q_\alpha, Q_\beta\} = \{\overline{Q}_{\dot{\alpha}}, \overline{Q}_{\dot{\beta}}\} = 0,$$
$$\{Q_\alpha, \overline{Q}_{\dot{\alpha}}\} = 2\sigma^\mu_{\alpha\dot{\alpha}} P_\mu,$$
$$[P^\mu, Q_\alpha] = [P^\mu, \overline{Q}_{\dot{\alpha}}] = 0,$$
$$[Q_\alpha, J^{\mu\nu}] = \frac{1}{2}(\sigma^{\mu\nu})_\alpha^{\ \beta} Q_\beta. \tag{3.1}$$

As $J^{\mu\nu}$ is the generalized angular momentum operator the last line in eq. (3.1) implies that Q_α is a spin-$\frac{1}{2}$ operator. Applying Q_α to a field will change the spin of it by $\frac{1}{2}$. This means

---

[7]In its minimal extension to the Standard Model supersymmetry does not incorporate gravity but many quantum gravity models are supersymmetric

supersymmetry generators convert fermions to bosons and vice versa.

The superalgebra in eq. (3.1) is actually the smallest extension of the Poincare-algebra as it is possible to introduce further anticommuting symmetry generators. Their maximal number is fixed to $N = 8$. Because the MSSM is a minimal extension of the Standard Model, it deals with only one set of anticommuting symmetry generators and is therefore referred to be a $N = 1$ supersymmetric theory.

A representation in the form of differential operators can be given by introducing superspace. Superspace is a manifold obtained by enlarging Minkowski space, whose coordinates are label with x^μ, with four anticommuting numbers: θ^α and $\overline{\theta}^{\dot{\alpha}}$, where α, $\dot{\alpha} \in \{1, 2\}$ (see Appendix 10.4 for the definition of anticommuting numbers). A representation of the superalgebra reads

$$
\begin{aligned}
P^\mu &= i\partial^\mu, \\
J^{\mu\nu} &= i(x^\mu \partial^\nu - x^\nu \partial^\mu), \\
Q_\alpha &= i(\partial_\alpha + i\sigma^\mu_{\alpha\dot{\alpha}} \overline{\theta}^{\dot{\alpha}} \partial_\mu), \\
\overline{Q}_{\dot{\alpha}} &= i(-\overline{\partial}_{\dot{\alpha}} - i\theta^\alpha \sigma^\mu_{\alpha\dot{\alpha}} \partial_\mu).
\end{aligned}
\tag{3.2}
$$

3.2 A Generic Supersymmetric Model in Superspace Formulation

This chapter outlines the generic ingredients and terms of a supersymmetric model. To this end it is practical to work in the language of superspace and superfields. Superfields are functions on superspace.

The superfields[8] relevant for the MSSM are the chiral superfield $\hat{\Phi}$, the antichiral superfield $\hat{\overline{\Phi}}$ and the vector superfield $\hat{V}$. Chiral superfields are defined by the restriction $\overline{\mathcal{D}}_{\dot{\alpha}}\hat{\Phi} = 0$, antichiral superfields by $\mathcal{D}_\alpha \hat{\overline{\Phi}} = 0$ (see appendix 10.4 for the definition of chiral covariant derivatives) and vector superfields by the condition of being real $\hat{V}^\dagger = \hat{V}$.

All superfields can be decomposed into component fields on Minkowski space. The component decomposition of the above fields read[9]

$$
\hat{\Phi}(x, \theta, \overline{\theta}) = A(x) + \sqrt{2}\theta\psi(x) + \theta\theta F(x) - i\theta\sigma^\mu\overline{\theta}\partial_\mu A(x) - \frac{1}{4}\theta\theta\overline{\theta}\overline{\theta}\partial_\mu\partial^\mu A(x) - \frac{i}{\sqrt{2}}\theta\theta\overline{\theta}\overline{\sigma}^\mu\partial_\mu\psi(x),
$$

$$
\hat{\overline{\Phi}}(x, \theta, \overline{\theta}) = A^\dagger(x) + \sqrt{2}\overline{\theta}\overline{\psi}(x) + \overline{\theta}\overline{\theta} F^\dagger(x) + i\theta\sigma^\mu\overline{\theta}\partial_\mu A^\dagger(x) - \frac{1}{4}\theta\theta\overline{\theta}\overline{\theta}\partial_\mu\partial^\mu A^\dagger(x) - \frac{i}{\sqrt{2}}\overline{\theta}\overline{\theta}\theta\sigma^\mu\partial_\mu\overline{\psi}(x),
$$

$$
\hat{V}(x, \theta, \overline{\theta}) = \theta\sigma^\mu\overline{\theta}v_\mu + i\theta\theta\overline{\theta}\overline{\lambda}(x) - i\overline{\theta}\overline{\theta}\theta\lambda(x) + \frac{1}{2}\theta\theta\overline{\theta}\overline{\theta}D(x),
\tag{3.3}
$$

where $A(x)$ and $F(x)$ are complex scalar fields, $\psi(x)$ and $\lambda(x)$ are left-handed Weyl spinors, $D(x)$ is a real scalar field and v_μ is a vector field.

---

[8]Superfield are throughout this thesis labeled with a hat.

[9]For tho vector superfield Wess-Zumino-gauge is applied.

The superfields transform under a generic gauge transformation as

$$\hat{\Phi} \to \mathrm{e}^{-2ig\hat{\Lambda}}\hat{\Phi},$$

$$\hat{\bar{\Phi}} \to \hat{\bar{\Phi}}\mathrm{e}^{2ig\hat{\bar{\Lambda}}},$$

$$\mathrm{e}^{2g\hat{V}} \to \mathrm{e}^{-2ig\hat{\bar{\Lambda}}}\mathrm{e}^{2g\hat{V}}\mathrm{e}^{2ig\hat{\Lambda}}, \tag{3.4}$$

where $\hat{\Lambda} = \hat{\Lambda}^a T^a$ and $\hat{V} = \hat{V}^a T^a$. $\hat{\Lambda}^a$ is an arbitrary chiral superfield, the T^a are the generetors of the gauge group in question and g is the gauge coupling constant of the gauge group.

One can therefore construct the important gauge invariant term $\int \mathrm{d}^4\theta\, \hat{\bar{\Phi}}\mathrm{e}^{2g\hat{V}}\hat{\Phi}$. If one introduces the gauge covariant derivative $D_\mu = \partial + igT^a v_\mu^a$ its component decomposition reads

$$\int \mathrm{d}^4\theta \hat{\bar{\Phi}}\mathrm{e}^{2g\hat{V}}\hat{\Phi} = F^\dagger F + (D_\mu A)^\dagger (D^\mu A) + \overline{\psi}\overline{\sigma}^\mu i D_\mu \psi$$

$$- \sqrt{2}g\left(-i(A^\dagger T^a A)\lambda^a + i\overline{\lambda}^a (A T^a A^\dagger)\right) + g(A^\dagger T^a A)D^a. \tag{3.5}$$

Therefore this term gives rise to the kinetic terms of the components of the chiral and antichiral superfields A, $A^\dagger$, ψ and $\overline{\psi}$ as well as their minimal coupling to the gauge fields v_μ^a and their superpartners λ^a and $\overline{\lambda}^a$ and terms involving the auxiliary fields F, $F^\dagger$ and D.

With the field-strength chiral superfields $\hat{W}_\alpha := -\frac{1}{4}\overline{\mathcal{D}}\mathcal{D}(\mathrm{e}^{-2gV}\mathcal{D}_\alpha \mathrm{e}^{2gV})$ one can write down a gauge invariant term yielding the kinetic terms of the gauge fields and their superpartners:

$$\int \mathrm{d}^2\theta \frac{1}{16g^2}\hat{W}^{\alpha a}\hat{W}_\alpha^a + h.c. = \frac{1}{2}D^a D^a - \frac{1}{4}F_{\mu\nu}^a F^{a\mu\nu} + \frac{i}{2}\overline{\lambda}^a \overline{\sigma}^\mu (D_\mu \lambda^a) + \frac{i}{2}\lambda^a \sigma^\mu (D_\mu \overline{\lambda}^a). \tag{3.6}$$

A third generic term in a supersymmetric theory arises from the superpotential $W(\hat{\Phi})$ which is a holomorphic function in the chiral superfields:

$$\int \mathrm{d}^2\theta \, W(\hat{\Phi}). \tag{3.7}$$

A renormalizable superpotential is given by $W(\hat{\Phi}) = c_i\hat{\Phi} + \frac{m_{ij}}{2}\hat{\Phi}_i\hat{\Phi}_j + \frac{g_{ijk}}{3!}\hat{\Phi}_i\hat{\Phi}_j\hat{\Phi}_k$. The component decomposition of the corresponding terms is

$$\int \mathrm{d}^2\theta \, \hat{\Phi}_1 = F_1,$$

$$\int \mathrm{d}^2\theta \, \hat{\Phi}_1\hat{\Phi}_2 = A_1 F_2 + F_1 A_2 - \psi_1\psi_2,$$

$$\int \mathrm{d}^2\theta \, \hat{\Phi}_1\hat{\Phi}_2\hat{\Phi}_3 = F_1 A_2 A_3 + A_1 F_2 A_3 + A_1 A_2 F_3 - A_1\psi_2\psi_3 - \psi_1 A_2\psi_3 - \psi_1\psi_2 A_3. \tag{3.8}$$

The Lagrangian for a supersymmetric theory is therefore given by

$$\mathcal{L}_{\text{SUSY}} = \mathcal{L}_{\text{matter}} + \mathcal{L}_{\text{gauge}} + \mathcal{L}_{\text{superpot}}$$
$$= \int \mathrm{d}^4\theta \hat{\bar{\Phi}} \mathrm{e}^{2g\hat{V}} \hat{\Phi} + \left(\int \mathrm{d}^2\theta \frac{1}{16g^2} \hat{W}^{\alpha a} \hat{W}^a_\alpha + h.c. \right) + \left(\int \mathrm{d}^2\theta \, W(\hat{\Phi}) + h.c. \right) \quad (3.9)$$

Observing the component decomposition eq. (3.5), (3.6) and (3.8) of the three parts of this Lagrangian one observes that the F and D fields have no kinetic term and are therefore auxiliary fields which can be eliminated by their equation of motion $\frac{\partial \mathcal{L}}{\partial \phi} = \partial_\mu \frac{\partial \mathcal{L}}{\partial(\partial_\mu \phi)}$ with $\phi \in \{F, D\}$. Doing this one obtains

$$\mathcal{L}_D = \frac{1}{2} D^a D^a + g A^\dagger T^a D^a A \qquad \Rightarrow \qquad D^a = -A^\dagger T^a A,$$
$$\mathcal{L}_D = -\frac{1}{2} \left(A^\dagger T^a A \right)^2. \tag{3.10}$$

and

$$\mathcal{L}_F = F_i^\dagger F_i + \left(c_i F_i + m_{ij} F_i A_j + \frac{g_{ijk}}{2} F_i A_j A_k + h.c. \right) \qquad \Rightarrow \qquad F_i^\dagger = -\frac{\partial W(A)}{\partial A_i}$$
$$\mathcal{L}_F = -\left| \frac{\partial W(A)}{\partial A_i} \right|^2 \tag{3.11}$$

3.3 The Minimal Supersymmetric Standard Model

After having introduced components of a generic supersymmetric model a possible realization of supersymmetry in nature - the Minimal Supersymmetric Standardmodel (MSSM) - is discussed in this section. The field content of the MSSM is summarized in table **??**. In comparison to the Standard Model each particle has a superpartner which differs in its spin by $\frac{1}{2}$. The superpartners of fermions have Spin 0 and are referred to as sfermions. The name of each sfermion is given by the name of its Standard Model partner with an additional "s-" in front of it, e.g. selectron or up-squark. The superpartners of bosons have spin $\frac{1}{2}$ and get an additional "-ino" at the end of their name, e.g. higgsino as the superpartner of the Higgs or bino as superpartner of the B-boson.

Apart from this doubling of the field content of the Standard Model, there is one modification within the Higgs sector, i.e. there are two instead of one Higgs superfield. These are necessary to avoid an anomaly in the electroweak gauge symmetry and to give masses to both up- and down-type quarks [19, page 8].

Note that the "chirality" of sfermions is understood to be the chirality of their superpartners. Of course scalar particles have no handedness. The Lagrangian[10] for the MSSM reads

Superfield	Components	$SU(3)_C \times SU(2)_L \times U(1)_Y$
$\hat{\Phi}$	$A,\ \psi$	
$\hat{V}$	$\lambda,\ v_\mu$	
$\hat{Q}$	$\tilde{q}_L = \begin{pmatrix} \tilde{u}_L \\ \tilde{d}_L \end{pmatrix},\ q_L = \begin{pmatrix} u_L \\ d_L \end{pmatrix}$	$(3,\ 2,\ \frac{1}{6})$
$\hat{U}$	$\tilde{u}_R^\dagger,\ u_R$	$(3^*,\ 1,\ -\frac{2}{3})$
$\hat{D}$	$\tilde{d}_R^\dagger,\ d_R$	$(3^*,\ 1,\ +\frac{1}{3})$
$\hat{L}$	$\tilde{l}_L = \begin{pmatrix} \tilde{\nu}_L \\ \tilde{e}_L \end{pmatrix},\ l_L = \begin{pmatrix} \nu_L \\ e_L \end{pmatrix}$	$(1,\ 2,\ -\frac{1}{2})$
$\hat{E}$	$\tilde{e}_R^\dagger,\ e_R$	$(1,\ 1,\ 1)$
$\hat{H}_d$	$H_d,\ \tilde{H}_d$	$(1,\ 2,\ -\frac{1}{2})$
$\hat{H}_u$	$H_u,\ \tilde{H}_u$	$(1,\ 2,\ +\frac{1}{2})$
$\hat{V}_Y$	$\lambda_Y,\ B_\mu$	$(1,\ 1,\ 0)$
$\hat{V}_w^a$	$\lambda_w^a,\ W_\mu^a$	$(1,\ 3,\ 0)$
$\hat{V}_s^a$	$\lambda_s^a,\ G_\mu^a$	$(8,\ 1,\ 0)$

Table 3.1: The table shows the field content of the MSSM in terms of the superfields and their components. The first two lines show the decomposition of the generic superfields (cf. subsection (3.3)).

The third column shows the representation (for $SU(3)_C$ and $SU(2)_L$) in which the fields transform and in which the generator in the covariant derivative needs to be inserted as well as the charges of the fields for $U(1)_Y$. For $SU(3)_C$ the "8" refers to the adjoint representation (see appendix 10.2), the "3" to the fundamental and the "3*" to the antifundamental representation $T_{antifund}^a = -\frac{\lambda^a}{2}$. For $SU(2)_L$ "3" refers to the adjoint representation and "2" to the fundamental representation. For both $SU(2)_L$ and $SU(3)_C$ a "1" indicates the the trivial representation.

$$\mathcal{L}_{\text{MSSM}} = \int \mathrm{d}^4\theta \left[\hat{\bar{Q}} \mathrm{e}^{2g_Y \hat{V}_Y + 2g_w \hat{V}_w + 2g_s \hat{V}_s} \hat{Q} + \hat{\bar{U}} \mathrm{e}^{2g_Y \hat{V}_Y + 2g_w \hat{V}_w - 2g_s \hat{V}_s^T} \hat{U} + \hat{\bar{D}} \mathrm{e}^{2g_Y \hat{V}_Y + 2g_w \hat{V}_w - 2g_s \hat{V}_s^T} \hat{D} \right.$$

$$+ \hat{\bar{L}} \mathrm{e}^{2g_Y \hat{V}_Y + 2g_w \hat{V}_w} \hat{L} + \hat{\bar{E}} \mathrm{e}^{2g_Y \hat{V}_Y + 2g_w \hat{V}_w} \hat{E}$$

$$\left. + \hat{\bar{H}}_d \mathrm{e}^{2g_Y \hat{V}_Y + 2g_w \hat{V}_w} \hat{H}_d + \hat{\bar{H}}_u \mathrm{e}^{2g_Y \hat{V}_Y + 2g_w \hat{V}_w} \hat{H}_u \right]$$

$$+ \int \mathrm{d}^2\theta \left[\frac{1}{16g_Y^2} \hat{W}_Y^\alpha \hat{W}_{Y\alpha} + \frac{1}{16g_w^2} \hat{W}_w^{a\alpha} \hat{W}_{w\alpha}^a + \frac{1}{16g_s^2} \hat{W}_s^{a\alpha} \hat{W}_{s\alpha}^a \right] + h.c.$$

$$+ \int \mathrm{d}^2\theta \, W_{\text{MSSM}} + h.c.$$

$$+ \mathcal{L}_{\text{soft}}. \tag{3.12}$$

Apart from the kinetic and minimal coupling terms in the first four lines of eq. (3.12) and the softly breaking part of the Lagrangian in the last line of eq. (3.12) which will be discussed in **??**, there is a superpotential W_{MSSM}:

$$W_{\text{MSSM}} = y_d \hat{H}_d \hat{Q} \hat{D} + y_u \hat{H}_u \hat{Q} \hat{U} + y_e \hat{H}_d \hat{L} \hat{E} - \mu \hat{H}_d \hat{H}_u, \tag{3.13}$$

which will in regard of its form be justified in section 3.3.2. After eliminating auxiliary fields the Higgs potential is generated. In contrast to the Standard Model the quadrilinear term in the Higgs potential is given in terms of the gauge couplings and therefore no independent parameter. From the Higgs potential both H_u and H_d acquire a vacuum expectation value:

$$\langle H_u \rangle = \frac{1}{\sqrt{2}} \begin{pmatrix} 0 \\ v_u \end{pmatrix} \qquad\qquad \langle H_d \rangle = \frac{1}{\sqrt{2}} \begin{pmatrix} v_d \\ 0 \end{pmatrix} \tag{3.14}$$

whose quotient is an important parameter of the electroweak MSSM.

$$\tan\beta := \frac{v_u}{v_d} \tag{3.15}$$

As in the Standard Model this spontaneous symmetry breaking and the presence of Yukawa-terms (first three terms of eq. (3.13)) lead to masses of the fermions.[11] Apart from that there are also other terms like quark-squark-higgsino interactions. In addition there is the μ-term which is responsible for Higgsino and Higgs masses.

3.3.1 Supersymmetry Breaking and Mass Eigenstates

?? In order to explain why supersymmetric particles have not been found so far supersymmetry has to be broken. Like in electroweak symmetry breaking supersymmetry is preserved at some

---

[10]This is the Lagrangian on the classical level, i.e. there are neither gauge fixing nor ghost terms.

[11]Note the sum convention of $SU_{\text{L}}(2)$ doublets: $\hat{H}_u \hat{Q} = (\hat{H}_u)_\alpha \hat{Q}_\beta \epsilon^{\alpha\beta}$ to ensure gauge invariance (see appendix 10.3 for the definition of $\epsilon^{\alpha\beta}$).

high energy scale but its vacuum state is not supersymmetric. However there is no consensus on how supersymmetry is broken. But by ignoring the exact mechanism and parameterizing it by introducing appropriate terms in the Lagrangian one accounts for it in an absolutely viable way.

Terms which break supersymmetry should be soft, i.e. they should have coupling constants with positive mass dimension.

$$
\begin{aligned}
\mathcal{L}_{\text{soft}} = & -M_{\tilde{Q}}^2 |\tilde{q}_L|^2 - M_{\tilde{U}}^2 |\tilde{u}_R|^2 - M_{\tilde{D}}^2 |\tilde{d}_R|^2 \\
& - M_{\tilde{L}}^2 |\tilde{l}_L|^2 - M_{\tilde{E}}^2 |\tilde{e}_R|^2 - M_{H_d}^2 |H_d|^2 - M_{H_u}^2 |H_u|^2 \\
& + \frac{1}{2} \left(M_1 \lambda_Y \lambda_Y + M_2 \lambda_w^a \lambda_w^a + M_3 \lambda_s^a \lambda_s^a \right) + h.c. \\
& - \left(A_d y_d H_d \tilde{q}_L \tilde{d}_R^\dagger + A_u y_u H_u \tilde{q}_L \tilde{u}_R^\dagger + A_e y_e H_d \tilde{l}_L \tilde{e}_R^\dagger - B\mu H_d H_u \right) + h.c.
\end{aligned}
\tag{3.16}
$$

The softly breaking terms in the MSSM comprise masses of the squarks, sleptons, Higgs-bosons and gauginos. The last line in eq. (3.16) resembles the superpotential in eq. (3.13). In fact the only two differences are that the superfields are replaced by their scalar components and that additional parameters with mass dimension one have been added. A_d, A_u, A_e are 3×3 matrices in family space.

There are fields in the MSSM which are no eigenstate of the mass operator $P^\mu P_\mu$ but have a mass matrix which is non-diagonal. This is true for neutral higgsinos and gauginos which mix to neutralinos and charged higgsinos and gauginos which mix to charginos to yield physical particles with definite mass. However, for this thesis only the mass matrix for electrically charged sfermions is given because this will change significantly when introducing R-symmetry in the next section. The Lagrangian describing these masses reads

$$
\mathcal{L}_{m_{\tilde{q}}, m_{\tilde{e}}} = - \begin{pmatrix} \tilde{u}_L^\dagger & \tilde{u}_R^\dagger \end{pmatrix} M_{\tilde{u}}^2 \begin{pmatrix} \tilde{u}_L \\ \tilde{u}_R \end{pmatrix} - \begin{pmatrix} \tilde{d}_L^\dagger & \tilde{d}_R^\dagger \end{pmatrix} M_{\tilde{d}}^2 \begin{pmatrix} \tilde{d}_L \\ \tilde{d}_R \end{pmatrix} - \begin{pmatrix} \tilde{e}_L^\dagger & \tilde{e}_R^\dagger \end{pmatrix} M_{\tilde{e}}^2 \begin{pmatrix} \tilde{e}_L \\ \tilde{e}_R \end{pmatrix}.
\tag{3.17}
$$

where the mass matrix is given by

$$
M_{\tilde{f}}^2 = \begin{pmatrix} M_{\tilde{f}LL}^2 & m_f X_f^* \\ m_f X_f & M_{\tilde{f}RR}^2 \end{pmatrix}.
\tag{3.18}
$$

The diagonal terms are given by the sum of the fermion mass squared m_f^2, the appropriate soft breaking term, e.g. $M_{\tilde{Q}}^2$ for left handed squarks and a contribution from the elimination of D-fields. In fact this last term splits the masses of fermions and sfermions already without explicit supersymmetry breaking. This is because the generation of fermion masses requires the breaking of gauge symmetry which is not possible without breaking supersymmetry. However

the off-diagonal terms are given by

$$X_f = A_f + \mu^* \left\{ \cot\beta, \tan\beta \right\} \tag{3.19}$$

with $\cot\beta$ for up-type squarks and $\tan\beta$ for down-type sfermions and $A_f \in \{A_d, A_u, A_e\}$.

3.3.2 R-Parity

The MSSM does not include any terms which violate baryon (B) or lepton number (L)[12] like

$$W_{\Delta\mathrm{B}=1} = \lambda \hat{U}\hat{D}\hat{D} \qquad \text{or} \qquad W_{\Delta\mathrm{L}=1} = \lambda'\hat{L}\hat{Q}\hat{D} \tag{3.20}$$

in the superpotential although this would be possible from the perspective of gauge invariance and renormalizability. However, this has not been oberserved experimentally. The most famous constraint on them is the non-observation of proton decay which restricts at least one of the parameters λ or λ' to be extremely small [19]. Forbidding these terms by postulating a conservation of B and L might not be the best solution since both B and L are known to be violated in nature by non-perturbative effects [23].

A possible way out is the postulation of the conservation of R-parity

$$P_R = (-1)^{3(\mathrm{B}-\mathrm{L})+2s} \tag{3.21}$$

where s is the spin of the particle on which the R-parity operator is applied to. R-parity is a multiplicative quantum number which is constructed to be $+1$ for each Standard Model particle and -1 for each supersymmetric partner. Apart from the prohibition of the terms in eq. (3.20) this has important consequences:

- There has to be a lightest supersymmetric particle (LSP) which is absolutely stable. This is a candidate for dark matter.

- At colliders like the LHC there must always be an even number of supersymmetric particles be produced, if at all.

The superpotential of the MSSM (see, eq. (3.13)) is chosen in such a way that it is the only renormalizable and gauge invariant potential which respects R-parity.

---

[12]The chiral superfield $\hat{Q}$ carries baryon number $\frac{1}{3}$, whereas $\mathrm{B} = -\frac{1}{3}$ for $\hat{D}$, $\hat{U}$ and $\mathrm{B} = 0$ for all other superfields. The only multiplets carrying a non-zero lepton number are $\hat{L}$ with $\mathrm{L} = 1$ and $\hat{E}$ with $\mathrm{L} = -1$.

4 R-Symmetry

R-symmetry is an additional continuous symmetry which extends supersymmetry in a non-trivial way. This is actually covered in the Haag-Lopuszanski-Sohnius theorem [22] but often concealed.

This section introduces R-symmetry and discusses briefly a minimal viable extension of the MSSM including R-symmetry, the MRSSM. Thereby some general features of the model are mentioned before the focus is laid on the strongly interacting sector which is the central topic of the thesis.

4.1 R-Symmetry Transformation

For a $N = 1$ supersymmetric theory, R-symmetry is a global $U(1)$ symmetry. It must not be confused with R-parity which is a discrete $\mathbb{Z}_2$ symmetry. A continuous global symmetry implies according to Noether's theorem a conserved charge. In the case of R-symmetry it is called R-charge and one therefore refers to R-symmetry as $U_R(1)$.

The defining property of $U_R(1)$ is that the anticommuting coordinates θ^α and $\overline{\theta}^{\dot{\alpha}}$ transform like

$$\theta \to \mathrm{e}^{i\tau}\theta, \qquad\qquad \overline{\theta} \to \mathrm{e}^{-i\tau}\overline{\theta}, \qquad\qquad (4.1)$$

where τ parametrizes the transformation. This in turn implies that the supersymmetry generators (see eq. **??**) transform like

$$Q \to \mathrm{e}^{-i\tau}Q \qquad\qquad \overline{Q} \to \mathrm{e}^{i\tau}\overline{Q} \qquad\qquad (4.2)$$

and R-symmetry does not commute with supersymmetry

$$[R, Q] = -Q \qquad\qquad \left[R, \overline{Q}\right] = \overline{Q}, \qquad\qquad (4.3)$$

meaning that superpartners do not have the same R-charge. The transformation of chiral and vector superfields reads

$$\begin{aligned} \hat{\Phi}(x, \theta, \overline{\theta}) &\to \mathrm{e}^{ir_{\hat{\Phi}}\tau}\,\hat{\Phi}(x, \mathrm{e}^{i\tau}\theta, \mathrm{e}^{-i\tau}\overline{\theta}), \\ \hat{V}(x, \theta, \overline{\theta}) &\to \hat{V}(x, \mathrm{e}^{i\tau}\theta, \mathrm{e}^{-i\tau}\overline{\theta}), \end{aligned} \qquad\qquad (4.4)$$

i.e. the chiral superfields transform with arbitrary R-charge where the R-charge of vector superfield is restricted to be zero by the condition that they are real. If one inserts the component decomposition eq. (3.3) of the superfields one can read off the R-charges of the component fields.

Superfield		Boson		Fermion	
$\hat{\Phi}$	$r_{\hat{\Phi}}$	A	$r_{\hat{\Phi}}$	ψ	$r_{\hat{\Phi}} - 1$
$\hat{V}$	0	v^{μ}	0	λ	$+1$

Table 4.1: This table shows the R-charges of a generic chiral and vector superfield.

4.2 The Minimal R-Symmetric Supersymmetric Standard Model

If one imposes R-symmetry upon the MSSM one is faced with a certain arbitrariness, i.e. the choice of the R-charges of the chiral superfields. A minimal R-symmetric extension of the MSSM is the minimal R-symmetric supersymmetric Standard Model (MRSSM) [24]. In this model the R-charges are chosen in such a way, that every Standard Model particle has R-charge zero. Following this one obtains the R-charges of all particles which are summed up in table 4.2 [30].

Field	Superfield		Boson		Fermion	
gauge Vector	$\hat{V}_s^a,\ \hat{V}_w^a,\ \hat{V}_Y$	0	$G_{\mu}^a,\ W_{\mu}^a,\ B_{\mu}$	0	$\lambda_s^a,\ \lambda_w^a,\ \lambda_Y$	$+1$
matter	$\hat{L},\ \hat{E}$	$+1$	$\tilde{l}_l,\ \tilde{e}_R^{\dagger}$	$+1$	$l_L,\ e_R$	0
	$\hat{Q},\ \hat{D},\ \hat{U}$	$+1$	$\tilde{q}_L,\ \tilde{d}_R^{\dagger},\ \tilde{u}_R^{\dagger}$	$+1$	$q_L,\ d_R,\ u_R$	0
H-Higgs	$\hat{H}_{d,u}$	0	$H_{d,u}$	0	$\tilde{H}_{d,u}$	-1
R-Higgs	$\hat{R}_{d,u}$	$+2$	$R_{d,u}$	$+2$	$\tilde{R}_{d,u}$	$+1$
adjoint chiral	$\hat{O},\ \hat{T},\ \hat{S}$	0	$\sigma^a,\ \omega^a,\ \rho$	0	$\chi_s^a,\ \chi_w^a,\ \chi_Y$	-1

Table 4.2: This table lists the R-charges of all superfields and their components in the MRSSM. The fields of the R-Higgs and the adjoint chiral superfields are not present in the MSSM

The gauge, matter and H-Higgs fields are the fields of the MSSM. Below the horizontal line one finds the fields which are not present in the MSSM, i.e. the R-Higgs and adjoint chiral fields. These occur for the following reason.

In the MSSM the gauginos are Majorana particles. Their mass terms reads in 2-spinor notation

$$\mathcal{L}_{\text{Majorana mass}} = -m\lambda\lambda + h.c. \tag{4.5}$$

which is not R-invariant because the Weyl fermion λ has R-charge $+1$. Giving no mass to the gauginos is phenomenologically not possible. The only way to account for a fermion mass is to write down a Dirac mass term

$$\mathcal{L}_{\text{Dirac mass}} = -m\chi\lambda + h.c., \tag{4.6}$$

where χ is another Weyl-spinor. This means that the 4-spinor of every gaugino is a Dirac-

instead of a Majorana-spinor, e.g. for the gluino:

$$
\tilde{g}_{\text{MSSM}} = \begin{pmatrix} -i\lambda_s \\ +i\bar{\lambda}_s \end{pmatrix} \qquad\qquad \tilde{g}_{\text{MRSSM}} = \begin{pmatrix} -i\lambda_s \\ +i\bar{\chi}_s \end{pmatrix}. \tag{4.7}
$$

In order to get a R-symmetric mass term on has to choose the R-charge of the new Weyl-spinor χ to be the opposite of λ.

This explains the necessity of enlarging the field content if one imposes R-symmetry.

Of course the new Weyl-spinor χ must have also a superpartner. One chooses this superpartner to be a scalar, i.e. the additional Weyl fermion comes from a chiral superfield. In order to maintain gauge invariance this chiral superfield has to transform in the adjoint representation, hence the name adjoint chiral in table 4.2. To fix notation the component decomposition of the eight chiral supermultiplets assosiated to the gluons is given by

$$
\hat{O}^a(x,\theta,\bar{\theta}) = \sigma^a + \sqrt{2}\theta i \chi_s^a + \dots \qquad\qquad a = 1,\dots,8. \tag{4.8}
$$

The scalar components σ^a are referred to as scalar gluons and the Weyl spinors χ^a are called octinos.

The same argument as for the adjoint chiral superfields explains the existence of additional Higgs-superfields which are referred to as R-Higgs fields.

Apart from these extensions R-symmetry also forbids terms which are allowed by supersymmetry. For the above choice of R-charges the μ-term in (3.13) and the A-terms in the last line of (3.16) are absent in the MRSSM. Inspecting eq. (3.19) implies that there is no squark mixing in the MRSSM. As a consequence terms which allow flavor violating processes like $\mu \to e\gamma$ in the MSSM are suppressed in the MRSSM [24]. Quite interestingly Dirac gauginos can be heavier than Majorana gauginos without being less natural in view of the hierarchy problem [25–27]. Finally the production cross section of strongly interacting particles is suppressed [26, 28]. It is this last feature which is going to be observed further in this thesis. To this end the colored sector of the MRSSM in now considered in more detail.

4.3 The R-Symmetric Supersymmetric Quantum Chromodynamics

The subject of this thesis is the phenomenology of the strongly coupling sector of the MRSSM. The R-symmetric supersymmetric quantum chromodynamics (RSQCD) is therefore considered closer. Its Lagrangian for an arbitrary massless quark reads

$$
\mathcal{L}_{\text{RSQCD}} = \int \mathrm{d}^4\theta \; \left(\hat{\bar{Q}}_L \mathrm{e}^{2g_s \hat{V}_s} \hat{Q}_L + \hat{\bar{Q}}_R \mathrm{e}^{-2g_s \hat{V}_s^T} \hat{Q}_R + \hat{\bar{O}} \mathrm{e}^{2g_s \hat{V}_s^{\text{fund}}} \hat{O} \right)
$$
$$
+ \left(\int \mathrm{d}^2\theta \frac{1}{16g_s^2} \hat{W}_s^{a\alpha} \hat{W}_{s\alpha}^a + h.c. \right) + \mathcal{L}_{\text{soft}} \tag{4.9}
$$

where $\hat{Q}_L$ and $\hat{Q}_R$ refer to the left- and right-handed superfield of the quark. Note that each field in the first line of eq. (4.9) transforms in a different representation of $SU_C(3)$, i.e. the fundamental, the antifundamental and the adjoint one. From now on T^a stands for the fundamental representation of the generators of $SU(3)_C$. In terms of components fields these expressions are given by

$$
\int \mathrm{d}^4\theta \, \hat{\bar{Q}}_L \mathrm{e}^{2g_s \hat{V}_s} \hat{Q}_L = F_L^\dagger F_L + (D_\mu \tilde{q}_L)^\dagger (D^\mu \tilde{q}_L) + \overline{q}_L \overline{\sigma}^\mu i D_\mu q_L
$$
$$
- \sqrt{2} g_s \left(-i(\tilde{q}_L^\dagger T^a q_L)\lambda^a + i\overline{\lambda}^a (\overline{q}_L T^a \tilde{q}_L) \right) + g_s \tilde{q}_L^\dagger T^a D^a \tilde{q}_L, \qquad (4.10)
$$

$$
\int \mathrm{d}^4\theta \, \hat{\bar{Q}}_R \mathrm{e}^{-2g_s \hat{V}_s^T} \hat{Q}_R = F_R^\dagger F_R + (D_\mu \tilde{q}_R)^\dagger (D^\mu \tilde{q}_R) + \overline{q}_R \overline{\sigma}^\mu i D_\mu q_R
$$
$$
+ \sqrt{2} g_s \left(-i(\tilde{q}_R T^{*a} q_R)\lambda^a + i\overline{\lambda}^a (\overline{q}_R T^{*a} \tilde{q}_R^\dagger) \right) - g_s \tilde{q}_R T^{*a} D^a \tilde{q}_R^\dagger, \quad (4.11)
$$

$$
\int \mathrm{d}^4\theta \, \hat{\bar{O}} \mathrm{e}^{2g_s \hat{V}_s^{\mathrm{fund}}} \hat{O} = F_O^\dagger F_O + (D_\mu \sigma^a)^\dagger (D^\mu \sigma^a) + \overline{\chi} \sigma^\mu i D_\mu \chi
$$
$$
- \sqrt{2} g_s \left(-i(\sigma_b^\dagger (-if_{abc})(-i\chi^c))\lambda^a + i\overline{\lambda}^a (i\overline{\chi}_b(+if_{abc})\sigma^{c\dagger}) \right)
$$
$$
- ig_s \sigma^{b\dagger} f^{abc} D^a \sigma^c, \qquad (4.12)
$$

where in the gauge covariant derivative $D_\mu = \partial_\mu + ig_s T^a G_\mu^a$ the generator T^a needs to be replaced by $-T^{*a}$ or $-if^{abc}$ if applied to a field transforming in the antifundamental or adjoint representation respectively.

The soft breaking Lagrangian accounts for the squark, gaugino and scalar gluon masses. These mass terms arise from a hidden sector spurion. For gauginos the D-type spurion is given by $\hat{W}'_\alpha = \theta_\alpha D$ and mediates super symmetry breaking at the mediation scale M: $\int \mathrm{d}\theta^2 \frac{\hat{W}'_\alpha}{M} W_s^\alpha \hat{O}$. After integrating out the spurion one obtains [29, 30]

$$
\mathcal{L}_{\mathrm{soft}} = - \frac{m_{\tilde{q}}^2}{2} (|\tilde{q}_L|^2 + |\tilde{q}_R|^2),
$$
$$
- m_\sigma^2 \, |\sigma^a|^2 - m_g (\lambda\chi - \sqrt{2} D^a \sigma^a + h.c.) \qquad (4.13)
$$

where the complex scalar gluons which are also referred to as sgluons

$$
\sigma = \frac{\phi_0 + i\sigma_0}{\sqrt{2}}, \qquad (4.14)
$$

constitute of two real ones with different masses. The equations of motion for the auxiliary fields are

$$
D^a = - g_s \tilde{q}_L^\dagger T^a \tilde{q}_L + g_s \tilde{q}_R T^{*a} \tilde{q}_R^\dagger + ig_s \sigma^{\dagger b} f^{abc} \sigma^c - \sqrt{2} m_g (\sigma^a + \sigma^{\dagger a}), \qquad (4.15)
$$
$$
F_i = 0 \qquad\qquad \mathrm{for} \qquad\qquad i = L, R, O \qquad (4.16)
$$

where D^a is still real as the purely imaginary parts to not contribute by virtue of the antisymmetry of the structure constants. After eliminating the auxiliary fields the complete Lagrangian reads in 4 spinor notation[13]

$$\begin{aligned}
\mathcal{L}_{\text{RSQCD}} =& |D_\mu \sigma|^2 + |D_\mu \tilde{q}_R|^2 + |D_\mu \tilde{q}_L|^2 + \overline{q} i \not{D} q + \overline{\tilde{g}}^a i \not{D} P_L \tilde{g}^a + \overline{\tilde{g}}^a i \not{D} P_R \tilde{g}^a - \frac{1}{4}(F_a^{\mu\nu})^2 \\
& - \sqrt{2} g_s \left(\overline{\tilde{g}}^a P_R (q^C T^a \tilde{q}_L) + (\tilde{q}_L^\dagger T^a \overline{q}^C) P_L \tilde{g}^a \right) \\
& + \sqrt{2} g_s \left(\overline{\tilde{g}}^a P_R (q T^{*a} \tilde{q}_R^\dagger) + (\tilde{q}_R T^{*a} \overline{q}) P_L \tilde{g}^a \right) \\
& - \sqrt{2} g_s \left(\overline{\tilde{g}}^a P_R (\tilde{g}^b (if^{abc}) \sigma^c) + (\sigma^{\dagger b}(-if^{abc}) \overline{\tilde{g}}^c) P_L \tilde{g}^a \right) \\
& - \frac{m_{\tilde{q}}^2}{2} (|\tilde{q}_L|^2 + |\tilde{q}_R|^2) - m_\sigma^2 |\sigma^a|^2 - m_g \overline{\tilde{g}}^a \tilde{g}^a \\
& - \frac{1}{2} \left(g_s \tilde{q}_L^\dagger T^a \tilde{q}_L - g_s \tilde{q}_R T^{*a} \tilde{q}_R^\dagger - i g_s \sigma^{\dagger b} f^{abc} \sigma^c + \sqrt{2} m_g (\sigma^a + \sigma^{\dagger a}) \right)^2
\end{aligned} \tag{4.17}$$

Observe that there is no 3 sgluon vertex, because of the antisymmetry of the structure constants f^{abc}. As already alluded to there are two distinct sgluons with different masses. The mass of the pseudoscalar σ_0^a is given by the soft breaking parameter $m_{\sigma_0} = m_\sigma$ whereas the mass of the scalar ϕ^0 is given by

$$m_{\phi_0} = \sqrt{m_{\sigma_0}^2 + 4 m_{\tilde{g}}^2}. \tag{4.18}$$

The Feynman rules infered from this Lagrangian are given in Appendix 10.5.

---

[13]How a 4 spinor is composed of Weyl-spinors is given in the Appendix 10.3

5 Squark and Gluino Production at Tree Level

Comment on sgluon production: which channels, calculate cross section for at least one configuration of masses.

In this chapter the production of strongly interacting supersymmetric particles[14] in the MRSSM is considered. The various processes and their associated cross section is compared to their analogues in the MSSM.

5.1 Partonic Processes and their Cross Section

For the following calculation the top quark is excluded from the initial state as it is too heavy to be significantly present in hadrons. For consistency reasons also the stop is excluded from the final states. One therefore deals with $n_f - 1 = 5$ quark flavors. In view of the renormalization to be performed at the 1-loop level the results are given in $D = 4 - 2\epsilon$ dimensions and it has been distinguished between the gauge coupling g_s from the gluon-quark-quark vertex and its supersymmetric analogue $\hat{g}_s$ from the gluino-squark-quark vertex. The usual Mandelstam variables s, t, u and the following modifications of them are used[15]

$$
\begin{aligned}
s &= (k_a + k_b)^2 = (p_1 + p_2)^2 \\
t &= (k_a - p_1)^2 = (k_b - p_2)^2 \\
u &= (k_a - p_2)^2 = (k_a - p_2)^2 \\
t_{\tilde{g}} &= t - m_{\tilde{g}}^2 \qquad\qquad\qquad\qquad t_{\tilde{q}} = t - m_{\tilde{q}}^2 \\
u_{\tilde{g}} &= u - m_{\tilde{g}}^2 \qquad\qquad\qquad\qquad u_{\tilde{q}} = u - m_{\tilde{q}}^2
\end{aligned}
\tag{5.1}
$$

---

[14]The production of sgluons is excluded from the analysis for their mass is chosen to be too large to significantly produce them.

[15]The kinematics of the process is like denoted in fig. 5.1.
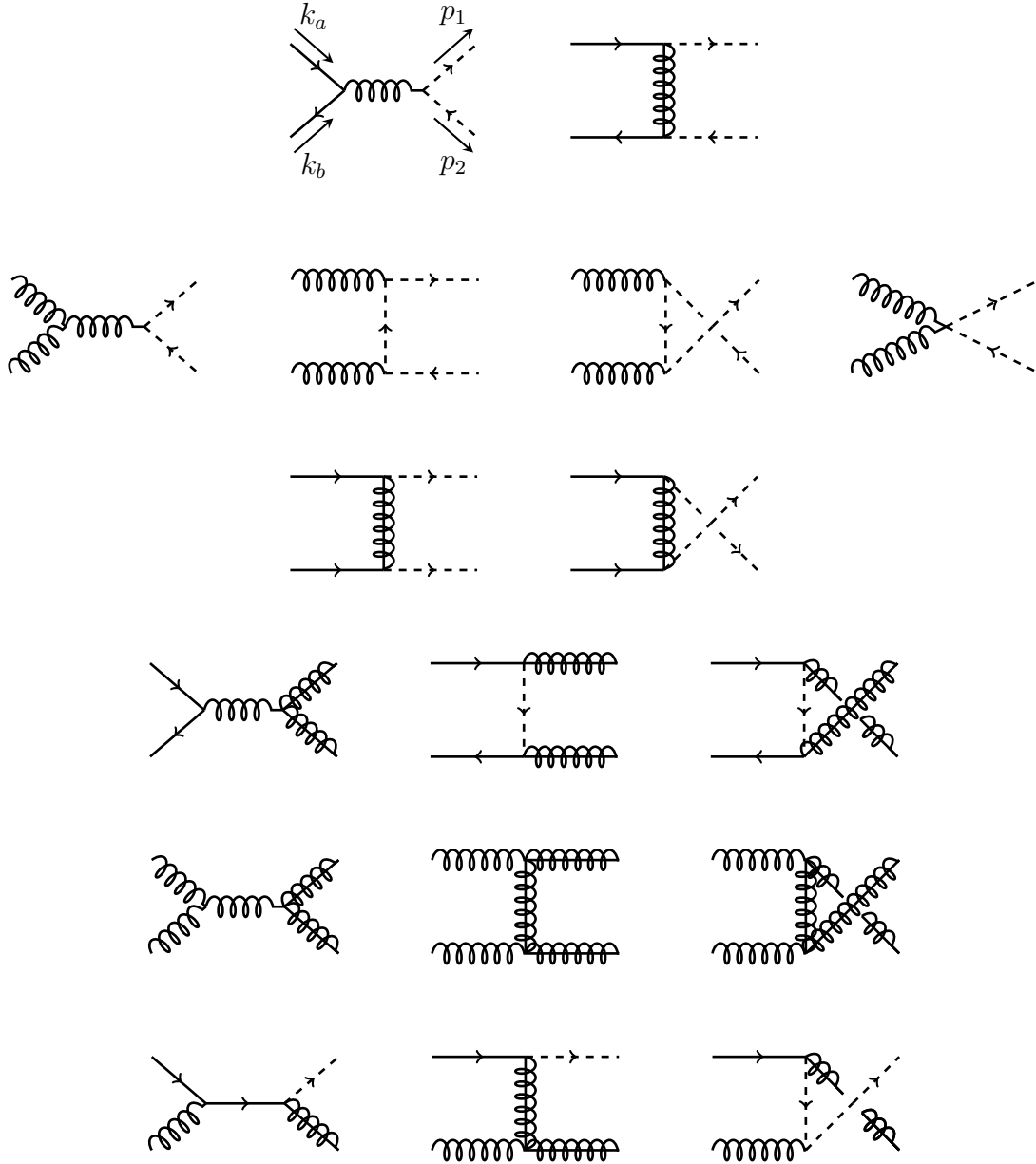
Figure 5.1: Tree level diagrams for squark and gluino production at tree level in the MRSSM. The processes $GG \to \tilde{q}\bar{\tilde{q}}$ and $qG \to \tilde{q}\tilde{g}$ are identical to those in the MSSM. The processes $q\bar{q} \to \tilde{q}\bar{\tilde{q}}$ and $qq \to \tilde{q}\tilde{q}$ involve the production of less chiralities than in the MSSM. Also in the $q\tilde{q} \to \tilde{g}\bar{\tilde{g}}$ channel only half of the t-channel squark chiralities occur in the MRSSM. (Anti-)Gluino production via initial gluons $GG \to \tilde{g}\bar{\tilde{g}}$ proceeds via the same diagrams like in the MSSM but its cross section is twice as much in the MRSSM for gluino and antigluino are distinguishable particles.

Using the Feynman rules in the Appendix 10.5 one obtains the following sums over absolute squared Feynman amplitudes.

$$
\sum |\mathcal{M}^B|^2(q_i\bar{q}_j \to \tilde{q}\tilde{q}^\dagger) = \delta_{ij}\left[8N_cC(F)g_s^4\frac{(n_f-1)}{s^2} + 4N_cC(F)\hat{g}_s^4\frac{1}{t_{\tilde{g}}^2} - 8C(F)g_s^2\hat{g}_s^2\frac{1}{t_{\tilde{g}}s}\right](tu - m_{\tilde{q}}^4)
$$
$$
+ (1-\delta_{ij})4N_cC(F)\hat{g}_s^4\frac{tu - m_{\tilde{q}}^4}{t_{\tilde{g}}^2} \tag{5.2}
$$

$$
\sum |\mathcal{M}^B|^2(GG \to \tilde{q}\tilde{q}^\dagger) = 4(n_f-1)g_s^4\left[2N_c^2C(F)\left(1 - 2\frac{t_{\tilde{q}}u_{\tilde{q}}}{s^2}\right) - 2C(F)\right]
$$
$$
\left[1 - \epsilon - 2\frac{sm_{\tilde{q}}^2}{t_{\tilde{q}}u_{\tilde{q}}}\left(1 - \frac{sm_{\tilde{q}}^2}{t_{\tilde{q}}u_{\tilde{q}}}\right)\right] \tag{5.3}
$$

$$
\sum |\mathcal{M}^B|^2(q_iq_j \to \tilde{q}\tilde{q}) = \delta_{ij}2\hat{g}_s^4N_cC(F)\left[\frac{1}{t_{\tilde{g}}^2} + \frac{1}{u_{\tilde{g}}^2}\right](tu - m_{\tilde{q}}^4)
$$
$$
+ (1-\delta_{ij})4\hat{g}_s^4N_cC(F)\frac{tu - m_{\tilde{q}}^4}{t_{\tilde{g}}^2} \tag{5.4}
$$

$$
\sum |\mathcal{M}^B|^2(q\bar{q} \to \tilde{g}\tilde{g}) = 8N_c^2C(F)g_s^4\left[\frac{2m_{\tilde{g}}^2s + t_{\tilde{g}}^2 + u_{\tilde{g}}^2}{s^2} - \epsilon\right]
$$
$$
+ 4N_c^2C(F)g_s^2\hat{g}_s^2\left[\frac{m_{\tilde{g}}^2s + t_{\tilde{g}}^2}{st_{\tilde{q}}} + \frac{m_{\tilde{g}}^2s + u_{\tilde{g}}^2}{su_{\tilde{q}}} + \epsilon\left(\frac{t_{\tilde{g}}}{t_{\tilde{q}}} + \frac{u_{\tilde{g}}}{u_{\tilde{q}}}\right)\right]
$$
$$
+ 2C(F)(N_c^2-1)\hat{g}_s^4\left(\frac{t_{\tilde{g}}^2}{t_{\tilde{q}}^2} + \frac{u_{\tilde{g}}^2}{u_{\tilde{q}}^2}\right) \tag{5.5}
$$

$$
\sum |\mathcal{M}^B|^2(GG \to \tilde{g}\bar{\tilde{g}}) = 16N_c^3C(F)g_s^4\left(1 - \frac{t_{\tilde{g}}u_{\tilde{g}}}{s^2}\right)
$$
$$
\left[\frac{s^2}{t_{\tilde{g}}u_{\tilde{g}}}(1-\epsilon)^2 - 2(1-\epsilon) + 4\frac{m_{\tilde{g}}^2s}{t_{\tilde{g}}u_{\tilde{g}}}\left(1 - \frac{m_{\tilde{g}}^2s}{t_{\tilde{g}}u_{\tilde{g}}}\right)\right] \tag{5.6}
$$

$$
\sum |\mathcal{M}^B|^2(qg \to \tilde{q}\tilde{g}) = 2g_s^2\hat{g}_s^2\left[2N_c^2C(F)\left(1 - 2\frac{su_{\tilde{q}}}{t_{\tilde{g}}^2}\right) - 2C(F)\right]
$$
$$
\left[(-1+\epsilon)\frac{t_{\tilde{g}}}{s} + \frac{2(m_{\tilde{g}}^2 - m_{\tilde{q}}^2)t_{\tilde{g}}}{su_{\tilde{q}}}\left(1 + \frac{m_{\tilde{q}}^2}{u_{\tilde{q}}} + \frac{m_{\tilde{g}}^2}{t_{\tilde{q}}}\right)\right] \tag{5.7}
$$

Having calculated the absolute squared Feynman amplitudes one obtains the partonic cross sections (see Appendix 10.7) via

$$
\frac{d^2\sigma^B}{dt\,du} = \frac{K_{ab}}{s^2}\frac{\pi S_\epsilon}{\Gamma(1-\epsilon)}\left[\frac{tu - m_1^2m_2^2}{\mu^2s}\right]^{-\epsilon}\Theta(tu - m_1^2m_2^2)
$$
$$
\Theta(s - 4m^2)\delta(s + t + u - m_1^2 - m_2^2)\sum |\mathcal{M}^B|^2 \tag{5.8}
$$

where m_1 (m_2) is the mass of the first (second) final state particle and m is their arithmetic

mean. The leading order cross sections are

$$\sigma^B(q_i\bar{q}_j \to \tilde{q}\tilde{q}^\dagger) = \delta_{ij}\frac{g_s^4}{16\pi s}(n_f - 1)\left[\frac{4}{27} - \frac{16m_{\tilde{q}}^2}{27s}\right]$$
$$+ \delta_{ij}\frac{g_s^2\hat{g}_s^2}{16\pi s}\left[\left(\frac{4}{27} + \frac{8m_-^2}{27s}\right)\beta_{\tilde{q}} + \left(\frac{8m_{\tilde{g}}^2}{27s} + \frac{8m_-^4}{27s^2}\right)L_1\right]$$
$$+ \frac{\hat{g}_s^4}{16\pi s}\left[-\frac{8}{9}\beta_{\tilde{q}} + \left(-\frac{4}{9} - \frac{8m_-^2}{9s}\right)L_1\right] \tag{5.9}$$

$$\sigma^B(GG \to \tilde{q}\tilde{q}^\dagger) = \frac{(n_f - 1)g_s^4}{16\pi s}\left[\left(\frac{5}{24} + \frac{31m_{\tilde{q}}^2}{12s}\right)\beta_{\tilde{q}} + \left(\frac{4m_{\tilde{q}}^2}{3s} + \frac{m_{\tilde{q}}^4}{3s^2}\right)\ln\frac{1-\beta_{\tilde{q}}}{1+\beta_{\tilde{q}}}\right] \tag{5.10}$$

$$\sigma^B(q_i q_j \to \tilde{q}\tilde{q}) = \frac{\hat{g}_s^4}{16\pi s}\left[-\frac{8}{9}\beta_{\tilde{q}} + \left(-\frac{4}{9} - \frac{8m_-^2}{9s}\right)L_1\right] \tag{5.11}$$

$$\sigma^B(q\bar{q} \to \tilde{g}\bar{\tilde{g}}) = \frac{g_s^4}{16\pi s}\left[\frac{16}{9} + \frac{32m_{\tilde{g}}^2}{9s}\right]\beta_{\tilde{g}}$$
$$+ \frac{\hat{g}_s^2 g_s^2}{16\pi s}\left[\left(-\frac{4}{3} - \frac{8m_-^2}{3s}\right)\beta_{\tilde{g}} + \left(\frac{8m_{\tilde{g}}^2}{3s} + \frac{8m_-^4}{3s^2}\right)L_2\right]$$
$$+ \frac{\hat{g}_s^4}{16\pi s}\left[\left(\frac{32}{27} + \frac{32m_-^4}{27(m_-^4 + m_{\tilde{q}}^2 s)}\right)\beta_{\tilde{g}} - \frac{64m_-^2}{27s}L_2\right] \tag{5.12}$$

$$\sigma^B(GG \to \tilde{g}\bar{\tilde{g}}) = \frac{g_s^4}{16\pi s}\left[\left(-6 - \frac{51m_{\tilde{g}}^2}{2s}\right)\beta_{\tilde{g}} + \left(-\frac{9}{2} - \frac{18m_{\tilde{g}}^2}{s} + \frac{18m_{\tilde{g}}^4}{s^2}\right)\ln\frac{1-\beta_{\tilde{g}}}{1+\beta_{\tilde{g}}}\right] \tag{5.13}$$

$$\sigma^B(qG \to \tilde{q}\tilde{g}) = \frac{g_s^2\hat{g}_s^2}{16\pi s}\left[\frac{\kappa}{s}\left(-\frac{7}{9} - \frac{32m_-^2}{9s}\right) + \left(-\frac{8m_-^2}{9s} + \frac{2m_{\tilde{q}}^2 m_-^2}{s^2} + \frac{8m_-^4}{9s^2}\right)L_3\right.$$
$$\left. + \left(-1 - \frac{2m_-^2}{s} + \frac{2m_{\tilde{q}}^2 m_-^2}{s^2}\right)L_4\right] \tag{5.14}$$

where the abbreviations [31]

$$\beta_{\tilde{q}} = \sqrt{1 - \frac{4m_{\tilde{q}}^2}{s}} \qquad\qquad \beta_{\tilde{g}} = \sqrt{1 - \frac{4m_{\tilde{g}}^2}{s}}$$
$$m_-^2 = m_{\tilde{g}}^2 - m_{\tilde{q}}^2 \qquad\qquad \kappa = \sqrt{(s - m_{\tilde{g}}^2 - m_{\tilde{q}}^2)^2 - 4m_{\tilde{g}}^2 m_{\tilde{q}}^2}$$
$$L_1 = \ln\frac{s + 2m_-^2 - s\beta_{\tilde{q}}}{s + 2m_-^2 + s\beta_{\tilde{q}}} \qquad\qquad L_2 = \ln\frac{s - 2m_-^2 - s\beta_{\tilde{g}}}{s - 2m_-^2 + s\beta_{\tilde{g}}}$$
$$L_3 = \ln\frac{s - m_-^2 - \kappa}{s - m_-^2 + \kappa} \qquad\qquad L_4 = \ln\frac{s + m_-^2 - \kappa}{s + m_-^2 + \kappa} \tag{5.15}$$

are used. In the following the considered processes of the MRSSM are compared to those of the MSSM.

The process $q_i \bar{q}_j \to \tilde{q}\tilde{q}^{\dagger}$

The production of a squark and an antisquark through a quark and an antiquark in the initial state originates from two types of Feynman diagrams. The first one has an s-channel gluon and is the same in the MSSM and in the MRSSM. The second one exhibits a difference due to the t-channel gluino which is no Majorana particle in the MRSSM. To see this one can either

Figure 5.2: Tree level diagrams for $q\bar{q} \to \tilde{q}\tilde{q}^{\dagger}$

just apply the Feynman rules in Appendix 10.5 or think of the conservation of R-charge: Left handed squarks have R-charge +1 and right handed squarks have R-charge -1. Antiparticles have the opposite R-charge of their corresponding particles. The final state particles have to meet the total R-charge zero from the initial state. Because of this one only has $\tilde{q}_L \bar{\tilde{q}}_L$ and $\tilde{q}_R \bar{\tilde{q}}_R$ as the final states in the MRSSM whereas in the MSSM one actually has four instead of two t-channel diagrams: The corresponding final states are $\tilde{q}_L \bar{\tilde{q}}_L$, $\tilde{q}_R \bar{\tilde{q}}_R$, $\tilde{q}_L \bar{\tilde{q}}_R$ and $\bar{\tilde{q}}_R \tilde{q}_L$. Consequently contributions from the t-channel diagrams are suppressed in the MRSSM in comparison to the MSSM. As visible in fig. 5.5 this suppression grows with the masses. The reason for this lies in the gluino mass dependence of the t-channel diagrams which is explained in the discussion of squark production.

If the initial state quarks are of different flavor the s-channel diagram is absent.

The process $GG \to \tilde{q}\tilde{q}^{\dagger}$

This process has the same cross section as in the MSSM for also in the MSSM only like chirality squark and antisquark $\tilde{q}_A \tilde{q}_A^{\dagger}$ with $A \in L, R$ can be produced.

The process $q_i q_j \to \tilde{q}\tilde{q}$

In the MRSSM only the production of unlike chirality squarks $\tilde{q}_L \tilde{q}_R$ is allowed whilst in the MSSM also like chirality squarks can be produced. This is again a consequence of the conservation of R-charge. The upshot of this is a suppression of squark production in the MRSSM in comparison to the MSSM. To be more explicit the suppression of squark production in the MRSSM grows with the gluino mass. This can be understood as follows: As in the MRSSM a left handed squark needs to be produced with a right handed squark one can read off from the Feynman rules given in Appendix 10.5 that the gluino propagator $i\frac{\not{p}+m_{\tilde{g}}}{p^2-m_{\tilde{g}}^2}$ is sandwiched between the projectors P_L and P_R which leads to the cancellation of the gluino mass in the numerator. Therefore for small momenta of the gluino compared to the gluino mass one gets $\mathcal{M} \sim \frac{1}{m_{\tilde{g}}^2}$ in the MRSSM while in the MSSM one finds a suppression proportional to $\frac{1}{m_{\tilde{g}}}$.

When considering squark production one has to sum over all $|\mathcal{M}|^2$ with different helicity. The diagrams for those different final state helicities are shown for flavor like squark production in tab. 5.1 and for flavor unlike squark production in tab. 5.2 for the MSSM and the MRSSM. To avoid double counting one needs to weight $|\mathcal{M}|^2(qq \to \tilde{q}_L\tilde{q}_L)$ and $|\mathcal{M}|^2(qq \to \tilde{q}_R\tilde{q}_R)$ with a statistical factor of $\frac{1}{2}$ as one integrates over all momenta of both particles to arrive at the cross section.

MSSM		MRSSM	
$u \to \tilde{u}_L^\dagger$ / $u \to \tilde{u}_R^\dagger$	$u \to \tilde{u}_L^\dagger$ / $u \to \tilde{u}_R^\dagger$	$u \to \tilde{u}_L^\dagger$ / $u \to \tilde{u}_R^\dagger$	$u \to \tilde{u}_L^\dagger$ / $u \to \tilde{u}_R^\dagger$
$u \to \tilde{u}_L^\dagger$ / $u \to \tilde{u}_L^\dagger$	$u \to \tilde{u}_L^\dagger$ / $u \to \tilde{u}_L^\dagger$		
$u \to \tilde{u}_R^\dagger$ / $u \to \tilde{u}_R^\dagger$	$u \to \tilde{u}_R^\dagger$ / $u \to \tilde{u}_R^\dagger$		

Table 5.1: All Feynman diagrams contributing to flavor like squark production in the MSSM and the MRSSM for the example of u-quarks. For the MSSM the absolute squared Feynman amplitudes from the diagrams with chirality like squarks need to be weighted with a factor of $\frac{1}{2}$.

MSSM		MRSSM	
$u \to \tilde{u}_L^\dagger$ / $d \to \tilde{d}_R^\dagger$	$u \to \tilde{u}_R^\dagger$ / $d \to \tilde{d}_L^\dagger$	$u \to \tilde{u}_L^\dagger$ / $d \to \tilde{d}_R^\dagger$	$u \to \tilde{u}_R^\dagger$ / $d \to \tilde{d}_L^\dagger$
$u \to \tilde{u}_L^\dagger$ / $d \to \tilde{d}_L^\dagger$			
$u \to \tilde{u}_R^\dagger$ / $d \to \tilde{d}_R^\dagger$			

Table 5.2: All Feynman diagrams contributing to flavor unlike squark production in the MSSM and the MRSSM for the example of u- and d-quarks.

Because of the absence of chirality like squarks in the final state in the MRSSM (and a missing interference of the two diagrams in tab. 5.1 in the column of the MRSSM) the partonic cross section of flavor like and unlike squarks is the same in the MRSSM, i.e. on the partonic level:

$$\sigma^{\mathrm{B}}_{\mathrm{Part,\ MRSSM}}(uu \to \tilde{u}_L\tilde{u}_R) = \sigma^{\mathrm{B}}_{\mathrm{Part,\ MRSSM}}(ud \to \tilde{u}_L\tilde{d}_R) + \sigma^{\mathrm{B}}_{\mathrm{Part,\ MRSSM}}(ud \to \tilde{u}_R\tilde{d}_L). \quad (5.16)$$

That is however not true in the MSSM because for flavor like squarks there is a non vanishing interference of the t- and u-channel diagram of the processes $qq \to \tilde{q}_L\tilde{q}_L$ and $qq \to \tilde{q}_R\tilde{q}_R$. This

term is given in [31, p.7]

The process $q\bar{q} \to \tilde{g}\bar{\tilde{g}}$

In contrast to the MSSM no statistical factor of $\frac{1}{2}$ is taken into account when turning from $|\mathcal{M}|^2$ to σ. This is because gluino and antigluino are distinguishable particles. Still in comparison to the MSSM cross section [31, p.9] only the first line in 5.12 is doubled up as the other two lines originate from an t or u channel squark which occurs in only one instead of two chiralities. Furthermore an interference term from the t and u channel diagram which occurs in the MSSM is absent in the MRSSM.

The process $GG \to \tilde{g}\bar{\tilde{g}}$

As in the previous process the MRSSM cross section for $GG \to \tilde{g}\bar{\tilde{g}}$ receives no statistical factor of $\frac{1}{2}$ like in the MSSM. As there are no further differences between MSSM and MRSSM in this channel, the MRSSM cross section is simply twice as large as in the MSSM.

The process $qG \to \tilde{q}\tilde{g}$

This process is exactly the same in the MSSM and MRSSM for the are two differences between the models which exactly cancel each other: Firstly in the MRSSM there is not only the production of a squark and a gluino but also the production of a squark and an antigluino. But on the other hand R-charge needs to be conserved which dictates that a "left-handed" squark can only be produced with an antigluino and a "right-handed" squark can only be produced with a gluino (see table 4.2).

In order to account for the confinement of quarks and gluons within hadrons the hadronic cross sections for the considered processes are calculated in the next subsection.

5.2 Hadronic Cross Section

Quarks, antiquarks and gluons are no free particles but are confined within hadrons. As hadrons consist of a variety of the just mentioned partons which share the hadron's momentum one does not have a definite initial state in hadron collisions which is assumed in the previous subsection. Fortunately the hadronic cross section for the production of a final state X, e.g. $X = \tilde{q}\tilde{q}$, can be obtained by convolving the partonic cross section with parton density functions of the initial hadrons.

$$\sigma_{\text{Had}}^{\text{B}}(P_1 P_2 \to X) = \int \mathrm{d}x_1 \mathrm{d}x_2 \, f_{P_1/H_1}(x_1) f_{P_2/H_2}(x_2) \, \sigma_{\text{Part}}^{\text{B}}(P_1 P_2 \to X, s = x_1 x_2 S). \quad (5.17)$$

The parton density functions $f_{P_i/H_j}(x)$ and the momentum fractions x_i are explained below. The hadrons center-of-mass energy is denoted with $\sqrt{S}$ where $\sqrt{s}$ denotes the partons center-of-mass energy.

As the production of the final state X may proceed via various initial partons one has to sum over all possible possibilities arising from the initial hadrons H_1 and H_2:

$$\sigma^B_{\mathrm{Had}}(H_1 H_2 \to X) = \sum_{i,j} \sigma^B_{\mathrm{Had}}(P_i P_j \to X) \tag{5.18}$$

where the sum runs over all partons P_i (P_j) which are in the hadron H_1 (H_2).

To get an intuitive idea of this factorization regard the hadrons as extended objects consisting of partons[16] which are permanently interacting which each other. Now consider two colliding hadrons in their center-of-mass frame. Due to Lorentz contraction the hadrons appear as thin discs and the parton's mutual interactions are time-delayed within this frame. This effectively means that a hadron at the time of collision is virtually frozen.

maybe picture of colliding disks

This in turn implies that the hadron consists at the time of collision of a definite number of partons which can be thought of as carrying a definite fraction of the hadron's momentum $p_{\mathrm{Part}} = x p_{\mathrm{Had}}$ with $x \in (0,1)$. The parton density function $f_{P/H}(x)$ can therefore be understood as the probability of finding a parton P within the hadron H carrying x of its momentum.

They actually depend on an arbitrary energy scale referred to as the factorization scale μ_F. The μ_F evolution is given within the scope of preturbation theory by coupled integro-differential equations named after Gribov, Lipatov, Dokshitzer, Altarelli and Parisi: the DGLAP-equations. For further reading on parton density functions and factorization see [33] and [34]. See [35] for how to determine parton density functions.

Fig. 5.3 shows a parton density function set for the proton. One can see that the partons most probable to carry a high fraction of momentum are the valence quarks. For lower values of x gluons constitute the major component of the proton.

Fig.5.5 shows the hadronic cross section for the production of various squarks in the MRSSM. These can only be produced by their non supersymmetric partner, e.g. two up-squarks can only be produced by two up-quarks. Because the partonic cross section for these processes are the same, cf. eq. 5.16, one can see the influence of the parton density functions quite nicely: The up-squark production is the dominant contribution to squark production. Apart from the solid lines in fig.5.5 which correspond to the production of first generation squarks, also the cross section of mixed first and second generation (dashed lines) and second generation (dotted lines) squarks is shown. The dashed dotted line shows the cross section of the charged conjugated particles of the dominant channel.

---

[16]The proton is considered as composed of three valence quarks: Two up-quarks and one down-quark. In addition there are gluons and seaquarks, i.e. virtual quark-antiquark pairs.
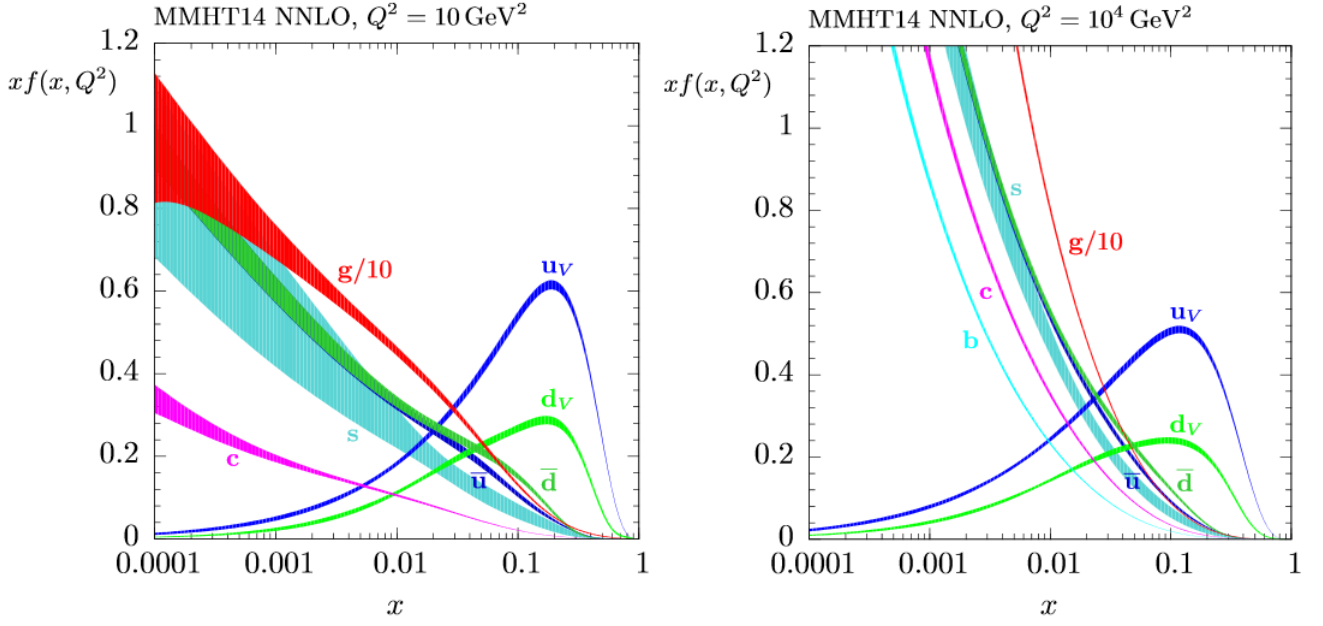
Figure 5.3: Parton density function of the proton, taken from `MMHT2014` [32] with 68% confidence level. The parton density function is multiplied by x in order to counteract its peak at $x \to 0$. The parton density function is given at two different factorisaction scales $\mu_F = Q$
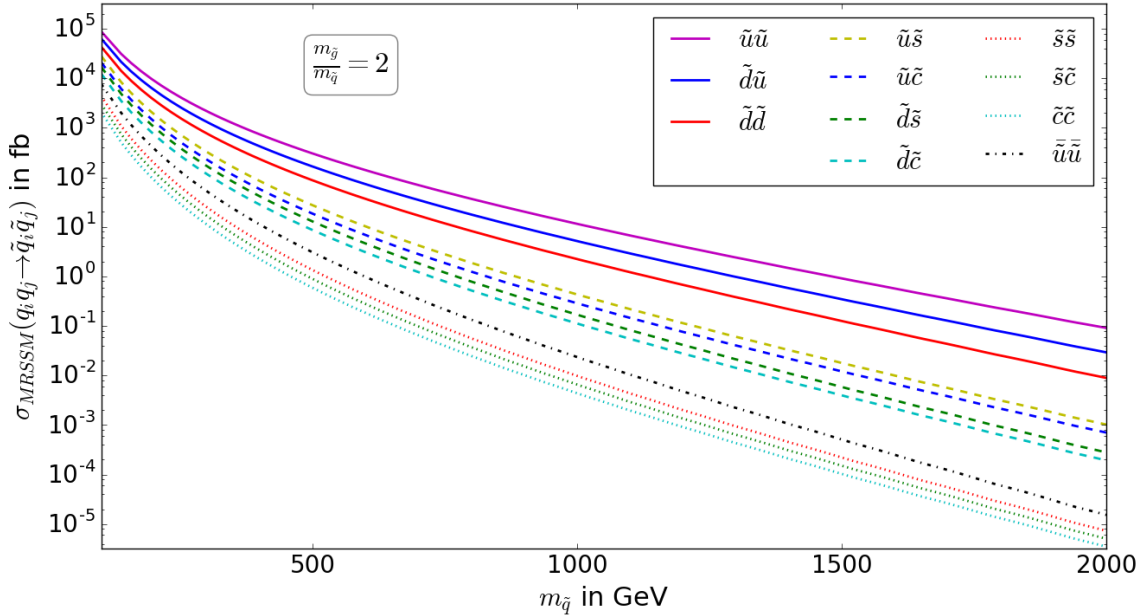
Figure 5.4: Hadronic cross section for squark production in the MRSSM at the LHC at $\sqrt{S} = 13\,\text{GeV}$. The ratio of the gluino and squark mass is fixed to 2. The parton densities used are `MMHT2014` LO with $\alpha_s(M_Z) = 0.135$ in the 5-flavor scheme [32]. As renormalization and factorization scale $\mu_R = \mu_F = \frac{m_1 + m_2}{2}$ has been chosen, where m_i are the final state particle masses.

REFER TO Kribs, Martin: SNOWMASS WHITEPAPER
REFER TO Vernoica Sanz: How many SUpersymmetries?

The following paragraph discusses fig. 5.5, 5.6 and 5.7, i.e. the hadronic cross section of all considered processes for three successive mass ratios of the gluino and squark: $\frac{m_{\tilde{g}}}{m_{\tilde{q}}} = 0.9$, 2 and 5. Also the corresponding fraction of final states is shown.

For the small mass ratio $\frac{m_{\tilde{g}}}{m_{\tilde{q}}} = 0.9$ and small squark masses the dominant contribution comes from gluino (antigluino) production. This is even more dominant in the MRSSM which can be explained by the above mentioned factor of 2 difference in the $GG \to \tilde{g}\tilde{g}(\overline{\tilde{g}})$ channel which comes from the distinguishable gluino and antigluino in the MRSSM. Furthermore there is the above mentioned destructive interference term in the $q\bar{q} \to \tilde{g}\tilde{g}(\overline{\tilde{g}})$ channel which makes the cross section in the MRSSM dominant over the one in the MSSM.

For a growing squark mass the previously subdominant gluino-squark production takes over and becomes dominant. A salient difference between the MSSM and the MRSSM is that squark production is strongly suppressed in the MRSSM. While in the MSSM it becomes dominant above about 1700 GeV it is subsubdominant for the whole displayed squark mass in the MRSSM. This suppression has also already been explained above.

Turning from $\frac{m_{\tilde{g}}}{m_{\tilde{q}}} = 0.9$ to $\frac{m_{\tilde{g}}}{m_{\tilde{q}}} = 2$ suppresses quite strongly the production of gluinos in all pertaining channels. For the MSSM one finds above 500 GeV a growing dominance of squark production. The same happens in the MRSSM but for a significantly higher squark mass of about 1300 GeV. This suppression of squark production in the MRSSM increases with a growing gluino masses which can be seen when going from $\frac{m_{\tilde{g}}}{m_{\tilde{q}}} = 0.9$ to $\frac{m_{\tilde{g}}}{m_{\tilde{q}}} = 2$ or even $\frac{m_{\tilde{g}}}{m_{\tilde{q}}} = 5$ in fig. 5.7. This reflects the gluino mass dependence explained in detail in section 5.1. See also 5.9 for a visualization of this behavior.

Note also that for sufficiently large squark masses squark production becomes the dominant process, see fig. 5.5 and 5.6. This is because the production of heavy particles requires large longitudinal momenta of the colliding partons, i.e. large x. Looking at the parton density functions in fig. 5.3 one sees that within the proton the partons most likely to carry large momentum are quarks. So looking at large x the proton basically consists of quarks and because the only process involving only quarks in the initial state is squark production, this channel dominates for high masses.

The total cross section in the MRSSM is increasingly smaller than in the MSSM in particular from about 500 GeV onwards. The is because for masses below that the $GG \to \tilde{q}\tilde{q}^{\dagger}$ channel which is the same for both models is the dominant one.

When raising the gluino squark mass ratio further to $\frac{m_{\tilde{g}}}{m_{\tilde{q}}} = 5$ the above described tendency continues. This is all processes including a gluino get even more negligible and squark production gets further suppressed. While in the MSSM it becomes dominant over $GG \to \tilde{q}\tilde{q}^{\dagger}$ at
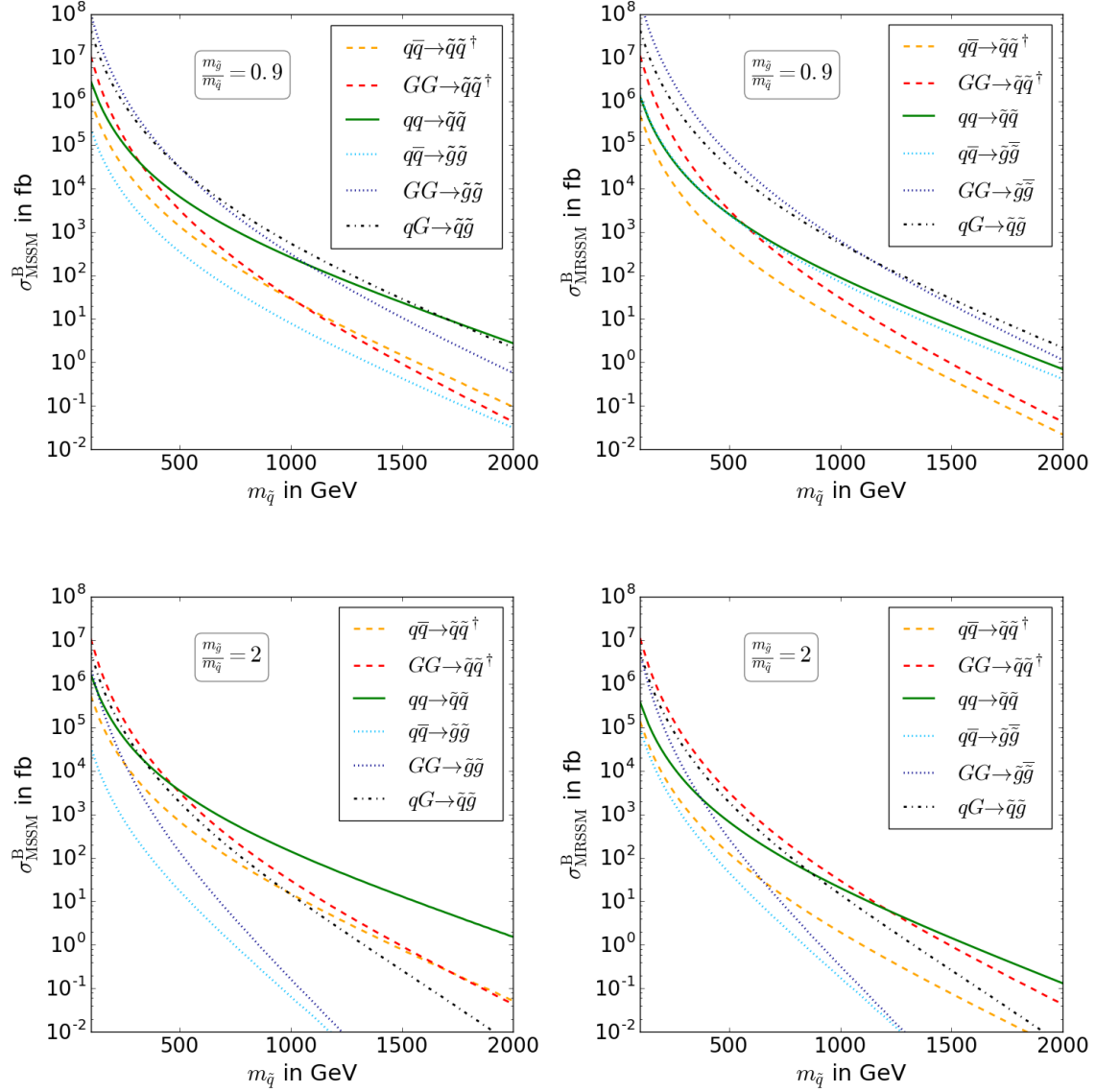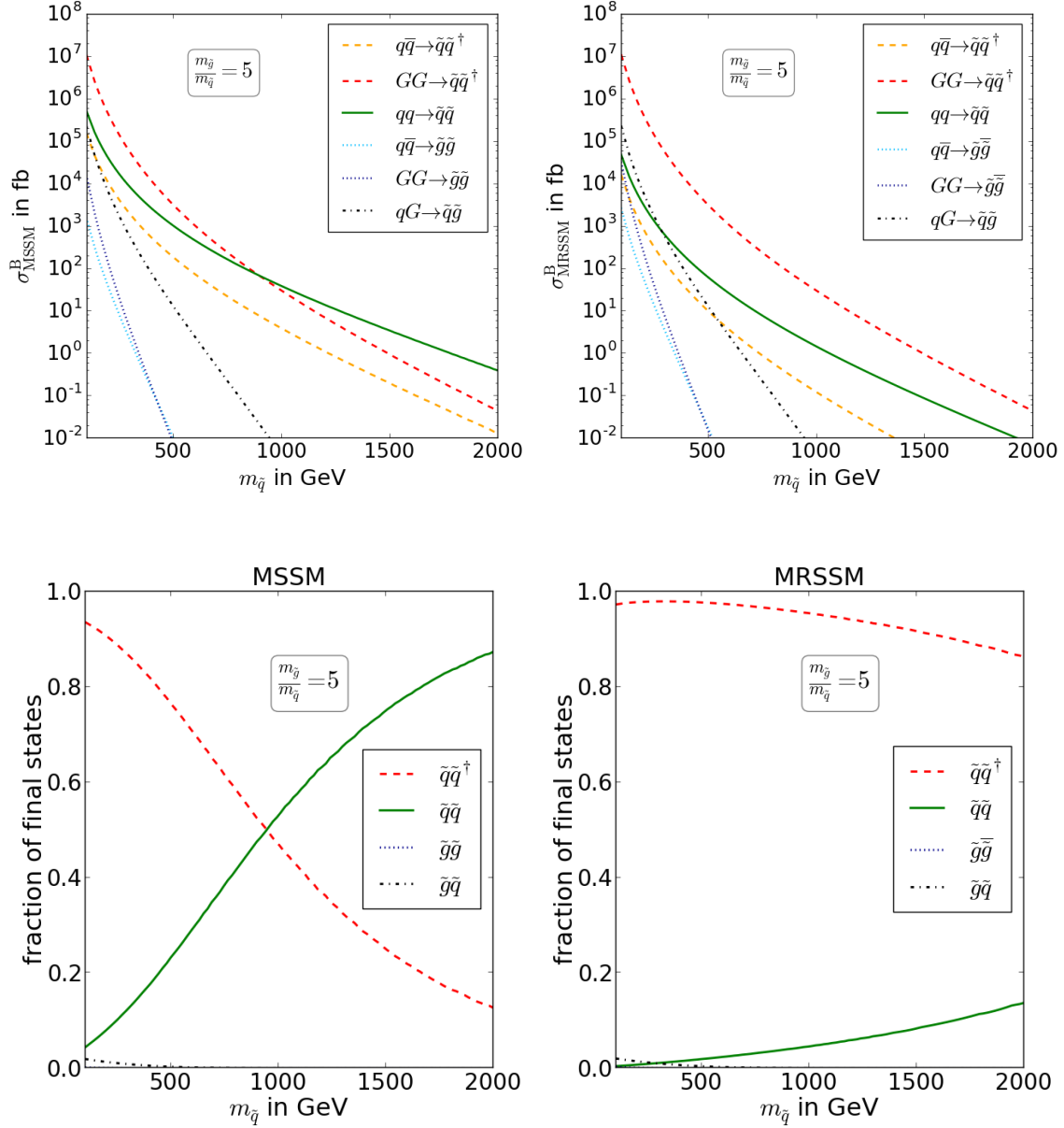
Figure 5.5: Hadronic cross section for squark and gluino production in the MSSM (left-hand side) and MRSSM (right-hand side) at the LHC with $\sqrt{S} = 13\,\text{GeV}$. The ratio of gluino and squark mass is fixed to 0.9 (first row) and 2 (second row). In the final state it has been summed over all squark flavors expect for t-squarks. For the channels $qq \to \tilde{q}\tilde{q}$ and $qG \to \tilde{q}\tilde{G}$ also the charge conjugated process is included. The parton densities used are MMHT2014 LO with $\alpha_s(M_Z) = 0.135$ in the 5-flavor scheme [32]. As renormalization and factorization scale $\mu_R = \mu_F = \frac{m_1 + m_2}{2}$ has been chosen, where m_i are the final state particle masses.
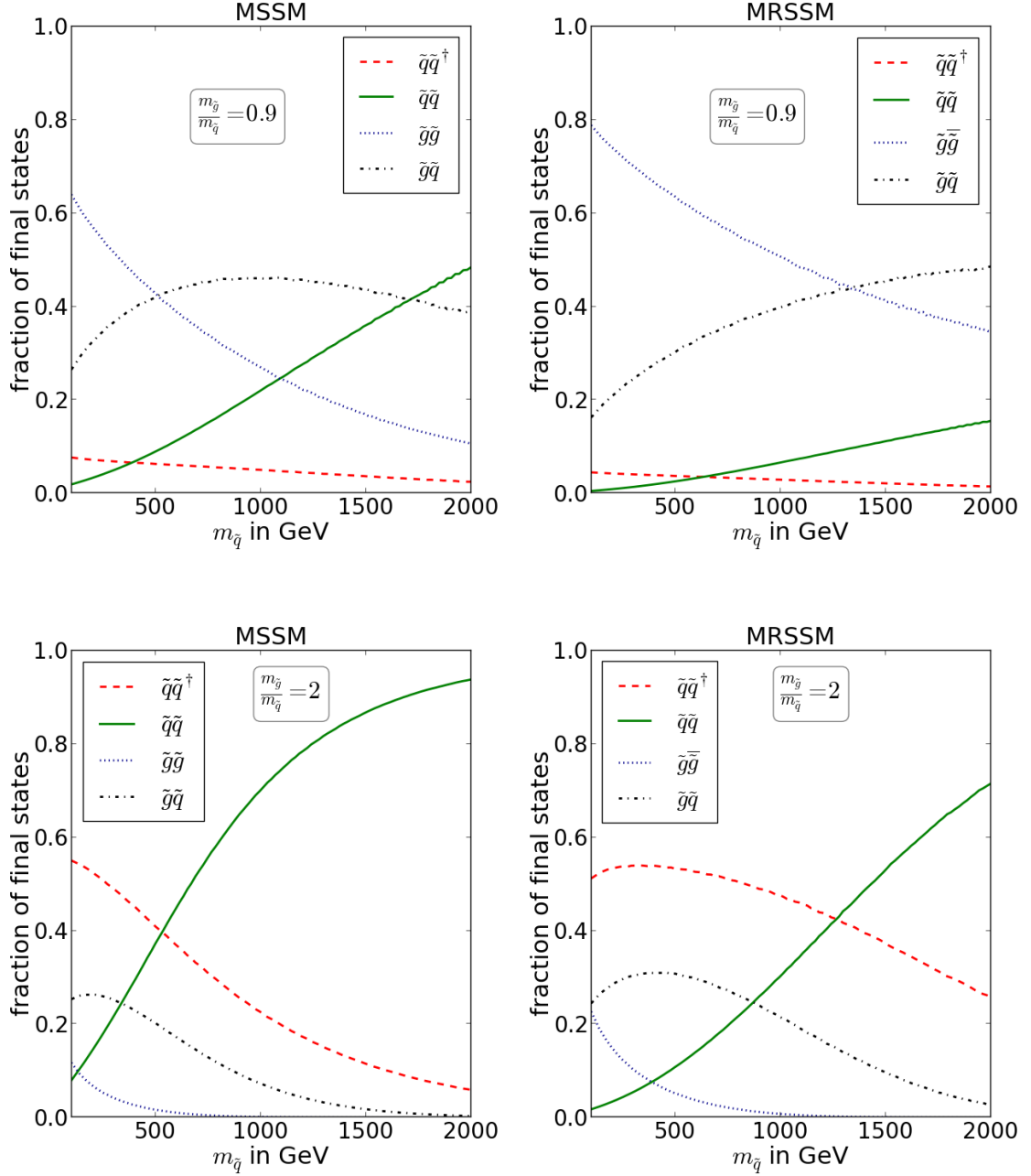
Figure 5.6: Relative contributions of the indicated final states on the total hadronic cross section in the MSSM (left-hand side) and MRSSM (right-hand side) at the LHC with $\sqrt{S} = 13\,\text{GeV}$. The ratio of gluino and squark mass is fixed to 0.9 (first row) and 2 (second row). In the final state it has been summed over all squark flavors expect for t-quarks. For the channels $qq \to \tilde{q}\tilde{q}$ and $qG \to \tilde{q}\tilde{G}$ also the charge conjugated process is included. The parton densities and the renormalization and factorization scale are chosen as in fig. 5.5.

$m_{\tilde{q}} \approx 1000\,\mathrm{GeV}$ it is subdominant in the MRSSM in the whole displayed mass range. even though it does not fall that steeply as the dominant channel.

Figure 5.7: Hadronic cross section for squark and gluino production (in the first row) and relative contributions of the indicated final states on the total hadronic cross section (in the second row) in the MSSM (left-hand side) and MRSSM (right-hand side) at the LHC which $\sqrt{S} = 13\,\mathrm{GeV}$. The ratio of gluino and squark mass is fixed to 5. In the final state it has been summed over all squark flavors expect for staus. For the channels $qq \rightarrow \tilde{q}\tilde{q}$ and $qG \rightarrow \tilde{q}\tilde{G}$ also the charge conjugated process is included. The parton densities and the renormalization and factorization scale are chosen as in fig. 5.5.

The contour plots 5.8 underline the already announced difference between squark production

in the MRSSM and the MSSM. The main difference is a suppression of the cross section for higher gluino masses in the MRSSM. Fig.5.9 shows the Born cross section of squark production including all possible flavors for a fixed mass of the gluino $m_{\tilde{g}} = 2000\,\mathrm{GeV}$ (top) and the squark $m_{\tilde{q}} = 1000\,\mathrm{GeV}$ (bottom). The figure includes errors of the calculation which come from the parton density functions and the renormalization and factorization scale.

The 68% uncertainty from the central value pdf-set is obtained by performing the calculation with all eigenvector sets of the central value and taking the minimum and maximum at each point as deviations from the calculation with the central set.

The error from the renormalization scale μ_R and the factorization scale μ_F is obtained by varying both parameters with a factor of $\frac{1}{2}$ and two. For each parameter combination the cross section has been calculated. Out of these nine numbers for each point the minimum and maximum has been chosen to estimate the error originating from the scale.

The total error is then obtained by Gauß's propagation of uncertainties:

$$\Delta\sigma = \sqrt{(\Delta\sigma_{\mathrm{pdf}})^2 + (\Delta\sigma_{\mathrm{scale}})^2}. \tag{5.19}$$

The uncertainty coming from the scale variation has been found much greater than the one from the parton density functions. The error from the phase space integration is negligible, i.e. $\Delta\sigma_{\mathrm{int}} < 1\%_0$.

As a summary of the comparison between MSSM and MRSSM gluino production one can say, that the gluino production is enhanced in the MRSSM due to distinguishable gluino and antigluino. In order to meet missing experimental evidence for supersymmerty this suggests that gluinos might be heavier than squarks in the MRSSM. Focusing on $\frac{m_{\tilde{g}}}{m_{\tilde{q}}} \geq 2$ the most significant change between the considered models is the growing suppression of squark production for a increasing gluino mass. This is why this channel is going to be investigated at next-to-leading order within this thesis. The ensuing sections provide the prerequisites for this calculation.

$m_{\tilde{g}} \setminus m_{\tilde{q}}$	500	1000	1500
1000			
1500			
2000			

Table 5.3: Table
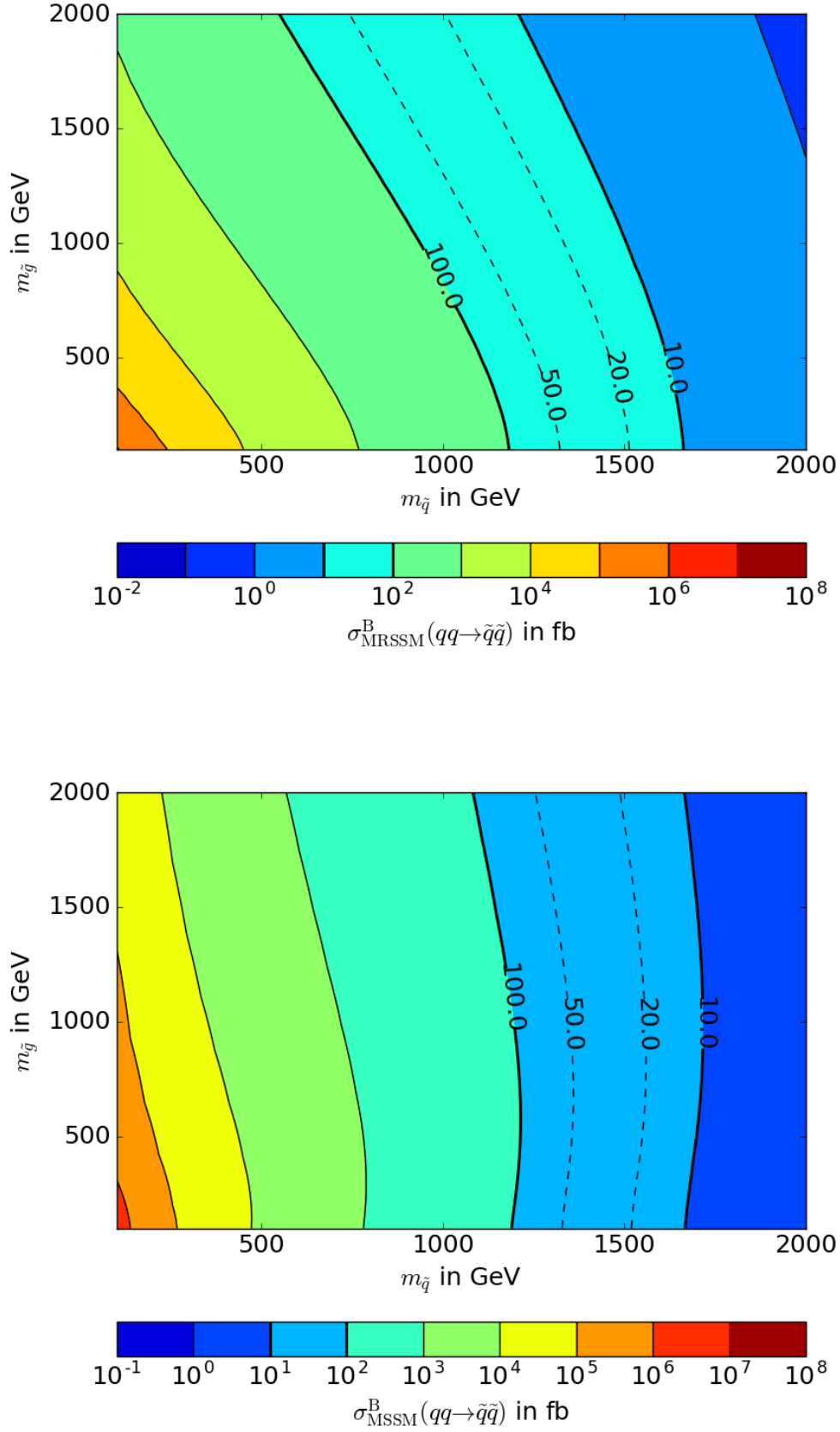
Figure 5.8: Contour plot for squark production cross section including all possible flavors (also charged) in the MRSSM (top) and MSSM (bottom)
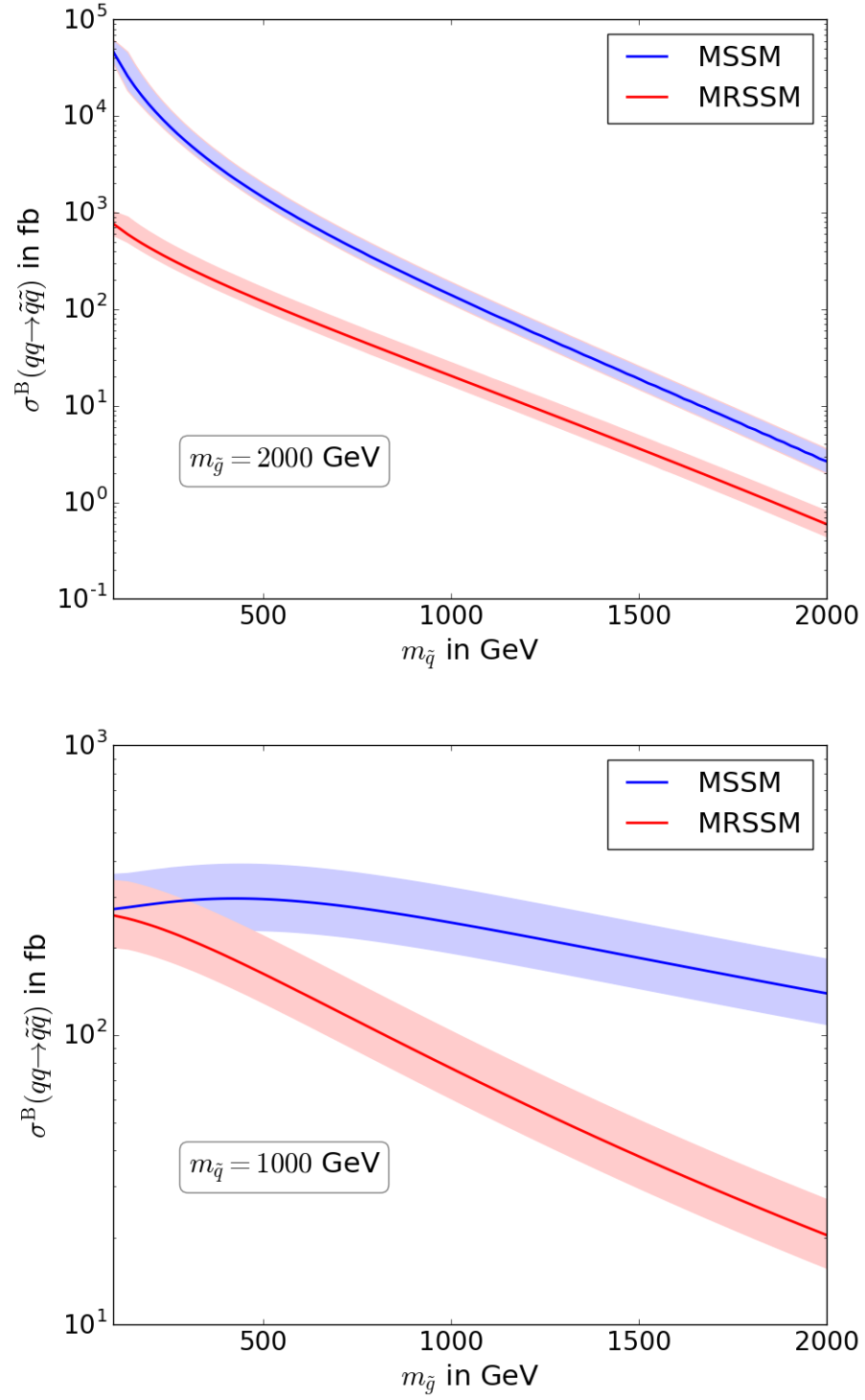
Figure 5.9: add error bars

6 Virtual and Real Corrections

The results calculated in the previous chapter are not the full theoretical predictions for the different processes but only the first term in a perturbation theory of α_s.

This section describes the necessary steps in the calculation of the squark production cross section at next-to-leading-order, i.e. its $\mathcal{O}(\alpha_s)$-correction.

Reason validity of perturbation theory in this context.

6.1 Virtual Correction

According to quantum field theory the $\mathcal{O}(\alpha_s)$ correction to a tree level process includes the computation of one-loop diagrams such as shown in fig. 6.1. To yield $\mathcal{O}(\alpha_s)$ corrections in the cross section the interference term between the one-loop amplitude $\mathcal{M}^{1L}$ and the Born amplitude $\mathcal{M}^{B}$ needs to be considered. However the virtual amplitude

$$\mathcal{M}^{V} = \mathcal{M}^{B}\mathcal{M}^{1L*} + \mathcal{M}^{1L}\mathcal{M}^{B*} = 2\Re\left(\mathcal{M}^{B}\mathcal{M}^{1L*}\right) \tag{6.1}$$

contains divergences. These come from integrals over undetermined momentum and energy of particles running in loops. Due to their origin these divergences are referred to as ultraviolet
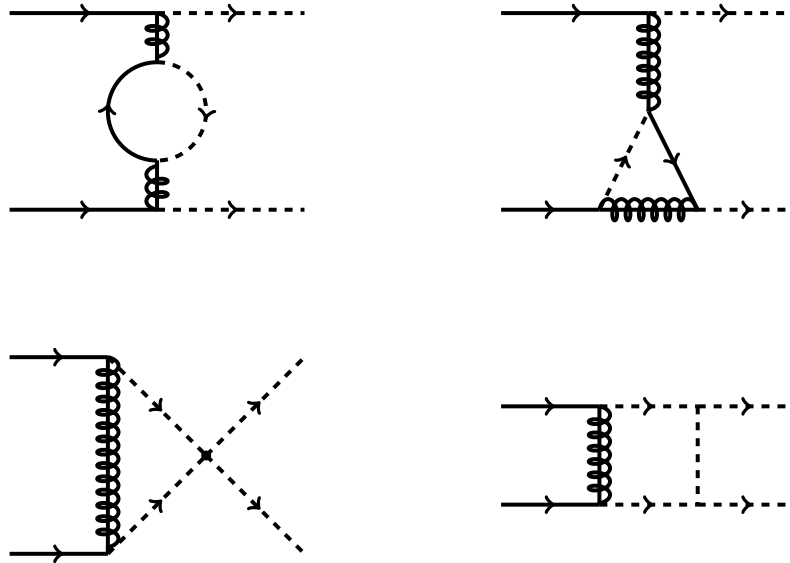
Figure 6.1: A selection of diagrams contributing to the 1-loop matrix element for squark production. Each diagram is a representative of a certain diagram type. In the first line an example for a self-energy and a vertex-correction diagram is shown. The second line lists typical box-diagrams: a three-point box and a four-point box.

(UV) and infrared divergences (IR). Ultraviolet divergences occur when loop momenta and energy tend to infinity which corresponds to arbitrary short distance interactions. However, these divergences are cured by first regularizing them and then introducing appropriate coun-

terterms[17] in the Lagrangian to cancel the extracted singularities. The second step is called renormalization and can be understood as a redefinition or rescaling of parameters and fields in the Lagrangian in the first place:

$$\phi^0/\sigma^0 \to \sqrt{Z_{\phi^0/\sigma^0}}\phi^0/\sigma^0 \qquad\qquad \tilde{q}_{L/R} \to \sqrt{Z_{\tilde{q}_{L/R}}}\tilde{q}_{L/R}$$

$$P_L\tilde{g} \to \sqrt{Z_{\tilde{g}}^L}P_L\tilde{g} \qquad\qquad P_R\tilde{g} \to \sqrt{Z_{\tilde{g}}^R}P_R\tilde{g}$$

$$q \to \sqrt{Z_q}q \qquad\qquad G_\mu \to \sqrt{Z_G}G_\mu \tag{6.2}$$

$$g_s \to g_{s\text{ bare}} \qquad\qquad m_{\tilde{q}}^2 \to m_{\tilde{q}\text{ bare}}^2$$

$$m_\sigma^2 \to m_{\sigma\text{ bare}}^2 \qquad\qquad m_{\tilde{g}} \to m_{\tilde{g}\text{ bare}} \tag{6.3}$$

In this thesis the computation of amplitudes is performed in $D = 4 - 2\epsilon$ dimensions in order to regularize infinities. Ultraviolet divergences show then up as single poles in ϵ. The renormalization will be discussed in detail in section 7 and 8.1.

Having removed the ultraviolet divergences the matrix element is not free of divergences as it comprises infrared divergences. These split into soft and collinear (or mass) singularities[18] which cannot be removed by means of renormalization. These additional singularities show up as single and double poles of ϵ in the matrix element $\mathcal{M}^{1L}$ and the virtual cross section which is obtained after performing the 2-body phase space integration as in eq. 5.8 but over $\left|\mathcal{M}^V\right|^2$:

$$\frac{\mathrm{d}^2\sigma^V}{\mathrm{d}t\,\mathrm{d}u} = \frac{K_{ab}}{s^2}\frac{\pi S_\epsilon}{\Gamma(1-\epsilon)}\left[\frac{tu - m_1^2m_2^2}{\mu^2 s}\right]^{-\epsilon}\Theta(tu - m_1^2m_2^2)$$
$$\Theta(s - 4m^2)\delta(s + t + u - m_1^2 - m_2^2)\sum|\mathcal{M}^V|^2. \tag{6.4}$$

The single poles correspond to soft or collinear divergences whereas the double poles correspond to the coincidence of soft and collinear divergences.

6.2 Real Corrections

A crucial thing to recognize in the calculation of the $\mathcal{O}(\alpha_s)$ correction to the squark production cross section is that not only virtual corrections but also real corrections give rise to this physical observable. This is because one does not measure the final state partons but the jets in which they hadronize in due to confinement. This means that a radiation of a massless particle whose energy tends to zero or the radiation of a particle which is collinear to one of the final state particles is in experiment measured as a two jet event even though there are three particles in the final state of the calculation. However real corrections also contain divergences. Including these contributions to the cross section causes the cancellation of single poles coming from soft divergences and the cancellation of double poles. At this point the only

---

[17]These counterterms have to be of the same $\mathcal{O}(\hbar)$ as the loop diagrams they are constructed to cancel [36].

[18]The names differ in the literature. Often infrared divergences are used as a synonym for soft divergences.

singularities which are left in the cross section are the collinear ones.

To see how these are removed consider the second diagram in fig. 6.3. The propagator of the quark which radiates off a gluon gives a contribution of the form

$$\frac{1}{(p_q + p_g)^2 - m_q^2} = \frac{1}{p_q \cdot p_g} = \frac{1}{2 E_q E_g (1 - \beta_q \cos\theta_{qg})} \qquad \text{with } \beta_q = \frac{\vec{p}_q}{E_q} \qquad (6.5)$$

to the the diagram in question. Here p_q, p_g (E_q, E_g) are the quark's and gluon's four-momentum (energy) and θ_{qg} is the angle between the quark's and gluon's three-momentum. One observes two potentially singular limits

$$\text{soft gluon}: \qquad E_g \to 0 \qquad\qquad\qquad\qquad\qquad (6.6)$$

$$\text{collinear particles}: \qquad \theta_{qg} \to 0 \qquad \text{if } m_q \to 0. \qquad\qquad (6.7)$$

Within these limits the inner quark can almost be considered as on-shell which means that it may travel a long distance between the emission of a gluon and taking part in the actual interaction. This suggest that some divergences may come from the incoming hadron and are actually not associated with the interaction. In fact this turns out to be the case: The remaining collinear divergences have a generic form (evtl. angeben) and can, by redefinition, be absorbed into the parton density functions. This procedure is referred to as mass factorization [33]. In fact the Kinoshita-Lee-Naunberg-Theorem [37], [38] guarantees the finiteness of sufficiently inclusive observables.

Figure 6.2 summarizes the required steps to render the next-to-leading-order cross section finite.
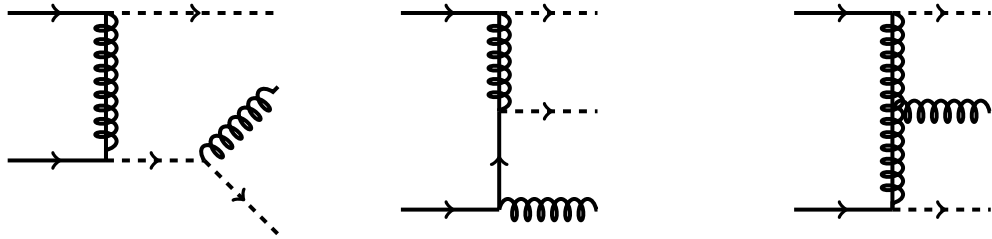
6.2.1 Real Gluon Radiation

A representative set of Feynman-diagrams for real gluon emission are shown in fig. 6.3. In order to extract the singularities the so called two-cut method has been adopted. This is the phase space has been divided into different regimes: a soft part, a hard collinear part and a hard non-collinear part.

In the soft part the energy of the outgoing gluon is only integrated up to $\delta_s \frac{\sqrt{s}}{2}$ where δ_s is a cut on which the final result must not depend on.

6.2.2 Real Quark Radiation
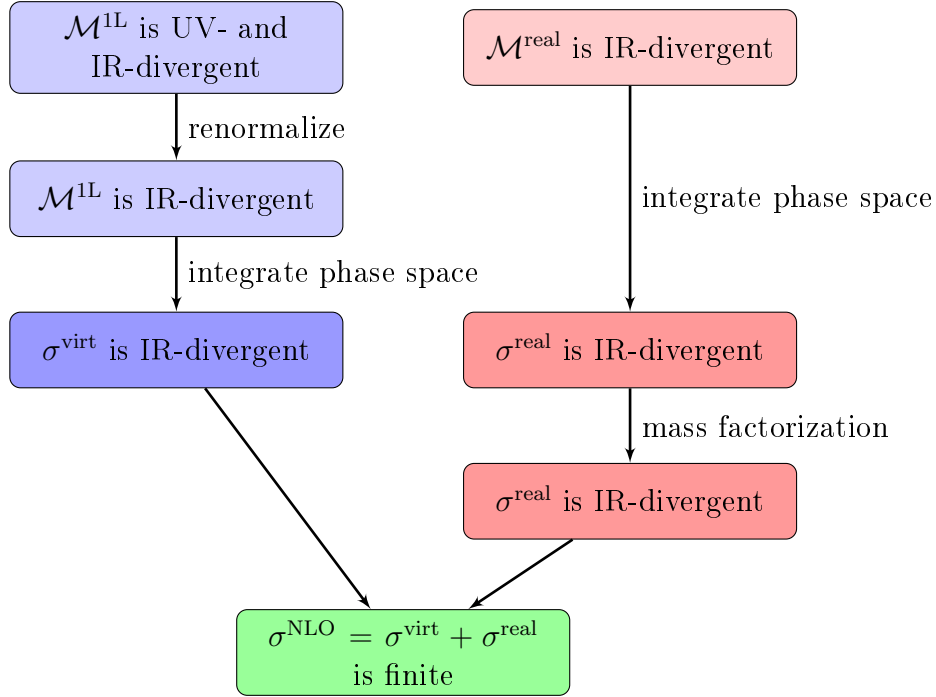
Figure 6.2: This scheme illustrates the necessary steps in the computation of the next-to-leading order cross section which are required to render it finite.

Figure 6.3: A selection of real gluon emission diagrams contributing to squark production. Again each diagram is a representative of a certain diagram type. The first one is final state gluon emission, the second one initial state gluon radiation and the third one is the radiation of a gluon from a virtual particle within the diagram.
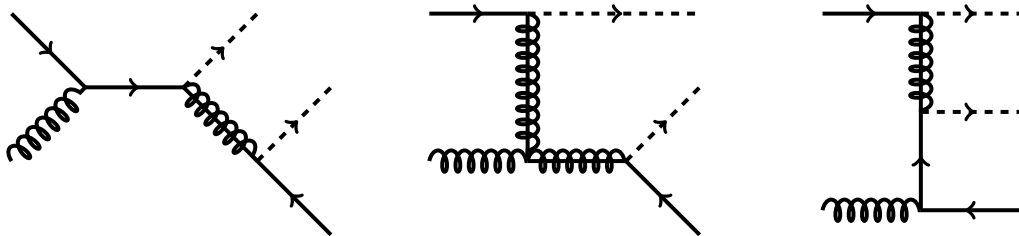
Figure 6.4: A selection of real quark emission diagrams contributing to squark production. The first two diagrams have a gluino propagator which may go on-shell. In this regime of phase space these diagrams should not be included in the correction to squark-production but to a tree-level contribution to squark-gluino-production.

7 Renormalization of the MRSSM

In order to improve the prediction of cross sections one has to take quantum corrections into account. These are associated with loops in the corresponding Feynman diagrams. Computing these loop diagrams one might encounter infinities which arise from certain momentum configurations of the unspecified loop momenta. These infinities can be classified due to their origin. Infinities which are associated with loop momenta which tend to infinity are referred to as ultraviolet(UV) divergences. Infinities arising from loop momenta approaching zero can occur in loops with massless particles and are called infrared(IR) singularities.

These infinities are not physical and must therefore be removed to get sensible predictions. To this end one regularizes them to extract them from the quantity in question. UV-divergences can be removed by means of renormalization, i.e. counterterms are inserted into the Lagrangian to cancel UV-divergences. Infrared and collinear divergenves are removed by adding up all possible contributions which give rise to the considered observable.

7.1 Regularization Schemes

Dimensional Regularization (DREG)

Dimensional regularization(DREG) is a very common procedure for regularizing infinities which was devised by t'Hooft and Veltman [39]. In this scheme loop momenta, gamma- and epsilon-tensors, phase space and fields are defined in D dimensions. As in every regularization scheme a parameter with mass dimension needs to be introduced. In DREG that is the μ parameter which ensures that the loop integrals still have mass dimension 4:

$$\int \frac{\mathrm{d}^4 p}{(2\pi)^4} \rightarrow \mu^{4-D} \int \frac{\mathrm{d}^D p}{(2\pi)^D}. \tag{7.1}$$

One often writes $D = 4 - 2\epsilon$. Then the divergences of the loop integral manifest in $\frac{1}{\epsilon}$ poles. However DREG suffers a flaw in supersymmetry. As the degrees of freedom of a massless gauge boson are $D-2$ but the degrees of freedom of its superpartner are 2 there is a mismatch if $D \neq 4$. As a consequence there are 2ϵ degrees of freedom associated with the gluon[19] which do not have a supersymmetric partner. Therefore DREG violates supersymmetry.

Dimensional Reduction (DRED)

Dimensional reduction (DRED) was introduced to rectify the imperfections of DREG, i.e. it preserves supersymmetry[20]. DRED promotes only loop momenta to D dimensions. All other

---

[19]These degrees of freedom are identified with scalars and are therefore referred to as ϵ scalars

[20]It is not clear if DRED preserves supersymmetry at all orders in perturbation theory but it does preserve supersymmetry at the 1-loop level.

quantities which are D dimensional in DREG stay in 4 dimensions.

maybe refer to Collins: Renormalization

7.2 Regularization Scheme Dependences

To discuss the subject of this and ensuing subsections it is useful to introduce the effective action Γ. A formal introduction of Γ can be found in [2]. In short Γ can be viewed as a modification of the classical action $\Gamma_{\text{cl}} = \int \mathcal{L}_{\text{cl}}$ by quantum effects:

$$\Gamma = \Gamma_{\text{cl}} + \mathcal{O}(\hbar) \tag{7.2}$$

This means that in addition to the vertices in the classical Lagrangian new vertices arise due to loop effects. As already alluded to loop corrections might a priori not be finite and then need to be rendered finite by the addition of counterterms. For $\mathcal{O}(\hbar)$ corrections one writes

$$\Gamma^{(\leq 1)} \to \Gamma^{(\leq 1)} + \Gamma^{(1), \text{ ct}} \tag{7.3}$$

These counterterms depend on the regularization (and renormalization) scheme. If one chooses to work with DREG supersymmetry will not be preserved at 1-loop order, i.e. $\Gamma^{(\leq 1)}_{\text{DREG}}$ is not supersymmetric. To maintain supersymmetry invariance of the renormalized effective action the counterterms will not only consist of supersymmetric counterterms $\Gamma^{(1), \text{ ct, sym}}_{\text{DREG}}$ but also of counterterms restoring supersymmetry $\Gamma^{(1), \text{ ct, trans}}_{\text{DREG}}$.

$$\Gamma^{(1), \text{ ct}}_{\text{DREG}} = \Gamma^{(1), \text{ ct, sym}}_{\text{DREG}} + \Gamma^{(1), \text{ ct, trans}}_{\text{DREG}} \tag{7.4}$$

Fortunately a supersymmetry conserving regularization scheme (at 1-loop level) is given by DRED [40]. One way to acquire supersymmetry restoring counterterms is therefore given by

$$\Gamma^{(\leq 1)}_{\text{DRED}} + \Gamma^{(1), \text{ ct}}_{\text{DRED}} \stackrel{!}{=} \Gamma^{(\leq 1)}_{\text{DREG}} + \Gamma^{(1), \text{ ct}}_{\text{DREG}}. \tag{7.5}$$

Equating also the finite terms in $\Gamma^{(1), \text{ ct, sym}}$ in DRED and DREG the choice of the supersymmetry restoring counterterms is fixed by [41]:

$$\Gamma^{(1),\text{ct,trans}}_{\text{DREG}} = \Gamma^{(\leq 1)}_{\text{DRED}} - \Gamma^{(\leq 1)}_{\text{DREG}}. \tag{7.6}$$

This equation justifies the label "trans" at the supersymmetry restoring counterterm because it actually describes the transition counterterm from DREG to DRED or vice versa.

In the case of the MRSSM it will turn out that the only supersymmetry violation comes from corrections associated with the gluon as already alluded to in section 7.1. However supersymmetry restoring will always already be included in δZ^{DREG}. Referring to the field

renormalization constants from eq. 6.2 this is

$$\delta Z^{\mathrm{DREG}} = \delta Z^{\mathrm{DREG,sym}} + \delta Z^{\mathrm{trans}} \tag{7.7}$$

where

$$\delta Z^{\mathrm{trans}} = \delta Z^{\mathrm{DREG}} - \delta Z^{\mathrm{DRED}} \tag{7.8}$$

is the supersymmetry restoring renormalization constant. Note the sign within this definition in comparison to eq. 7.6. The only point where particularly care is required is the coupling: The gauge coupling g_s and the Yukawa coupling $\hat{g}_s$ receive different supersymmetry restoring counterterms due to different loop diagrams. Therefore one has to make a difference between these couplings at 1-loop level. In order to match g_s to the experimentally measured coupling it is renormalized in the $\overline{\mathrm{MS}}$-scheme (with an additional manipulation for heavy particles, which will be explained in subsection 7.4). The Yukawa coupling $\hat{g}_s$ therefore needs to be added with the difference of the supersymmetry restoring counterterms from the $q\tilde{q}^{\dagger}\tilde{g}$ vertex and the $q\bar{q}G$ vertex at 1-loop in order to be renormalized in the same way.

7.3 On-Shell Renormalization

A part of the computation of the cross section at next-to-leading order is the calculation of renormalization constants. Field renormalization constants δZ and parameter renormalization constants δo with $o \in \{g, m\}$ are defined by

$$Z = 1 + \delta Z \qquad\qquad o_{\mathrm{bare}} = o + \delta o \tag{7.9}$$

where Z and o are defined by the multiplicative renormalization transformation, introduced in eq. 6.2 and 6.2. The field and mass renormalization constants have been calculated in DREG in the on-shell scheme. This has the advantage that when turning to the cross section no manipulation of the Green function to the S-matrix element has to be done, see section 8.1. The calculation has partially been performed by hand but was always checked with the mathematica output generated by the packages `FeynArts` [42] and `FormCalc` [43, 44].

The Quark Self-Energy

The quark self-energy splits into contribution from the Standard Model as well as a supersymmetric analogue which is already present in the MSSM.
The one-particle-irreducible diagrams evaluate to

$$i\Gamma^{\mathrm{1L}}_{q_i\bar{q}_j} = i\frac{g_s^2}{16\pi^2}\delta_{ij}C(F)\left[2\left(B_0(p^2,0,0) + B_1(p^2,0,0) - \frac{1}{2}\right)\slashed{p} - 2B_1(p^2,m_{\tilde{g}}^2,m_{\tilde{q}}^2)\slashed{p}\right]. \tag{7.10}$$
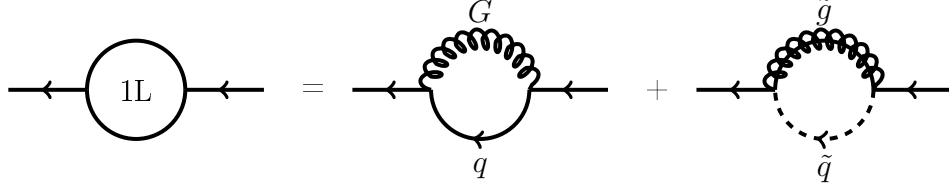
Figure 7.1: Feynman diagrams contributing to the self-energy of the quark at 1-loop level.

With the counterterm Feynman rule

$$i\Gamma^{1\mathrm{L,ct}}_{q_i\bar{q}_j} \hat{=} i \;\longleftarrow\!\!\times\!\!\longleftarrow\; j \hat{=} i\delta_{ij}\delta Z_q \slashed{p}$$

and the on-shell renormalization condition

$$\frac{\partial}{\partial \slashed{p}}\left[\Re(\Gamma^{1\mathrm{L}}_{q_i\bar{q}_j}) + \Gamma^{1\mathrm{L,ct}}_{q_i\bar{q}_j}\right]_{p^2=0} = 0 \tag{7.11}$$

where $\Re(\ldots)$ denotes the real part of $\ldots$ one finds

$$\delta Z_q = 2C(F)\frac{g_s^2}{16\pi^2}\Re\left[B_1(0, m_{\tilde{g}}^2, m_{\tilde{q}}^2)\right]. \tag{7.12}$$

Note that the Standard Model contribution to the quark renormalization constant equals zero as it is propotional to $B_0(0,0,0)$ and $B_1(0,0,0)$. These integrals have no mass scale and are due to their definition of their scaling in D dimensions [45] defined to be zero. Pictorially this may be understood as a cancellation of a positive UV-divergent part and a negative IR-divergent part. Note further that the term $\frac{1}{2}$ from eq. 7.10 has vanished because it has been absorbed in $B_0(p^2, 0, 0)|_{p^2\to 0}$.
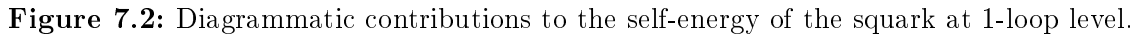
Doing the same calculation in DRED one finds that this very term $\frac{1}{2}$ is absent. Therefore the transition renormalization constant between DREG and DRED is given by

$$\delta Z_q^{\mathrm{trans}} = \delta Z_q^{\mathrm{DREG}} - \delta Z_q^{\mathrm{DRED}} = C(F)\frac{g_s^2}{16\pi^2}. \tag{7.13}$$

The Squark Self-Energy

The contributions to the self-energy of the left- and right-handed squark are the same for electroweak effects are neglected. Therefore to avoid unnecessary labeling $\Gamma_{\tilde{q}\tilde{q}^\dagger}$ stands in the following for $\Gamma_{\tilde{q}_L\tilde{q}_L^\dagger} = \Gamma_{\tilde{q}_R\tilde{q}_R^\dagger}$.

$$i\Gamma^{1\mathrm{L}}_{\tilde{q}_i\tilde{q}_j^\dagger} = i\frac{g_s^2}{16\pi^2}\delta_{ij}C(F)\left[A_0(m_{\tilde{q}}^2) + 0 - \left(4A_0(m_{\tilde{g}}^2) + 4B_1(p^2, 0, m_{\tilde{g}}^2)p^2\right)\right.$$
$$\left. + 4m_{\tilde{g}}^2 B_0(p^2, m_{\phi^0}^2, m_{\tilde{q}}^2) - \left(2B_1(p^2, 0, m_{\tilde{q}}^2)p^2 + B_0(p^2, 0, m_{\tilde{q}}^2)(m_{\tilde{q}}^2 + 3p^2)\right)\right]. \tag{7.14}$$

Figure 7.2: Diagrammatic contributions to the self-energy of the squark at 1-loop level.

Suppressing δ_{AB} with $A, B \in \{L, R\}$ which is present in the tree level propagator (see fig. 10.1) the counterterm Feynman rule is given by

$$i\Gamma^{1\mathrm{L,ct}}_{q_i\bar{q}_j} \,\hat{=}\, i \,\text{---}\!\!\!\blacktriangleleft\!\!\!\text{---}\!\!\!\times\!\!\!\text{---}\!\!\!\blacktriangleleft\!\!\!\text{---}\, j \,\hat{=}\, i\delta_{ij}\left[\delta Z_{\tilde{q}}(p^2 - m_{\tilde{q}}^2) - \delta m_{\tilde{q}}^2\right].$$

The on-shell renormalization conditions read

$$\frac{\partial}{\partial p^2}\left[\Re(\Gamma^{1\mathrm{L}}_{\tilde{q}_i\tilde{q}_j^\dagger}) + \Gamma^{1\mathrm{L,ct}}_{\tilde{q}_i\tilde{q}_j^\dagger}\right]_{p^2=m_{\tilde{q}}^2} = 0 \qquad\qquad \left[\Re(\Gamma^{1\mathrm{L}}_{\tilde{q}_i\tilde{q}_j^\dagger}) + \Gamma^{1\mathrm{L,ct}}_{\tilde{q}_i\tilde{q}_j^\dagger}\right]_{p^2=m_{\tilde{q}}^2} = 0. \qquad (7.15)$$

This results in the following renormalization constants

$$\begin{aligned}
\delta Z_{\tilde{q}} = \frac{g_s^2}{16\pi^2}C(F)\Re\Big[&4B_1(p^2, 0, m_{\tilde{g}}^2) + 2B_1(B_1(p^2, 0, m_{\tilde{q}}^2)) + 3B_0(p^2, 0, m_{\tilde{q}}^2) \\
&+ 4m_{\tilde{g}}^2\frac{\partial}{\partial p^2}B_1(p^2, 0, m_{\tilde{g}}^2) - 4m_{\tilde{g}}^2\frac{\partial}{\partial p^2}B_0(p^2, m_{\phi^0}^2, m_{\tilde{q}}^2) + 2m_{\tilde{q}}^2\frac{\partial}{\partial p^2}B_1(p^2, 0, m_{\tilde{q}}^2) \\
&+ 4m_{\tilde{q}}^2\frac{\partial}{\partial p^2}B_0(p^2, 0, m_{\tilde{q}}^2)\Big]_{p^2=m_{\tilde{q}}^2}
\end{aligned} \qquad (7.16)$$

and

$$\begin{aligned}
\delta m_{\tilde{q}}^2 = \frac{g_s^2}{16\pi^2}C(F)\Big[&A_0(m_{\tilde{q}}^2) - (4A_0(m_{\tilde{g}}^2) + 4B_1(m_{\tilde{q}}^2, 0, m_{\tilde{g}}^2)m_{\tilde{q}}^2) + 4m_{\tilde{g}}^2B_0(m_{\tilde{q}}^2, m_{\phi^0}^2, m_{\tilde{q}}^2) \\
&- (2B_1(m_{\tilde{q}}^2, 0, m_{\tilde{q}}^2)m_{\tilde{q}}^2 + 4B_0(m_{\tilde{q}}^2, 0, m_{\tilde{q}}^2)m_{\tilde{q}}^2)\Big].
\end{aligned} \qquad (7.17)$$

The squark self-energy exhibits no regularization dependence. The transition counterterms are therefore

$$\delta Z_{\tilde{q}}^{\text{trans}} = \delta m_{\tilde{q}}^{2 \ \text{trans}} = 0. \tag{7.18}$$

The Glunio Self-Energy

The 4-spinor of the gluino comprises two Weyl spinors which describe very different particles.

$$\tilde{g}^a = \begin{pmatrix} -i\lambda^a \\ i\overline{\chi}^a \end{pmatrix} \tag{7.19}$$

The left-handed part λ^a is associated with the superpartner of the gluon and therefore the "actual" gluino whereas the right-handed part $\overline{\chi}^a$ was introduced to assign a Dirac-mass to the gluino and may be referred to as the octino.

From the Lagrangian 4.17 one can see that the couplings of the two particles are quite distinct. This is reflected by different field renormalization constants of the left- and right-handed part of the gluino. As for the quarks the fermion (and momentum) flow is from the right to the
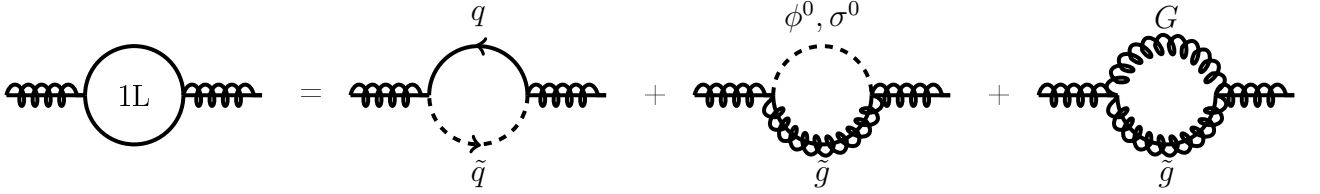
Figure 7.3: diagrammatic contributions to the self-energy of the squark at 1-loop level

left.

$$i\Gamma_{\tilde{g}^a\tilde{g}^b}^{1L} = i\frac{g_s^2}{16\pi^2}\delta_{ab}\left[-4T(F)\left((n_f - 1)B_1(p^2, 0, m_{\tilde{q}}^2) + B_1(p^2, m_t^2, m_{\tilde{q}}^2)\right)P_L\slashed{p}\right.$$
$$+ C(A)\left((B_0(p^2, m_{\tilde{g}}^2, m_{\phi^0}^2) - B_0(p^2, m_{\tilde{g}}^2, m_{\sigma^0}^2))m_{\tilde{g}} - (B_1(p^2, m_{\tilde{g}}^2, m_{\phi^0}^2) + B_1(p^2, m_{\tilde{g}}^2, m_{\sigma^0}^2))\slashed{p}\right)$$
$$\left. + C(A)\left((2 - 4B_0(p^2, 0, m_{\tilde{g}}^2))m_{\tilde{g}} - (1 - 2(B_0(p^2, 0, m_{\tilde{g}}^2) + B_1(p^2, 0, m_{\tilde{g}}^2)))\slashed{p}\right)\right] \tag{7.20}$$

Where $n_f = 6$ is the number of quark flavors.

The counterterm Feynman rule derived from multiplicative renormalization reads

$$i\Gamma_{\tilde{g}^a\tilde{g}^b}^{1L,\text{ct}} \;\hat{=}\; a \; \text{〜〜〜✕〜〜〜} \; b \;\hat{=}\; i\delta_{ab}\left[(\delta Z_{\tilde{g}}^L P_L + \delta Z_{\tilde{g}}^R P_R)\slashed{p} - \left(\frac{\delta Z_{\tilde{g}}^L + \delta Z_{\tilde{g}}^R}{2}m_{\tilde{g}} + \delta m_{\tilde{g}}\right)\right].$$

The on-shell renormalization conditions for the fields are

$$\frac{\partial}{\partial(P_L\slashed{p})}\left[\Re(\Gamma_{\tilde{g}^a\tilde{g}^b}^{1L}) + \Gamma_{\tilde{g}^a\tilde{g}^b}^{1L,\text{ct}}\right]_{\slashed{p}=m_{\tilde{g}}} = 0, \qquad \frac{\partial}{\partial(P_R\slashed{p})}\left[\Re(\Gamma_{\tilde{g}^a\tilde{g}^b}^{1L}) + \Gamma_{\tilde{g}^a\tilde{g}^b}^{1L,\text{ct}}\right]_{\slashed{p}=m_{\tilde{g}}} = 0 \tag{7.21}$$

where the derivative of $\Sigma = \Sigma^{VL} P_L \slashed{p} + \Sigma^{VR} P_R \slashed{p} + \Sigma^{SL} P_L + \Sigma^{SR} P_R$ with respect to $P_A \slashed{p}$ ($A \in \{L, R\}$) is defined by [46]

$$\frac{\partial}{\partial (P_A \slashed{p})} \Sigma \bigg|_{\slashed{p}=m} = \Sigma^{VA} + \frac{\partial}{\partial p^2} \left(m^2 \Sigma^{VL} + m^2 \Sigma^{VR} + m \Sigma^{SL} + m \Sigma^{SR} \right). \tag{7.22}$$

This leads to the following renormalization constants

$$\begin{aligned}
\delta Z_{\tilde{g}}^{L} = \frac{g_s^2}{16\pi^2} \Re \Big[& 4T(F) \left((n_f - 1) B_1(m_{\tilde{g}}^2, 0, m_{\tilde{q}}^2) + B_1(m_{\tilde{g}}^2, m_t^2, m_{\tilde{q}}^2) \right) \\
& + C(A)(B_1(m_{\tilde{g}}^2, m_{\tilde{g}}^2, m_{\phi^0}^2) + B_1(m_{\tilde{g}}^2, m_{\tilde{g}}^2, m_{\sigma^0}^2)) \\
& + C(A)(1 - 2(B_0(m_{\tilde{g}}^2, 0, m_{\tilde{g}}^2) + B_1(m_{\tilde{g}}^2, 0, m_{\tilde{g}}^2))) \\
& + 4T(F) m_{\tilde{g}}^2 \frac{\partial}{\partial p^2} \left(((n_f - 1)) B_1(p^2, 0, m_{\tilde{q}}^2) + B_1(p^2, m_t^2, m_{\tilde{q}}^2) \right) \\
& - 2C(A) m_{\tilde{g}} \frac{\partial}{\partial p^2} \left(B_0(p^2, m_{\tilde{g}}^2, m_{\phi^0}^2) - B_0(p^2, m_{\tilde{g}}^2, m_{\sigma^0}^2) - B_1(p^2, m_{\tilde{g}}^2, m_{\phi^0}^2) - B_1(p^2, m_{\tilde{g}}^2, m_{\sigma^0}^2) \right) \\
& - 4C(A) m_{\tilde{g}}^2 \frac{\partial}{\partial p^2} \left(-B_0(p^2, 0, m_{\tilde{g}}^2) + B_0(p^2, 0, m_{\tilde{g}}^2) \right) \Big]_{p^2 = m_{\tilde{g}}^2}
\end{aligned} \tag{7.23}$$

and

$$\begin{aligned}
\delta Z_{\tilde{g}}^{R} = \frac{g_s^2}{16\pi^2} \Re \Big[& C(A)(B_1(m_{\tilde{g}}^2, m_{\tilde{g}}^2, m_{\phi^0}^2) + B_1(m_{\tilde{g}}^2, m_{\tilde{g}}^2, m_{\sigma^0}^2)) \\
& + C(A)(1 - 2(B_0(m_{\tilde{g}}^2, 0, m_{\tilde{g}}^2) + B_1(m_{\tilde{g}}^2, 0, m_{\tilde{g}}^2))) \\
& + 4T(F) m_{\tilde{g}}^2 \frac{\partial}{\partial p^2} \left(((n_f - 1)) B_1(p^2, 0, m_{\tilde{q}}^2) + B_1(p^2, m_t^2, m_{\tilde{q}}^2) \right) \\
& - 2C(A) m_{\tilde{g}} \frac{\partial}{\partial p^2} \left(B_0(p^2, m_{\tilde{g}}^2, m_{\phi^0}^2) - B_0(p^2, m_{\tilde{g}}^2, m_{\sigma^0}^2) - B_1(p^2, m_{\tilde{g}}^2, m_{\phi^0}^2) - B_1(p^2, m_{\tilde{g}}^2, m_{\sigma^0}^2) \right) \\
& - 4C(A) m_{\tilde{g}}^2 \frac{\partial}{\partial p^2} \left(-B_0(p^2, 0, m_{\tilde{g}}^2) + B_0(p^2, 0, m_{\tilde{g}}^2) \right) \Big]_{p^2 = m_{\tilde{g}}^2}.
\end{aligned} \tag{7.24}$$

As for the quark there are constant terms amid the Passarino-Veltman integrals. These arise only in DREG but and not in DRED. The transition counterterms are

$$\delta Z_{\tilde{g}}^{A \text{ trans}} = \delta Z_{\tilde{g}}^{A \text{ DREG}} - \delta Z_{\tilde{g}}^{A \text{ DRED}} = C(A) \frac{g_s^2}{16\pi^2} \tag{7.25}$$

for $A \in \{L, R\}$. The gluino mass counterterm is ascertained by the condition

$$\left[\Re(\Gamma_{\tilde{g}^a \bar{\tilde{g}}^b}^{1\text{L}}) + \Gamma_{\tilde{g}^a \bar{\tilde{g}}^b}^{1\text{L,ct}} \right]_{\slashed{p}=m_{\tilde{g}}} = 0 \tag{7.26}$$

which is equivalent to

$$\delta m_{\tilde{g}} = \Re\left(m_{\tilde{g}}\frac{\Sigma^{VL} + \Sigma^{VR}}{2} + \frac{\Sigma^{SL} + \Sigma^{SR}}{2}\right) \tag{7.27}$$

and yields

$$\delta m_{\tilde{g}} = \frac{g_s^2}{16\pi^2}m_{\tilde{g}}^2 \,\Re\left[-2T(F)\left((n_f - 1)B_1(m_{\tilde{g}}^2, 0, m_{\tilde{q}}^2) + B_1(m_{\tilde{g}}^2, m_t^2, m_{\tilde{q}}^2)\right)\right.$$
$$+ C(A)\left(B_0(m_{\tilde{g}}^2, m_{\tilde{g}}^2, m_{\phi^0}^2) - B_0(m_{\tilde{g}}^2, m_{\tilde{g}}^2, m_{\sigma^0}^2) - B_1(m_{\tilde{g}}^2, m_{\tilde{g}}^2, m_{\phi^0}^2) - B_1(m_{\tilde{g}}^2, m_{\tilde{g}}^2, m_{\sigma^0}^2)\right)$$
$$\left.+ C(A)\left(1 - 2B_0(m_{\tilde{g}}^2, 0, m_{\tilde{g}}^2) + 2B_1(m_{\tilde{g}}^2, 0, m_{\tilde{g}}^2)\right)\right]. \tag{7.28}$$

Again there is a transition counterterm

$$\delta m_{\tilde{g}}^{\text{trans}} = \delta m_{\tilde{g}}^{\text{DREG}} - \delta m_{\tilde{g}}^{\text{DRED}} = C(A)\frac{g_s^2}{16\pi^2}m_{\tilde{g}}. \tag{7.29}$$

Apart from the renormalization constant of the gauge coupling and the supersymmetry restoring counterterm these are all renormalization constants needed from squark production at next to leading order. In fact the field renormalization constants of the gluino are not needed as they drop out when summing up all three counterterm Feynman diagrams. This can be seen when writing down the matrix amplitudes for the counterterm Feynman diagrams shown in fig. 7.4:

$$\mathcal{M}^{\text{B}} = -2g_s^2\frac{\langle v_2|P_R\slashed{k}_3|u_1\rangle}{t_{\tilde{g}}}T_{\delta\beta}^a T_{\gamma\alpha}^a + 2g_s^2\frac{\langle v_2|P_L\slashed{k}_3|u_1\rangle}{u_{\tilde{g}}}T_{\gamma\beta}^a T_{\delta\alpha}^a \tag{7.30}$$

$$\mathcal{M}_{\text{vertex}}^{\text{1L,ct}} = 2\mathcal{M}^B\left(\frac{\delta\hat{g}_s}{\hat{g}_s} + \frac{\delta Z_q}{2} + \frac{\delta Z_{\tilde{g}}^L}{2} + \frac{\delta Z_{\tilde{q}}}{2}\right) \tag{7.31}$$

$$\mathcal{M}_{\text{self}-\text{energy}}^{\text{1L,ct}} = 2g_s^2\left\langle v_2\left|P_R\, i\frac{\slashed{p} + m_{\tilde{g}}}{t_{\tilde{g}}}\left[i(\delta Z_{\tilde{g}}^L P_L + \delta Z_{\tilde{g}}^R P_R)\slashed{p}\right.\right.\right.$$
$$\left.\left.\left.-i\left(\frac{\delta Z_{\tilde{g}}^L + \delta Z_{\tilde{g}}^R}{2}m_{\tilde{g}} + \delta m_{\tilde{g}}\right)\right]i\frac{\slashed{p} + m_{\tilde{g}}}{t_{\tilde{g}}}P_L\right|u_1\right\rangle\Bigg|_{p=p_1-p_3} + \text{u} - \text{channel}$$
$$= -\mathcal{M}^B\delta Z_{\tilde{g}}^L + 2\frac{m_{\tilde{g}}}{t_{\tilde{g}}}\left(-2g_s^2\frac{\langle v_2|P_R\slashed{k}_3|u_1\rangle}{t_{\tilde{g}}}T_{\delta\beta}^a T_{\gamma\alpha}^a\right)\delta m_{\tilde{g}}$$
$$+ 2\frac{m_{\tilde{g}}}{u_{\tilde{g}}}\left(2g_s^2\frac{\langle v_2|P_L\slashed{k}_3|u_1\rangle}{u_{\tilde{g}}}T_{\gamma\beta}^a T_{\delta\alpha}^a\right)\delta m_{\tilde{g}}. \tag{7.32}$$

Where $\delta Z_{\tilde{g}}^R$ drops out already in $\mathcal{M}_{\text{self}-\text{energy}}^{\text{1L,ct}}$ as the octino does neither couple to quarks nor to squarks the renormalization constant for the actual gluino $\delta Z_{\tilde{g}}^L$ drops out when $\mathcal{M}_{\text{self}-\text{energy}}^{\text{1L,ct}}$ and $\mathcal{M}_{\text{vertex}}^{\text{1L,ct}}$ are added. This is also true in a more general case, i.e. the renormalization constants of virtual particles do always drop out.
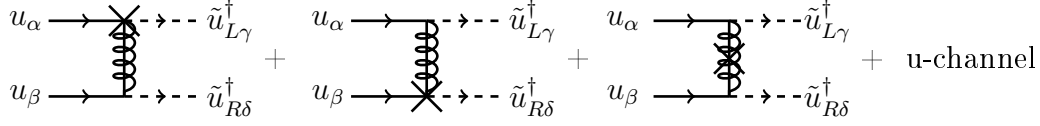
Figure 7.4: 1-Loop-level counterterm Feynman diagrams for squark production in the MRSSM. The Greek latters label the particle's color.

7.4 Renormalization of the Gauge Coupling

The gauge coupling g_s is renormalized in the $\overline{\text{MS}}$-scheme with the modification that additional logarithms are subtracted, i.e. light particles are treated in the $\overline{\text{MS}}$-scheme and heavy particles in the zero-momentum subtraction scheme. This is to decouple heavy particles from the running of $\alpha_s = \frac{g_s^2}{4\pi}$. This renormalization procedure allows to adopt the experimental values of α_s from the parton density functions. The running due to effects of heavy particles is then encoded in the logarithms of δg_s.

Extracting δg_s from the quark-quark-gluon vertex requires not only the computation of $i\Gamma^{1\text{L}}_{q_i \bar{q}_j G^\mu_a}$ but also the (re)evaluation of auxiliary field renormalization constants δZ^{aux}_q and δZ^{aux}_G in the above mentioned scheme. These will not be the same as the on-shell scheme.

The Quark Self-Energy Revisited

The quark self-energy has two contribution which are shown in figure 7.1. The first one corresponds to light particles the second one to heavy particles: $i\Gamma^{1\text{L}}_{q_i\bar{q}_j} = i\Gamma^{1\text{L,light}}_{q_i\bar{q}_j} + i\Gamma^{1\text{L,heavy}}_{q_i\bar{q}_j}$. For light particles only the UV-divergent[21] part is kept. The self energy corresponding to the heavy particles is taken at zero momentum $p^2 = 0$.

$$i\Gamma^{1\text{L,light}}_{q_i\bar{q}_j}\Big|_{\text{UV-div}} = iC(F)\frac{g_s^2}{16\pi^2}\Delta_\epsilon \slashed{p}\delta_{ij} \tag{7.33}$$

$$i\Gamma^{1\text{L,heavy}}_{q_i\bar{q}_j}(p^2=0) = -iC(F)\frac{g_s^2}{16\pi^2}2B_1(0, m_{\tilde{g}}^2, m_{\tilde{q}}^2)\slashed{p}\delta_{ij} \tag{7.34}$$

The renormalization constant for the evaluation of δg_s is determined by the condition

$$\frac{\partial}{\partial\slashed{p}}\left[\Gamma^{1\text{L,light}}_{q_i\bar{q}_j}\Big|_{\text{UV-div}} + \Gamma^{1\text{L,heavy}}_{q_i\bar{q}_j}(p^2=0) + \Gamma^{1\text{L,ct}}_{q_i\bar{q}_j}\right] = 0 \tag{7.35}$$

and computes to

$$\delta Z^{\text{aux}}_q = \frac{g_s^2}{16\pi^2}C(F)\left[-\Delta_\epsilon + 2B_1(0, m_{\tilde{g}}^2, m_{\tilde{q}}^2)\right]. \tag{7.36}$$

---

[21]In contrast to the MS-scheme in the $\overline{\text{MS}}$-scheme not only the pure ultraviolet divergence but also two additional transcendent numbers are subtracted. It is therefore common to define $\Delta_\epsilon = \frac{1}{\epsilon} - \gamma_{\text{E}} + \ln 4\pi$.
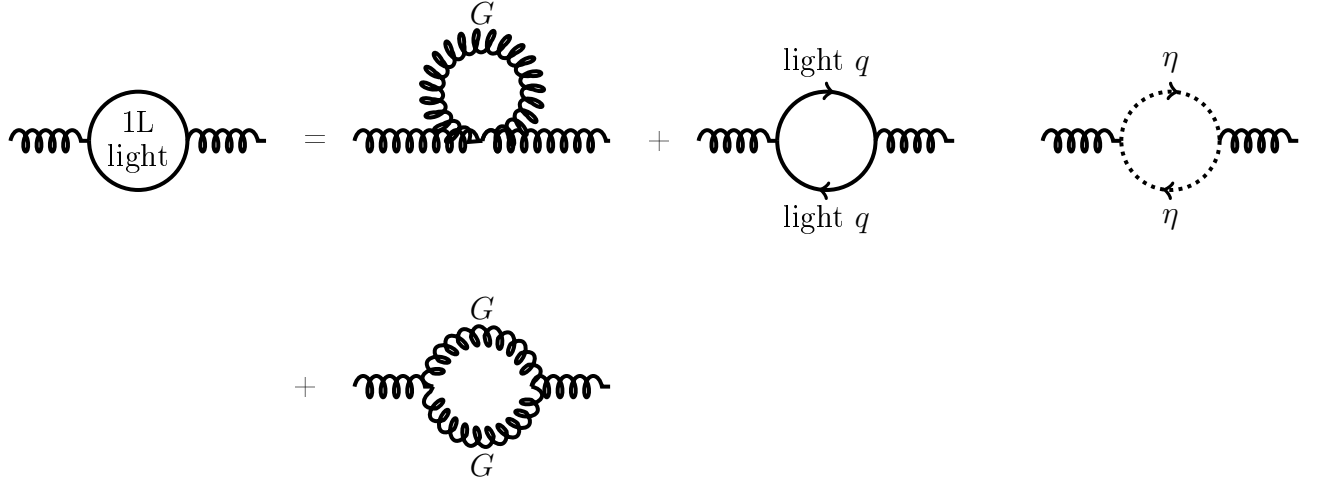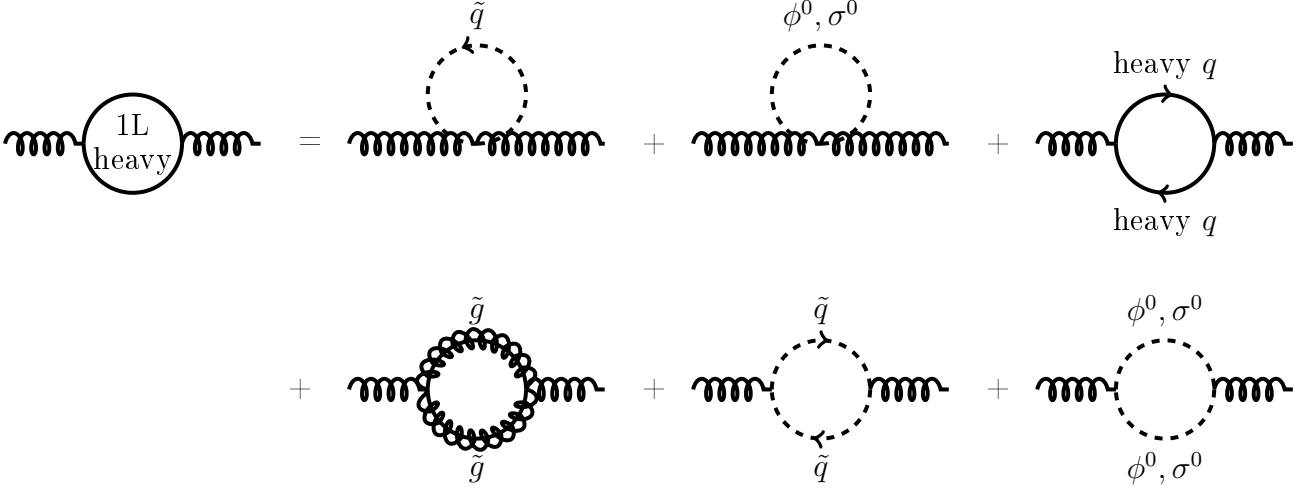
Figure 7.5: Contribution to the self-energy of the gluon originating from light particles

The Gluon Self-Energy

As for the quark self-energy there are again contributions to the self-energy originating from light and heavy particles. Again these are differently dealt with.

$$
\begin{aligned}
i\Gamma^{\text{1L,light}}_{G^a_\mu G^b_\nu}\Big|_{\text{UV-div}} &= i\frac{g_s^2}{16\pi^2}\Delta_\epsilon \left[0 - \frac{4(n_f-1)}{3}T(F)(p^2 g^{\mu\nu} - p^\mu p^\nu) + \frac{C(A)}{12}(p^2 g^{\mu\nu} + 2p^\mu p^\nu) \right.\\
&\quad \left. + \frac{C(A)}{12}(19 p^2 g^{\mu\nu} - 22 p^\mu p^\nu) \right]\delta_{ab}\\
&= i\frac{g_s^2}{16\pi^2}\Delta_\epsilon \left[-\frac{4(n_f-1)}{3}T(F) + \frac{5}{3}C(A) \right](p^2 g^{\mu\nu} - p^\mu p^\nu)\delta_{ab}
\end{aligned}
\tag{7.37}
$$

Both the contribution from the gluon loop and the one from the ghost loop are not proportional to $(p^2 g^{\mu\nu} - p^\mu p^\nu)$ but their sum is. The heavy particle contributions are calculated in the zero-

Figure 7.6: Contribution to the self-energy of the gluon originating from heavy particles, in the last diagram either ϕ^0 or σ^0 are running in the loop

momentum subtraction

$$
i\Gamma^{\text{1L,heavy}}_{G^a_\mu G^b_\nu}(p^2 = 0) = i\frac{g_s^2}{16\pi^2}\delta_{ab}\left[-4T(F)n_f\left(\Delta_\epsilon - \ln\frac{m_{\tilde{q}}^2}{\mu^2}\right)m_{\tilde{q}}^2 g^{\mu\nu} - C(A)\left(\Delta_\epsilon - \ln\frac{m_{\phi^0}^2}{\mu^2}\right)m_{\phi^0}^2 g^{\mu\nu}\right.
$$

$$
- C(A)\left(\Delta_\epsilon - \ln\frac{m_{\sigma^0}^2}{\mu^2}\right)m_{\sigma^0}^2 g^{\mu\nu} - \frac{4}{3}T(F)\left(\Delta_\epsilon - \ln\frac{m_t^2}{\mu^2}\right)(p^2 g^{\mu\nu} - p^\mu p^\nu)
$$

$$
- \frac{4}{3}C(A)\left(\Delta_\epsilon - \ln\frac{m_{\tilde{g}}^2}{\mu^2}\right)(p^2 g^{\mu\nu} - p^\mu p^\nu)
$$

$$
- \frac{2}{3}T(F)n_f\left(\Delta_\epsilon - \ln\frac{m_{\tilde{q}}^2}{\mu^2}\right)(p^2 g^{\mu\nu} - p^\mu p^\nu) + 4T(F)n_f\left(\Delta_\epsilon - \ln\frac{m_{\tilde{q}}^2}{\mu^2}\right)m_{\tilde{q}}^2 g^{\mu\nu}
$$

$$
- \frac{1}{6}C(A)\left(\Delta_\epsilon - \ln\frac{m_{\phi^0}^2}{\mu^2}\right)(p^2 g^{\mu\nu} - p^\mu p^\nu) + C(A)\left(\Delta_\epsilon - \ln\frac{m_{\phi^0}^2}{\mu^2}\right)m_{\phi^0}^2 g^{\mu\nu}
$$

$$
\left.- \frac{1}{6}C(A)\left(\Delta_\epsilon - \ln\frac{m_{\phi^0}^2}{\mu^2}\right)(p^2 g^{\mu\nu} - p^\mu p^\nu) + C(A)\left(\Delta_\epsilon - \ln\frac{m_{\phi^0}^2}{\mu^2}\right)m_{\phi^0}^2 g^{\mu\nu}\right]
$$

$$
= i\frac{g_s^2}{16\pi^2}\delta_{ab}\left[-\frac{4}{3}T(F)\left(\Delta_\epsilon - \ln\frac{m_t^2}{\mu^2}\right)(p^2 g^{\mu\nu} - p^\mu p^\nu)\right.
$$

$$
- \frac{4}{3}C(A)\left(\Delta_\epsilon - \ln\frac{m_{\tilde{g}}^2}{\mu^2}\right)(p^2 g^{\mu\nu} - p^\mu p^\nu)
$$

$$
- \frac{2}{3}T(F)n_f\left(\Delta_\epsilon - \ln\frac{m_{\tilde{q}}^2}{\mu^2}\right)(p^2 g^{\mu\nu} - p^\mu p^\nu)
$$

$$
- \frac{1}{6}C(A)\left(\Delta_\epsilon - \ln\frac{m_{\phi^0}^2}{\mu^2}\right)(p^2 g^{\mu\nu} - p^\mu p^\nu)
$$

$$
\left.- \frac{1}{6}C(A)\left(\Delta_\epsilon - \ln\frac{m_{\phi^0}^2}{\mu^2}\right)(p^2 g^{\mu\nu} - p^\mu p^\nu)\right] \tag{7.38}
$$

The counterterm Feynman rule for the gluon propagator is

$$i\Gamma^{\text{1L,ct}}_{G^a_\mu G^b_\nu} \; \hat{=} \; a, \mu \;\text{∿∿∿✕∿∿∿}\; b, \nu \; \hat{=} \; -i\delta Z_G \left(p^2 g^{\mu\nu} - p^\mu p^\nu\right) \delta_{ab}.$$

The renormalization condition for δZ_G^{aux} reads

$$\Gamma^{\text{1L,light}}_{G^a_\mu G^b_\nu}\bigg|_{\text{UV−div}} + \Gamma^{\text{1L,heavy}}_{G^a_\mu G^b_\nu}(p^2 = 0) - \delta Z_G^{\text{aux}} \left(p^2 g^{\mu\nu} - p^\mu p^\nu\right) \delta_{ab} = 0 \tag{7.39}$$

and yields

$$\begin{aligned}
\delta Z_G^{aux} = \frac{g_s^2}{16\pi^2} \Bigg\{ &\left[-\frac{4}{3}T(F)(n_f - 1) + \frac{5}{3}C(A) \right] \Delta_\epsilon + \left[-\frac{4}{3}T(F) \left(\Delta_\epsilon - \ln \frac{m_t^2}{\mu^2} \right) \right. \\
&- \frac{4}{3}C(A) \left(\Delta_\epsilon - \ln \frac{m_{\tilde{g}}^2}{\mu^2} \right) - \frac{2}{3}T(F)n_f \left(\Delta_\epsilon - \ln \frac{m_{\tilde{q}}^2}{\mu^2} \right) \\
&\left. - \frac{1}{6}C(A) \left(\Delta_\epsilon - \ln \frac{m_{\phi^0}^2}{\mu^2} \right) - \frac{1}{6}C(A) \left(\Delta_\epsilon - \ln \frac{m_{\sigma^0}^2}{\mu^2} \right) \right] \Bigg\}
\end{aligned} \tag{7.40}$$

where the first squared brackets come from light and the second one from heavy particles running in the loop.

The $q\bar{q}G$ Vertex Correction

As for the self energies the vertex correction is composed of loops from light particles from the Standard Model and additional heavy particle loops. The contributions from Standard Model
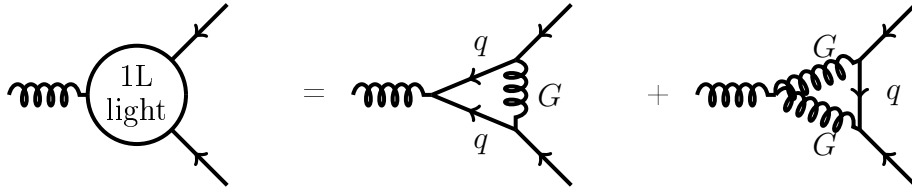

Figure 7.7: Contribution from light (Standard Model) particles to the $q\bar{q}G$ vertex correction

particles to the $q\bar{q}G$ yield

$$\begin{aligned}
i\Gamma^{\text{1L,light}}_{q_i \bar{q}_j G^a_\mu}\bigg|_{\text{UV−div}} &= -ig_s T^a_{ij}\gamma^\mu \frac{g_s^2}{16\pi^2} \left[\left(C(F) - \frac{C(A)}{2} \right) 2(B_0(0,0,0) - 2C_{00}(0,0,0,0,0)) \right. \\
&\quad \left. + C(A)(B_0(0,0,0) + 2C_{00}(0,0,0,0,0)) \right] \\
&= -ig_s T^a_{ij}\gamma^\mu \frac{g_s^2}{16\pi^2} \Delta_\epsilon \left[\left(C(F) - \frac{C(A)}{2} \right) + \frac{3}{2}C(A) \right].
\end{aligned} \tag{7.41}$$

The term in the curved brackets of eq. 7.41 corresponds to the first diagram in fig. 7.7 whereas the term with the prefactor $C(A)$ corresponds to the second diagram. The 3-point-function
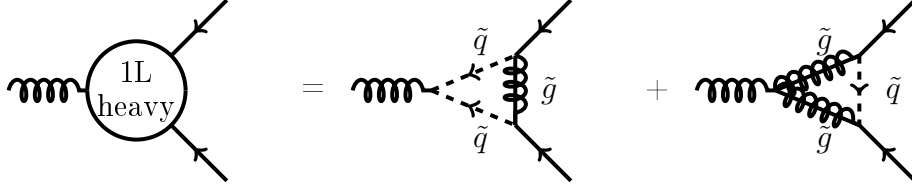
Figure 7.8: Contribution from heavy particles to the $q\bar{q}G$ vertex correction.

with only heavy particles running in the loop evaluates to

$$
\begin{aligned}
i\Gamma^{\text{1L,heavy}}_{q_i\bar{q}_jG^a_\mu}(p_i^2=0) &= -ig_sT^a_{ij}\gamma^\mu\frac{g_s^2}{16\pi^2}\left[\left(C(F)-\frac{C(A)}{2}\right)4C_{00}(0,0,0,m_{\tilde{g}}^2,m_{\tilde{q}}^2,m_{\tilde{q}}^2)\right.\\
&\qquad\qquad\left.+\,C(A)\left(B_0(0,m_{\tilde{g}}^2,m_{\tilde{q}}^2)-2C_{00}(0,0,0,m_{\tilde{g}}^2,m_{\tilde{q}}^2,m_{\tilde{q}}^2)\right)\right]\\
&= ig_sT^a_{ij}\gamma^\mu\frac{g_s^2}{16\pi^2}2C(F)B_1(0,m_{\tilde{g}}^2,m_{\tilde{q}}^2)
\end{aligned}
\tag{7.42}
$$

The argument $p_i^2=0$ of the vertex function denotes, that all external particles are taken on shell, i.e. at zero momentum.

In the second line identities from 10.6 have been used. The renormalization condition for the counterterm of the gauge coupling δg_s reads

$$
i\Gamma^{\text{1L,light}}_{q_i\bar{q}_jG^a_\mu}\bigg|_{\text{UV}-\text{div}}+i\Gamma^{\text{1L,heavy}}_{q_i\bar{q}_jG^a_\mu}(p_i^2=0)+\left[-ig_sT^a_{ij}\gamma^\mu\left(\frac{\delta g_s}{g_s}+\delta Z_q^{\text{aux}}+\frac{\delta Z_G^{\text{aux}}}{2}\right)\right]=0.
\tag{7.43}
$$

Finally one can read off $\frac{\delta g_s}{g_s}$

$$
\begin{aligned}
\frac{\delta g_s}{g_s} &= \frac{g_s^2}{16\pi^2}\left[\left(\frac{2}{3}T(F)(n_f-1)-\frac{11}{6}C(A)\right)\Delta_\epsilon+\left(\frac{5}{6}C(A)+\frac{2}{3}T(F)+\frac{1}{3}T(F)n_f\right)\Delta_\epsilon\right.\\
&\quad\left.-\frac{2}{3}C(A)\ln\frac{m_{\tilde{g}}^2}{\mu^2}-\frac{1}{3}T(F)n_f\ln\frac{m_{\tilde{q}}^2}{\mu^2}-\frac{2}{3}T(F)\ln\frac{m_t^2}{\mu^2}-\frac{1}{12}C(A)\left(\ln\frac{m_{\phi^0}^2}{\mu^2}+\ln\frac{m_{\sigma^0}^2}{\mu^2}\right)\right].
\end{aligned}
\tag{7.44}
$$

Note the only difference to the MSSM [31] is the appearence of the sgluon masses as well as a factor of two in front of the logarithm of the gluino mass which is due to twice as much degrees of freedom of the gluino in the MRSSM.

7.5 The Beta Function

The beta function describes the dependence of the gauge coupling g_s upon the energy scale μ. Writing down the action of a theory in D dimensions one needs to introduce an energy scale μ in order to keep the action dimensionless. But μ is no physical parameter and can be absorbed

into the fields and parameters. To this end one defines

$$g_{sB}(g_s, \mu) = \mu^\epsilon g_s \left(1 + \frac{\delta g_s}{g_s}\right) \tag{7.45}$$

which must not depend upon the unphysical scale μ, ergo

$$0 = \frac{\mathrm{d}g_{sB}}{\mathrm{d}\ln\mu} = \frac{\partial g_{sB}}{\partial\ln\mu} + \beta\frac{\partial g_{sB}}{\partial g_s} \tag{7.46}$$

where the definition of the beta function $\frac{\partial g_s}{\partial\ln\mu}$ has been inserted. Equation 7.46 serves to calculate $\beta(g_s, \epsilon)$. By equating coefficients and using the shortcuts

$$\frac{\beta_0^L}{2} = \frac{2}{3}T(F)(n_f - 1) - \frac{11}{6}C(A)$$
$$\frac{\beta_0^H}{2} = \frac{5}{6}C(A) + \frac{2}{3}T(F) + \frac{1}{3}T(F)n_f$$
$$L = -\frac{2}{3}C(A)\ln\frac{m_{\tilde{g}}^2}{\mu^2} - \frac{1}{3}T(F)n_f\ln\frac{m_{\tilde{q}}^2}{\mu^2} - \frac{2}{3}T(F)\ln\frac{m_t^2}{\mu^2} - \frac{1}{12}C(A)\left(\ln\frac{m_{\phi^0}^2}{\mu^2} + \ln\frac{m_{\sigma^0}^2}{\mu^2}\right)$$

so that

$$\frac{\delta g_s}{g_s} = \frac{g_s^2}{16\pi^2}\left(\frac{\beta_0^L}{2\epsilon_{\mathrm{UV}}} + \frac{\beta_0^H}{2\epsilon_{\mathrm{UV}}} + L\right) \tag{7.47}$$

one finds

$$\beta(g_s, \epsilon) = -\epsilon g_s\left(1 + \frac{g_s^2}{16\pi^2}L\right) + \beta(g_s) + \mathcal{O}(2 - \mathrm{loop}) \tag{7.48}$$

$$\beta(g_s) = \frac{g_s^3}{16\pi^2}\beta_0^L + \mathcal{O}(2 - \mathrm{loop}). \tag{7.49}$$

This is the beta function of QCD first found by Politzer [47] Gross and Wilczek [48]

7.6 Supersymmetry Restoring Counterterm

As already discussed in section 7.2 care is required in terms of supersymmetry restoring when renormalizing the gauge coupling g_s and the Yukawa coupling $\hat{g}_s$. In doing so one needs the already calculated transition counterterms of the quark, squark and gluino from eq. 7.13, 7.18 and 7.25 as well as the transition counterterm of the gluon.

The Gluon Self-Energy Revisited

The only regularization dependence of the gluon self-energy arises from the gluon loop, i.e. the last diagram in figure 7.5. With the definition of $\Gamma_{\text{DREG}}^{(1),\text{ct,trans}}$ in eq. 7.6 one obtains

$$i\Gamma_{\text{DREG},G_\mu^a G_\nu^b}^{(1),\text{ct,trans}} = -i\frac{1}{3}C(A)\frac{g_s^2}{16\pi^2}(p^2 g^{\mu\nu} - p^\mu p^\nu)\delta_{ab} \tag{7.50}$$

which translates to the transition counterterm

$$\delta Z_G^{\text{trans}} = \frac{C(A)}{3}\frac{g_s^2}{16\pi^2}. \tag{7.51}$$

The $q\bar{q}G$ Vertex Correction Revisited

The diagrams from which the supersymmetry restoring contributions to the gauge coupling correction come from are shown in figure 7.7 and evaluate to

$$i\Gamma_{\text{DREG},q_i\bar{q}_j G_\mu^a}^{(1),\text{ct,trans}} = -ig_s T_{ij}^a \gamma^\mu \frac{g_s^2}{16\pi^2}\left[\left(C(F) - \frac{C(A)}{2}\right) + \frac{C(A)}{2}\right] \tag{7.52}$$
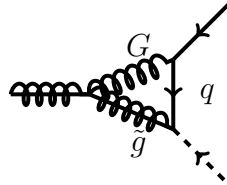
$$= -ig_s T_{ij}^a \gamma^\mu \left[\frac{\delta g_s^{\text{trans}}}{g_s} + \delta Z_q^{\text{trans}} + \frac{\delta Z_G^{\text{trans}}}{2}\right] \tag{7.53}$$

where the second line shows the supersymmetry restoring counterterms. This yields

$$\frac{\delta g_s^{\text{trans}}}{g_s} = -\frac{C(A)}{6}\frac{g_s^2}{16\pi^2}. \tag{7.54}$$

The $q\tilde{q}^\dagger\tilde{g}$ Vertex Correction

The supersymmetry restoring corrections to the Yukawa coupling originate from the diagram below. The supersymmetry restoring part is given by

Figure 7.9: Diagram of the supersymmetry restoring correction of the $q\tilde{q}\tilde{g}$ vertex

$$i\Gamma_{\text{DREG},q_i\tilde{q}_j\tilde{g}^a}^{(1),\text{ct,trans}} = -ig_s\sqrt{2}P_L T_{ij}^a \frac{g_s^2}{16\pi^2}C(A) \tag{7.55}$$

$$= -ig_s\sqrt{2}P_L T_{ij}^a \left[\frac{\delta\hat{g}_s^{\text{trans}}}{g_s} + \frac{\delta Z_q^{\text{trans}} + \delta Z_{\tilde{q}}^{\text{trans}} + \delta Z_{\tilde{g}}^{\text{trans}}}{2}\right]. \tag{7.56}$$

The supersymmetry restoring part of the Yukawa renormalization constants is therefore

$$\frac{\delta \hat{g}_s^{\text{trans}}}{g_s} = -\frac{C(F) - C(A)}{2} \frac{g_s^2}{16\pi^2}. \tag{7.57}$$

As a consequence of the two different supersymmetry restoring parts of the coupling renormalization constants an additional renormalization constant $\delta g_s^{\text{restore}}$ needs to be introduced. As described in section 7.2 it is given by

$$\frac{\delta g_s^{\text{restore}}}{g_s} = \frac{\delta \hat{g}_s^{\text{trans}}}{g_s} - \frac{\delta g_s^{\text{trans}}}{g_s} = \frac{g_s^2}{16\pi^2} \left(\frac{2C(A)}{3} - \frac{C(F)}{2} \right). \tag{7.58}$$

In short this means that the gauge coupling g_s is renormalized with δg_s given in 7.44 and the Yukawa coupling $\hat{g}_s$ is renormilzed with $\delta \hat{g}_s = \delta g_s + \delta g_s^{\text{restore}}$.

The finite correction $\delta g_s^{\text{restore}}$ is the same as in supersymmetric QCD which should not surprise too much as all its contributions originate from loops with gluons.

7.7 $\overline{\text{MS}}$ - Renormalization

To quickly check for UV-finiteness of a Greenfunction or a physical observable it is useful to have the extracted UV-divergences of the renormalization constants at hand. How these are obtained is described in 10.6.

$$\begin{aligned}
\delta Z_{\tilde{g}}^L &= -\frac{g_s^2}{16\pi^2 \epsilon_{\text{UV}}} 2\left[T(F) n_f + C(A) \right] \qquad & \delta Z_{\tilde{g}}^R &= -\frac{g_s^2}{16\pi^2 \epsilon_{\text{UV}}} 2C(A) \\
\delta m_{\tilde{g}} &= \frac{g_s^2}{16\pi^2 \epsilon_{\text{UV}}} \left[T(F) n_f - 2C(A) \right] m_{\tilde{g}} \\
\delta Z_{\tilde{q}} &= 0 & \delta m_{\tilde{q}}^2 &= 0 \\
\frac{\delta g_s}{g_s} &= \frac{g_s^2}{16\pi^2 \epsilon_{\text{UV}}} \left[T(F) n_f - C(A) \right] = 0 \\
\delta Z_{\phi^0} &= 0 & \delta m_{\phi^0}^2 &= -\frac{g_s^2}{16\pi^2 \epsilon_{\text{UV}}} \left[8T(F) n_f - 16C(A) \right] m_{\tilde{g}}^2 \\
\delta Z_{\sigma^0} &= 0 & \delta m_{\sigma^0}^2 &= 0 \\
\delta Z_G &= -\frac{g_s^2}{16\pi^2 \epsilon_{\text{UV}}} 2T(F) n_f
\end{aligned} \tag{7.59}$$

Note that the renormalization constants $\delta m_{\tilde{g}}$, $\delta m_{\phi^0}^2$ and $\delta m_{\sigma^0}^2$ are not independent from each other as the masses of the gluino and the two sgluons stam from only two parameters, i.e. $m_{\tilde{g}}$ and m_σ^2 from the softly breaking part of the Lagrangian, eq. 4.17. In additions it happens that the particle content of RSQCD is such that $\frac{\delta g_s}{g_s} = 0$. This means that the β function of g_s equals zero at 1-loop-level if one does not choose to decouple heavy particles from the running as has been done in this thesis. However at 2-loop-level there is a non-zero β function of g_s, which has been calculated by SARAH [49–52].

7.8 The Renormalized Matrix Element

After having renormalized the matrix element for squark production all UV-divergences are removed. This has been achieved by extending the model file, generated by `SARAH` with counterterm Feynman rules and the above calculated renormalization constants. The derivation of the counterterm Feynman rules has been performed by the author whereas the implementation in the modelfile was mainly done by another member of the group. The renormalization constants for masses and fields are calculated by functions like MASSRC and FIELDRC [46]. Their result has been checked with the above calculated renormalization constants.

To keep track of all divergences, the calculation has been performed with the option: DIMENSIONS $\to 0$. This is the only opportunity in `FormCalc` to really work in D dimensions, i.e. the result contains a quantity $Dminus4$ which equals -2ϵ in DREG. The absolute matrix element coming from `FormCalc` is given in terms of scalar integrals, like defined in appendix 10.6.

To extract infrared divergences `LoopTools` has been used. This tool provides the function SETLAMBDA which can be set to 0, -1 or -2 to extract the finite part, single pole or double pole of scalar integrals. This allows for numerically extracting the coefficients of ϵ^i with $i \in \{0, -1, -2\}$ of the absolute squared matrix amplitude. The respective poles of $|\mathcal{M}^{\mathrm{V}}_{\mathrm{MRSSM}}(uu \to \tilde{u}_L \tilde{u}_R)|^2$ are shown in figure **??**. In addition the tree-level absolute squared matrix amplitude with leading order α_s is compared with its analogue with next-to-leading order α_s and virtual absolute squared matrix amplitude. The latter is not given analytically. All $|\mathcal{M}|^2$ are color and spin averaged in the final state and summed over in the initial state.
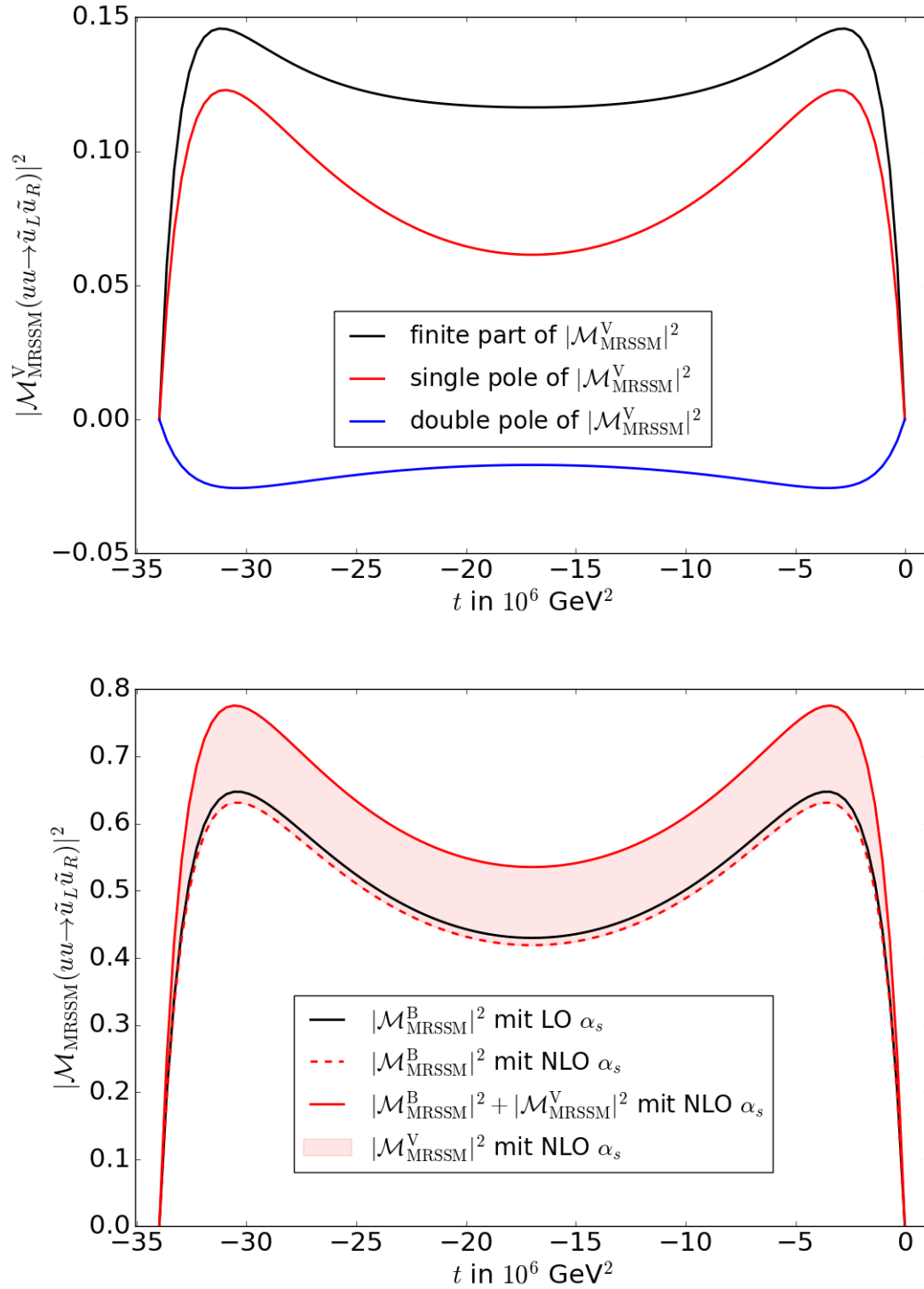
Figure 7.10: The figure at the top shows the coefficients of $\mathcal{O}(\epsilon^0)$, $\mathcal{O}(\epsilon^{-1})$ and $\mathcal{O}(\epsilon^{-2})$ terms of the absolute squared matrix element of $uu \to \tilde{u}_L \tilde{u}_R$ in the MRSSM as a function of the Mandelstam variable t. External helicities and colors are averaged. The parameters are fixed to $m_{\tilde{q}} = \mu = 1000\,\mathrm{GeV}$, $m_{\tilde{g}} = 2000\,\mathrm{GeV}$, $m_\sigma = 5000\,\mathrm{GeV}$ and $\sqrt{s} = 6000\,\mathrm{GeV}$ which is the partnoic center of mass energy.

The figure at the bottom shows the absolute squared matrix element of $uu \to \tilde{u}_L \tilde{u}_R$ in the MRSSM at tree-level with $\alpha_s = $ from the leading order parton density function MMHT2014 [32], and $\alpha_s = $ from the netxt-to-leading order parton density function as well as the contribution from the virtual absolute squared matrix element.

8 Squark Production at One-Loop

8.1 The LSZ Theorem

The LSZ theorem [53] or LSZ reduction formula prescribes how to obtain the S-matrix element, i.e. a physical observable, from the time ordered correlation function of the respective field operators. The time ordered correlation function of fields in an interacting theory can be calculated perturbatively with the aid of the Gell-Mann and Low theorem and the Wick theorem.

Considering a physical process with kinematics $\vec{k}_1 \ldots \vec{k}_n \to \vec{p}_1 \ldots \vec{p}_m$ and taking for the sake of simplicity only one scalar field ϕ the Fourier transform of the time ordered product of a correlation function is related to the corresponding S-matrix element like[22]

$$\prod_{i=1}^{n} \int \mathrm{d}x_i \; \mathrm{e}^{ip_i x_i} \prod_{j=1}^{m} \int \mathrm{d}y_j \; \mathrm{e}^{ik_j y_j} \left\langle \Omega | \mathcal{T} \left[\phi(x_1) \ldots \phi(x_n) \phi(y_1) \ldots \phi(y_m) \right] | \Omega \right\rangle$$

$$\sim \prod_{i=1}^{n} \frac{i\sqrt{Z}}{p_i^2 - m^2 + i\epsilon} \prod_{j=1}^{m} \frac{i\sqrt{Z}}{k_j^2 - m^2 + i\epsilon} \left\langle \vec{p}_1 \ldots \vec{p}_n | S | \vec{k}_1 \ldots \vec{k}_m \right\rangle . \tag{8.1}$$

Here $\mathcal{T}$ denotes the time ordering operator, $|\Omega\rangle$ is the ground state of the interacting theory and $\sqrt{Z}$ is the residue of the single particle pole in the two-point function

$$\int \mathrm{d}x \; \mathrm{e}^{ipx} \left\langle \Omega | \mathcal{T} \left[\phi(x)\phi(0) \right] | \Omega \right\rangle = \frac{i}{p^2 - m_0^2} + \frac{i}{p^2 - m_0^2} \left(\frac{i\Sigma(p^2)}{p^2 - m_0^2} \right) + \frac{i}{p^2 - m_0^2} \left(\frac{\Sigma(p^2)}{p^2 - m_0^2} \right)^2 + \ldots$$

$$= \frac{i}{p^2 - m_0^2 - \Sigma(p^2)} . \tag{8.2}$$

The parameter m_0 is the tree-level mass and the quantity $-i\Sigma(p^2)$ denotes the sum of all
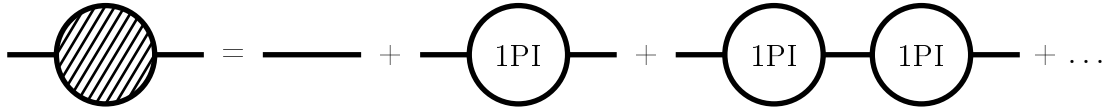
Figure 8.1: Diagrammatic figure of the two-point function of a scalar field: The propagator in an interaction theory can be calculated in a perturbation series in the coupling constant.

one-particle-irreducible contributions to the particle's self-energy. From eq. 8.2 one can read off the physical mass m^2 of the particle which is associated with the field ϕ. It is determined as the value of p^2 where the propagator has a pole, i.e.

$$\left[p^2 - m_0^2 - \Sigma(p^2) \right]_{p^2 = m^2} = 0 \tag{8.3}$$

---

[22]In this subsection the $\sim$ indicates that the poles on either side are the same provided that all momenta are close to their mass shell, i.e. $p_i^0 \to E_{\vec{p}_i}$ and $k_j^0 \to E_{\vec{k}_j}$.
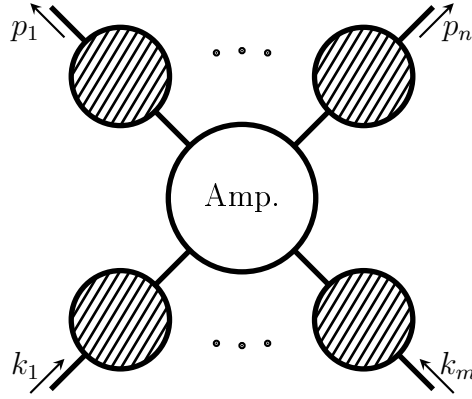
Close to the pole the denominator of eq. 8.2 can by expanded like

$$p^2 - m_0^2 - \Sigma(p^2) = (p^2 - m^2)\left(1 - \frac{\partial \Sigma(p^2)}{\partial p^2}\right)_{p^2=m^2} + \mathcal{O}((p^2 - m^2)^2). \tag{8.4}$$

The residue of the propagator can therefore be written as

$$Z = \left(1 - \frac{\partial \Sigma(p^2)}{\partial p^2}\right)^{-1}_{p^2=m^2}. \tag{8.5}$$

Now considers the full $(n+m)$-point function in scalar theory. One can decompose it into an amputated $(n+m)$-point function and "full" propagators like written in eq. 8.2 and depicted in fig. 8.1.

Figure 8.2: Diagrammatic figure of a "full" $(n+m)$-point function. Apart from the "full" propagators there is the "full" amputated $(n+m)$-point function

Inserting the expression

$$\frac{i}{p^2 - m_0^2 - \Sigma(p^2)} \sim \frac{iZ}{p^2 - m^2} \tag{8.6}$$

for the full propagators one notices the same singularity as in eq. 8.1. If one now compares the coefficients of these poles in eq. 8.1 one finds

$$\left\langle \vec{p}_1 \ldots \vec{p}_n \right| S \left| \vec{k}_1 \ldots \vec{k}_m \right\rangle = \sqrt{Z}^{n+m}.$$

Now it becomes visible why the renormalization in the on-shell scheme

$$\left.\frac{\partial \Sigma(p^2)}{\partial p^2}\right|_{p^2=m^2} \overset{!}{=} 0 \tag{8.7}$$

introduces no further manipulation when turning from the correlation function to the S-matrix-element because $Z = 1$ in on-shell renormalization. Furthermore the on-shell condition for the mass renormalization

$$\Sigma(p^2)|_{p^2=m^2} = 0 \tag{8.8}$$

means that the physical mass equals the tree level mass.

8.2 The Squark Production Cross Section at Next-to-Leading Order

The squark production cross section at next-to-leading order is composed out of three contributions. These are the Born or tree-level cross section, the virtual correction and the real correction.

$$\sigma^{\mathrm{NLO}} = \sigma^{\mathrm{B}} + \sigma^{\mathrm{V}} + \sigma^{\mathrm{R}} \tag{8.9}$$

All three contributions have to be calculated with next-to-leading parton density functions.
It has been checked that for multiple different and quite distinct choices of the parameters $m_{\tilde{q}}$ and $m_{\tilde{g}}$ the double as well as the single poles of the virtual and real correction cancel up to machine precision. As the real corrections have been calculated analytically it is possible to quote the double pole. With

$$\sigma^{\mathrm{R}}_{\mathrm{double\ pole}} = -\sigma^{\mathrm{V}}_{\mathrm{double\ pole}} = C(F)\frac{\alpha_s}{\pi}\sigma^{\mathrm{B}}\frac{1}{\epsilon^2} \tag{8.10}$$

it has a very succinct form.
The setup of the calculation is summarized in fig. 8.3. Both the virtual and the Born matrix amplitude have been generated with the `Mathematica` package `FeynArts`. To this end a modelfile generated by the `Mathematica` package `SARAH` has been adjusted by hand to include counterterm Feynman rules and the definition of those counterterms. The matrix amplitudes have been processed further to the absolute squared matrix amplitudes by the `Mathematica` package `FormCalc` which have then been converted to `C++` and stored in an output file.
This output file is in turn invoked by a `C++` code which evaluates the scalar integrals of the absolute squared matrix amplitudes numerically by using the package `LoopTools` [54]. Finally the phase space integration is performed by the integration routine "Cuhre" which is part of the `CUBA` library [55].
Comment on how real corrections are processed.
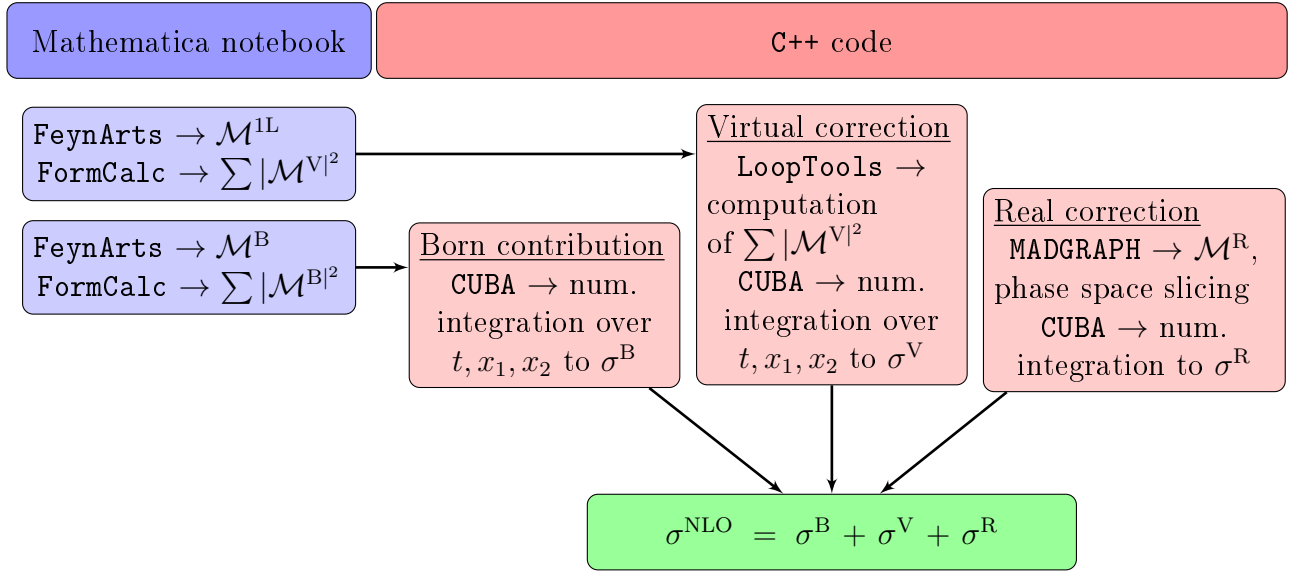
Figure 8.3: This scheme illustrates the setup of the computation of the next-to-leading order cross section. The absolute squared matrix amplitudes of the Born or tree-level contribution and the virtual correction are generated by `Mathematica` packages and imported into a `C++` code. Loop integrals are evaluated numerically using `Looptools`. For all three contributions the `CUBA`-library was used for the phase space and x_1 and x_2 integration to arrive at the cross sections σ^{B}, σ^{V} and σ^{V}.

8.2.1 Remark on Prefactors in the Calculation

For the discussion of results it will not been distinguished between virtual and real corrections. This is because they have not been separated strictly in the calculation: As already discussed both σ^{V} and σ^{R} are divergent, i.e. there are poles of the form $\frac{1}{\epsilon}$ and $\frac{1}{\epsilon^2}$. But these pole cancel completely. On the other hand there are also prefactors from the phase space integral and the loop integral, with can be expanded in a power series in ϵ. In short, the virtual and real correction to the cross section can be expressed with some coefficients $A - E$, which are functions of the parameters $m_{\tilde{g}}$ and $m_{\tilde{q}}$, in the following way

$$\sigma^{\mathrm{V}} = \left(1 + (A^{\mathrm{V}} + P_1)\epsilon + (B^{\mathrm{V}} + P_2)\epsilon^2 + \mathcal{O}(\epsilon^3)\right)\left(C^{\mathrm{V}} - \frac{D}{\epsilon} - \frac{E}{\epsilon^2}\right), \tag{8.11}$$

$$\sigma^{\mathrm{R}} = \left(1 + (A^{\mathrm{R}} + P_1)\epsilon + (B^{\mathrm{R}} + P_2)\epsilon^2 + \mathcal{O}(\epsilon^3)\right)\left(C^{\mathrm{R}} + \frac{D}{\epsilon} + \frac{E}{\epsilon^2}\right). \tag{8.12}$$

Here, the coefficients A, B and C are in general distinct in the virtual and real part, but D and E are the same as the poles of both contributions cancel exactly.

Now some of the prefactors, namely P_1 and P_2, are the same in both contributions. Just keeping them like in eq. (8.12) would slow the computation of the real part down by a factor

5 because this part of the calculation is done analytically. Therefore a speed-up has been achieved by discarding the common prefactors at the cost of loosing track about the origin of the next-to-leading order correction.

A common prefactor comes from the two-body phase space integral in eq. (6.4)

$$
\frac{(4\pi)^\epsilon}{\Gamma(1-\epsilon)} \left(\frac{tu - m_{\tilde{q}}^4}{\mu^2 s} \right)^{-\epsilon} = 1 + \epsilon \left(\ln 4\pi - \gamma_E - \ln \frac{tu - m_{\tilde{q}}^4}{\mu^2 s} \right) + \epsilon^2 \left(\frac{1}{2} \left(\ln 4\pi - \ln \frac{tu - m_{\tilde{q}}^4}{\mu^2 s} \right)^2 \right.
$$
$$
\left. + \frac{\gamma_E^2}{2} - \frac{\pi^2}{12} - \gamma_E \left(\ln 4\pi - \ln \frac{tu - m_{\tilde{q}}^4}{\mu^2 s} \right) \right) + \mathcal{O}(\epsilon^3). \tag{8.13}
$$

In addition the prefactor of a loop integral defined in `LoopTools` differs from the one usually, and therefore also here, used. The `LoopTools` definition [**?**] of a loop integral is

$$
T_{\mu_1\ldots\mu_P}^N = \frac{\mu^{4-D}}{i\pi^{\frac{D}{2}} r_\Gamma} \int \mathrm{d}^D q \frac{q_{\mu_1} \ldots q_{\mu_P}}{[q^2 - m_1^2][(q+p_1)^2 - m_2^2] \ldots [(q + p_1 + \ldots + p_{N-1})^2 - m_N^2]} \tag{8.14}
$$

where T^1 is an A-integral, T^2 is an B-integral, etc. and $r_\Gamma = \frac{\Gamma(1-\epsilon)^2 \Gamma(1+\epsilon)}{\Gamma(1-2\epsilon)}$, where $\Gamma(z)$ is the Gamma function. Comparing the prefactors of eq. (8.14) and eq. (10.26) one finds that one has to multiply the `LoopTools` output by

$$
r_\Gamma (4\pi)^\epsilon = 1 + \epsilon(\ln 4\pi - \gamma_E) + \epsilon^2 \left(\frac{\gamma_E^2}{2} - \frac{\pi^2}{12} + \frac{\ln^2 4\pi}{2} - \gamma_E \ln 4\pi \right) + \mathcal{O}(\epsilon^3) \tag{8.15}
$$

in order to have the same prefactors as in eq. (10.26). The right hand side of eq. (8.13) and eq. (8.15) are the prefactors discarded in the computation. Instead the prefactor ??? has been included in the virtual correction.

8.2.2 K-factors for Squark Production in the MRSSM

A common way to describe next-to-leading order corrections is stating the K-factor, which is defined to be the ratio of the complete next-to-leading order cross section σ^{NLO}, see eq. (8.9) and the leading order cross section σ^{LO}:

$$
K(X \to Y) = \frac{\sigma^{\mathrm{NLO}}(X \to Y)}{\sigma^{\mathrm{LO}}(X \to Y)}. \tag{8.16}
$$

The process in question is described by $X \to Y$. Figure 8.4 shows the K-factor for the production of up-squarks in the MRSSM for varying masses of both the squark ($m_{\tilde{g}} = 2000\,\mathrm{GeV}$) and the gluino $m_{\tilde{q}} = 1000\,\mathrm{GeV}$. The mass of the pseudoscalar has been fixed to $m_\sigma = 5000\,\mathrm{GeV}$ in both plots. It can be seen that the K-factor increases with increasing squark mass and decreases with increasing gluino mass. Note that the sum of virtual and real corrections gets negative for very light squarks. But this region of parameter space is already excluded

phenomenologically. Calculate uncertainties for multiple points(pdf, scale, integration)
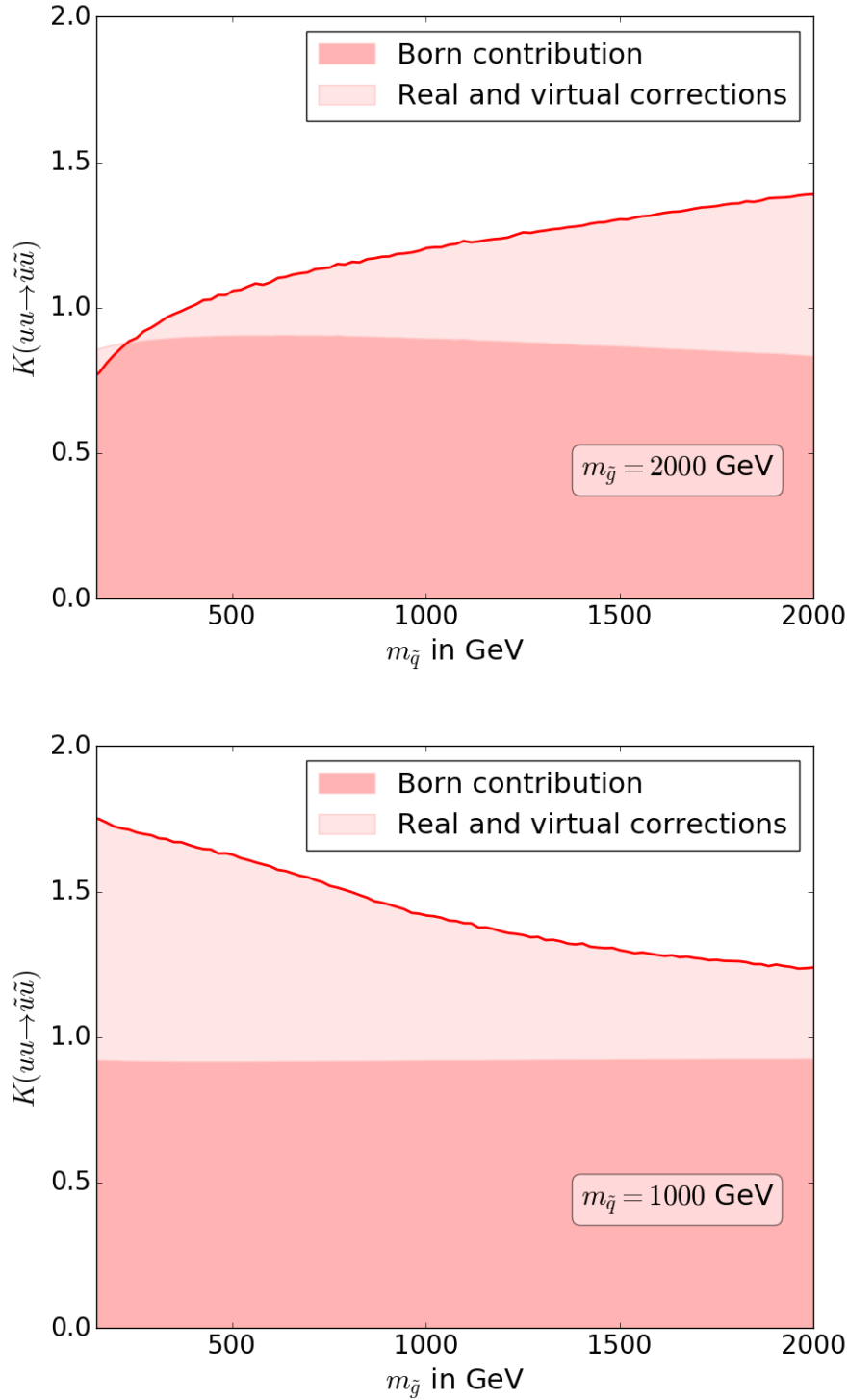
Figure 8.4: Dependence of the K-factor for the process $uu \to \tilde{u}\tilde{u}$ on the squark mass $m_{\tilde{q}}$ for fixed $m_{\tilde{g}} = 2000\,\text{GeV}$ (top) and on the gluino mass $m_{\tilde{g}}$ for fixed $m_{\tilde{q}} = 1000\,\text{GeV}$ (bottom).

8.3 The Cross Section in the Limit of Large Sgluon Masses

The cross section for squark production does not exist in the limit of an infinitely large sgluon mass, instead it was found that it diverges logarithmically.

$$\lim_{m_\sigma \to \infty} \sigma(qq \to \tilde{q}\tilde{q}) \sim \ln \frac{m_\sigma^2}{\mu^2} \tag{8.17}$$

This is actually expected as an effective field theory of the MRSSM where the sgluon is integrated out is no longer supersymmetric. This is because the sgluon is together with the octino part of a supermultiplet. Integrating out only the sgluon means that the octino misses its superpartner in the effective field theory. In this case the decoupling theorem [56] does no longer hold.

It is even possible to predict the logarithmic scaling of $\sigma(qq \to \tilde{q}\tilde{q})$ quantitatively. The coefficient of the logarithm is proportional to the difference of the one-loop β function coefficients of g_s and $\hat{g}_s$ in the effective theory with the heavy particle integrated out, see eq. (4) in [57].
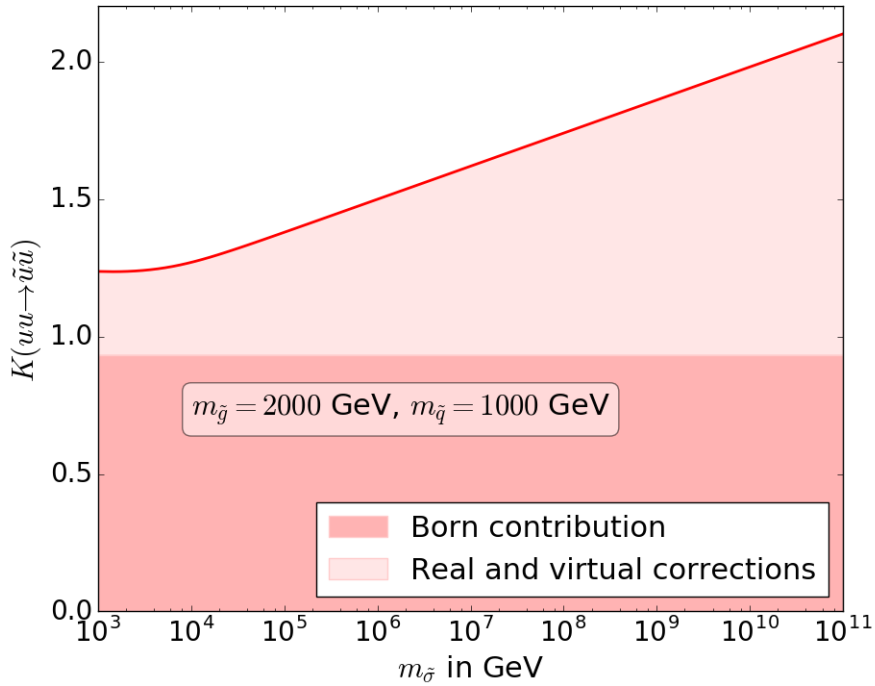
Figure 8.5: Dependence of the K-factor for the process $uu \to \tilde{u}\tilde{u}$ on the mass of the pseudoscalar sgluon. For $m_\sigma \approx 10^5$ GeV onwards want find a logarithmic scaling as predicted by [57].

9 Summary and Outlook

10 Appendix

10.1 System of Units and Metric

In this thesis the natural units are used, i.e. $c = \hbar(= k_B) = 1$. Furthermore the Minkowski metric is chosen to be

$$g^{\mu\nu} = \text{diag}(1, -1, -1, -1). \tag{10.1}$$

10.2 Constants of the Color Algebra $SU(N)$

[Marina von Steinkirch]
Tha Casimir operator $C(R)\mathbb{1}$ of a semi-simple Lie algebra in the irreducible representation R is given by

$$g^{ab}T^a(R)T^b(R) = C(R)\mathbb{1} \tag{10.2}$$

where $T^a(R)$ is the a-th generator of the matrix valued representation R, g^{ab} is the metric of group, $C(R)$ is the Quadratic Casimir invariant of the representation R and $\mathbb{1}$ is the identity in the representation space.
Apart from $C(R)$ it is common to define the Dynkin-Index $T(R)$:

$$\text{Tr}\left[T^a(R)T^b(R)\right] = T(R)\delta^{ab}. \tag{10.3}$$

The two constants are connected by

$$C(R) \cdot \dim(R) = T(R) \cdot \dim(G) \tag{10.4}$$

where $\dim(G)$ is the dimension of the group and $\dim(R)$ is the dimension of the irreducible representation R.
In the case of $SU(N)$ one has a diagonal metric $g^{ab} = \delta^{ab}$ and therefore 10.2 turns to

$$\sum_a (T^a(R))^2 = C(R)\mathbb{1}_{\dim(R)\times\dim(R)} \tag{10.5}$$

and one can write down the following useful formulae for the fundamental representation $R = F$: $T_{ij}^a = \frac{\lambda_{ij}^a}{2}$ and the adjoint representation $R = A$: $(T_{ij}^a)^{adj} = -if_{aij}$

$$T_{ik}^a T_{kj}^a = C(F)\mathbb{1}_{ij} \qquad\qquad \text{with } C(F) = \frac{N^2-1}{2N} = \frac{4}{3}$$

$$f^{abc}f^{dbc} = C(A)\delta^{ad} \qquad\qquad \text{with } C(A) = N = 3$$

$$\text{Tr}\left[T^a T^b\right] = T(F)\delta^{ab} \qquad\qquad \text{with } T(F) = \frac{1}{2} \qquad (10.6)$$

where λ_{ij}^a are for $N_c = 3$ the Gell-Mann matrices and f_{abc} are the structure constants of $SU(N_c)$.

10.3 Weyl basis and 2-spinor notation

As representation of the γ-matrices the Weyl or chiral representation is chosen:

$$\gamma^\mu = \begin{pmatrix} 0 & \sigma^\mu \\ \overline{\sigma}^\mu & 0 \end{pmatrix} \qquad\qquad \gamma_5 = \begin{pmatrix} -\mathbb{1}_2 & 0 \\ 0 & \mathbb{1}_2 \end{pmatrix} \qquad (10.7)$$

with

$$\sigma^\mu = \begin{pmatrix} \mathbb{1}_2 & \sigma^i \end{pmatrix}, \qquad\qquad \overline{\sigma}^\mu = \begin{pmatrix} \mathbb{1}_2 & -\sigma^i \end{pmatrix}, \qquad (10.8)$$

where σ^i are the Pauli matrices and $\mathbb{1}_n$ is the $n \times n$ unit matrix. The left and right handed projectors are then given by

$$P_L = \frac{1}{2}(\mathbb{1}_4 - \gamma_5)\begin{pmatrix} \mathbb{1}_2 & 0 \\ 0 & 0 \end{pmatrix} \qquad\qquad P_R = \frac{1}{2}(\mathbb{1}_4 + \gamma_5)\begin{pmatrix} 0 & 0 \\ 0 & \mathbb{1}_2 \end{pmatrix} \qquad (10.9)$$

The representation of generators of the Lorentz group on 4-spinor space are composed of the above matrices. Because of the block form of those it is not surprising that the representation on 4-spinor space is reducible to two representations on 2-spinor (Weyl spinor) spaces. It is therefore sensible to decompose a 4 spinor into a left and a right handed Weyl spinor[23]

$$\Psi = \begin{pmatrix} \psi_\alpha \\ \overline{\chi}^{\dot{\alpha}} \end{pmatrix} \qquad (10.10)$$

where $\alpha, \dot{\alpha} \in \{1, 2\}$. Left handed Weyl spinors are labeled with undotted and right handed Weyl spinors with dotted indices. One distinguishes 4 different Weyl spinors:

$$\psi^\alpha, \qquad \overline{\psi}^{\dot{\alpha}} = (\psi^\alpha)^*, \qquad \psi_\alpha = \epsilon_{\alpha\beta}\psi^\beta, \qquad \text{and} \qquad \psi_{\dot{\alpha}} = \epsilon_{\dot{\alpha}\dot{\beta}}\psi^{\dot{\beta}} = (\psi_\alpha)^*, \qquad (10.11)$$

---

[23]The projectors in the chiral basis (eq. 10.9) explain the names left and right handed Weyl spinors.

where $*$ denotes complex conjugation and indices are lowered with the antisymmetric $\epsilon_{\alpha\beta}$ ($\epsilon_{\dot{\alpha}\dot{\beta}}$), which obeys

$$\epsilon^{\alpha\beta} = \epsilon_{\beta\alpha}, \; \epsilon^{\dot{\alpha}\dot{\beta}} = \epsilon_{\dot{\beta}\dot{\alpha}} \qquad \text{and} \qquad \epsilon_{12} = \epsilon_{\dot{1}\dot{2}} = 1. \qquad (10.12)$$

By virtue of the antisymmetry of ϵ one finds the Lorentz invariant products:

$$\psi\chi := \psi^{\alpha}\chi_{\alpha} = -\chi_{\alpha}\psi^{\alpha} = \chi^{\alpha}\psi_{\alpha} = \chi\psi,$$
$$\overline{\psi}\overline{\chi} := \overline{\psi}_{\dot{\alpha}}\overline{\chi}^{\dot{\alpha}} = -\overline{\chi}^{\dot{\alpha}}\overline{\psi}_{\dot{\alpha}} = \overline{\chi}_{\dot{\alpha}}\overline{\psi}^{\dot{\alpha}} = \overline{\chi}\overline{\psi} \qquad (10.13)$$

To make the index structure of the Pauli matrices explicit one writes $\sigma^{\mu}_{\alpha\dot{\alpha}}$ and $\overline{\sigma}^{\mu\dot{\alpha}\alpha}$ for the formulae in 10.8. For the definition of the supersymmetry algebra in section 3.1 the representation of the generators of the Lorentz group on the left and right handed Weyl spinor space are introduced:

$$\frac{1}{2}(\sigma^{\mu\nu})_{\alpha}{}^{\beta} := \frac{i}{4}(\sigma^{\mu}\overline{\sigma}^{\nu} - \sigma^{\nu}\overline{\sigma}^{\mu})_{\alpha}{}^{\beta}$$
$$\frac{1}{2}(\overline{\sigma}^{\mu\nu})^{\dot{\alpha}}{}_{\dot{\beta}} := \frac{i}{4}(\overline{\sigma}^{\mu}\sigma^{\nu} - \overline{\sigma}^{\nu}\sigma^{\mu})^{\dot{\alpha}}{}_{\dot{\beta}} \qquad (10.14)$$

With the definition of bared and charge conjugated 4-spinors[24]

$$\overline{\Psi} := \Psi^{\dagger}\gamma^0, \qquad\qquad \Psi^C := i\gamma^2\gamma^0\overline{\Psi}^T \qquad (10.15)$$

one obtains:

$$\Psi = \begin{pmatrix} \psi_{\alpha} \\ \overline{\chi}^{\dot{\alpha}} \end{pmatrix}, \qquad\qquad \overline{\Psi} = \begin{pmatrix} \chi^{\alpha} & \overline{\psi}_{\dot{\alpha}} \end{pmatrix},$$
$$\Psi^C = \begin{pmatrix} \chi_{\alpha} \\ \overline{\psi}^{\dot{\alpha}} \end{pmatrix}, \qquad\qquad \overline{\Psi}^C = \begin{pmatrix} \psi^{\alpha} & \overline{\chi}_{\dot{\alpha}} \end{pmatrix}. \qquad (10.16)$$

The 4-spinor of an arbitrary quark q is given in terms of Weyl spinors q_L and $\overline{q}_R$ by

$$q = \begin{pmatrix} q_L \\ \overline{q}_R \end{pmatrix} \qquad (10.17)$$

whereas the 4-spinor of the Dirac gauginos is given in terms of the Weyl spinors λ and $\overline{\chi}$[25]

$$\tilde{g}^a = \begin{pmatrix} -i\lambda^a \\ i\overline{\chi}^a \end{pmatrix} \qquad (10.18)$$

---

[24]Ψ^T denotes the transpose of the spinor Ψ and $\Psi^{\dagger}$ is the Hermitian adjoint of Ψ.

[25]λ is the superpartner of the gluon, called the gluino and $\overline{\chi}$ is the Weyl spinor of the chiral superfield which is associated with the gluon, called the octino.

10.4 Anticommuting numbers

Anticommuting numbers θ^α are also referred to as Grassmann numbers and are defined by $\theta^\alpha \theta^\beta = -\theta^\beta \theta^\alpha$ and commute with ordinary numbers.

They occur in superspace formalism in the form of 2 tuples, i.e. θ^α with $\alpha = 1, 2$. The complex conjugate of this tuple is denoted with $\overline{\theta}^{\dot\alpha}$. Derivatives are defined by

$$\partial^\alpha \theta_\beta := \frac{\partial}{\partial \theta_\alpha} \theta_\beta := \delta^\alpha_\beta \qquad\qquad \partial_\alpha \theta^\beta := \frac{\partial}{\partial \theta^\alpha} \theta^\beta := \delta^\beta_\alpha$$

$$\overline{\partial}^{\dot\alpha} \overline{\theta}_{\dot\beta} := \frac{\partial}{\partial \overline{\theta}_{\dot\alpha}} \overline{\theta}_{\dot\beta} := \delta^{\dot\alpha}_{\dot\beta} \qquad\qquad \overline{\partial}_{\dot\alpha} \overline{\theta}^{\dot\beta} := \frac{\partial}{\partial \overline{\theta}^{\dot\alpha}} \overline{\theta}^{\dot\beta} := \delta^{\dot\beta}_{\dot\alpha} \qquad (10.19)$$

whereby one needs to be cautious as these definitions imply

$$\partial_\alpha = -\epsilon_{\alpha\beta} \partial^\beta \qquad\qquad \partial_{\dot\alpha} = -\epsilon_{\dot\alpha\dot\beta} \partial^{\dot\beta}. \qquad (10.20)$$

Integrals are defined by:

$$\int d\theta_\alpha \, (a + b\theta^\beta + c\theta^\beta \theta^\gamma) := b\delta^\beta_\alpha + c(\delta^\beta_\alpha \theta^\gamma - \delta^\gamma_\alpha \theta^\beta) \qquad \text{and}$$

$$\int d\theta_\alpha \, (a\overline{\theta}^{\dot\beta}) := (a\overline{\theta}^{\dot\beta}) \int d\theta_\alpha \qquad (10.21)$$

where the first line mirrows the claim of translation invariance. One furthermore introduces the shortcuts

$$\int d\theta^2 := \int \frac{1}{4} \epsilon_{\alpha\beta} d\theta^\alpha d\theta^\beta, \qquad \int d\overline{\theta}^2 := \int \frac{1}{4} \epsilon_{\dot\alpha\dot\beta} d\theta^{\dot\alpha} d\theta^{\dot\beta}, \qquad \text{and}$$

$$\int d^4\theta := \int d\theta^2 d\overline{\theta}^2. \qquad (10.22)$$

For the definition of (anti-)chiral superfields and the field strength chiral superfields it proves useful to introduce supersymmetry (or chiral) covariant derivatives

$$\mathcal{D}_\alpha := \frac{\partial}{\partial \theta^\alpha} - i(\sigma^\mu \overline{\theta})_\alpha \partial_\mu \qquad\qquad \mathcal{D}^{\dot\alpha} := \frac{\partial}{\partial \overline{\theta}_{\dot\alpha}} - i(\overline{\sigma}^\mu \theta)^{\dot\alpha} \partial_\mu$$

$$D^\alpha := \epsilon^{\alpha\beta} D_\beta = -\frac{\partial}{\partial \theta_\alpha} + i(\overline{\theta}\overline{\sigma}^\mu)^\alpha \partial_\mu \qquad \mathcal{D}_{\dot\alpha} := \epsilon_{\dot\alpha\dot\beta} \mathcal{D}^{\dot\beta} = -\frac{\partial}{\partial \overline{\theta}^{\dot\alpha}} + i(\sigma^\mu \theta)_{\dot\alpha} \partial_\mu. \qquad (10.23)$$

By construction they are supersymmetry invariant, i.e. they fulfill the following anticommutation relations with the supersymmetry generators from eq. 3.2:

$$\{Q_\alpha, \mathcal{D}_\beta\} = \{\overline{Q}_{\dot\alpha}, \mathcal{D}_\beta\} = \{Q_\alpha, \mathcal{D}_{\dot\beta}\} = \{\overline{Q}_{\dot\alpha}, \mathcal{D}_{\dot\beta}\} = 0 \qquad (10.24)$$

10.5 Feynman rules for the RSQCD

The following Feynman rules are derived from the Lagrangian of the R-symmetric supersymmetric quantum chromodynamics (RSQCD) eq. 4.17. When compared with the Feynman rules of the supersymmetric QCD the diagrams involving scalar gluons are new. In addition the gluon-quark-squark vertex is different in RSQCD for the gauginos are Dirac fermions. Note that for calculations involving fermions one needs to go in the opposite direction of the fermion flow which is given by a curved arrow next to the diagrams in fig. 10.2 and does not always agree with the flow of fermion number given by the direction of the Dirac propagator. This renders the evaluation of fermion number violating processes like $qq \rightarrow \tilde{q}\tilde{q}$ unambiguous, cf. [31].

① $(\sigma^0)^a$ ----------- $(\sigma^0)^b$ $\;\hat{=}\; \frac{i}{p^2-m_{\sigma^0}^2+i\varepsilon}\delta_{ab}$

② $(\phi^0)^a$ ----------- $(\phi^0)^b$ $\;\hat{=}\; \frac{i}{p^2-m_{\phi^0}^2+i\varepsilon}\delta_{ab}$

③ $\tilde{q}_{Ai}$ ----◄---- $\tilde{q}_{Bj}^{\dagger}$ $\;\hat{=}\; \frac{i\delta_{AB}}{p^2-m_{\tilde{q}}^2+i\varepsilon}\delta_{ij}$

④ q_i ————◄———— $\bar{q}_j$ $\;\hat{=}\; i\frac{\not{p}+m_q}{p^2-m_q^2+i\varepsilon}\delta_{ij}$

⑤ G_μ^a ⦙⦙⦙⦙⦙⦙⦙⦙ G_ν^b $\;\hat{=}\; -\,i\frac{g^{\mu\nu}}{p^2+i\varepsilon}\delta_{ab}$

⑥ $\tilde{g}^a$ ⦙⦙⦙⦙⦙⦙⦙⦙ $\bar{\tilde{g}}^b$ $\;\hat{=}\; i\frac{\not{p}+m_{\tilde{g}}}{p^2-m_{\tilde{g}}^2+i\varepsilon}\delta_{ab}$

⑦ c^a ·······◄······· $\bar{c}^b$ $\;\hat{=}\; \frac{i}{p^2+i\varepsilon}\delta_{ab}$

⑧ G_μ^a (to $\bar{q}i$ and q_j) $\;\hat{=}\; -\,ig_s T_{ij}^a\gamma^\mu$

⑨ G_μ^a (to $\tilde{q}_{Ai}^{\dagger}(-p_1)$ and $\tilde{q}_{Bj}(p_2)$) $\;\hat{=}\; -\,ig_s(p_2+p_1)^\mu T_{ij}^a\delta_{AB}$

⑩ G_μ^a, $\tilde{q}_{Ai}^{\dagger}$, G_ν^b, $\tilde{q}_{Bj}$ $\;\hat{=}\; ig_s^2 g^{\mu\nu}\left\{T^a,T^b\right\}_{ij}\delta_{AB}$

⑪ $G_\mu^a(p_a)$, $G_\rho^c(p_c)$, $G_\nu^b(p_b)$ $\;\hat{=}\; -\,g_s f_{abc}\left[g_{\mu\nu}(p_a-p_b)^\rho +\; g_{\nu\rho}(p_b-p_c)^\mu + g_{\rho\mu}(p_c-p_a)^\nu\right]$
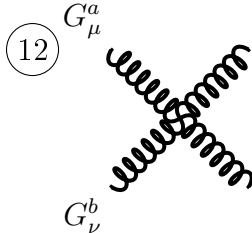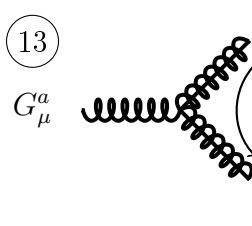
Figure 10.1: In the Feynman diagrams of the propagators the momentum is flowing from the right to the left hand side.
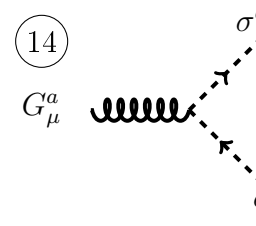In the Feynman diagrams of the vertices all momenta flow towards the vertex, i.e. in diagram 9 $-p_1$ is flowing towards the vertex.
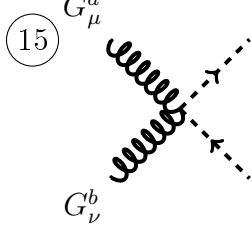The indices $A,B \in \{L,R\}$ label the left/right "handedness" of the squarks. The indices $i,j = 1,2,3$ are the color indices in the (anti)fundamental representation where $a,b,c,\dots = 1,\dots,8$ are the color indices of the adjoint representation.
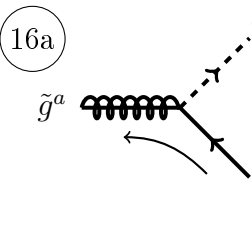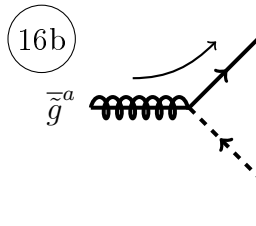
⑫ G^a_μ G^c_ρ G^b_ν G^d_σ

$$\hat{=} -ig_s^2[f^{abe}f^{cde}(g^{\mu\rho}g^{\nu\sigma} - g^{\mu\sigma}g^{\nu\rho}) + f^{ace}f^{bde}(g^{\mu\nu}g^{\rho\sigma} - g^{\mu\sigma}g^{\nu\rho})$$
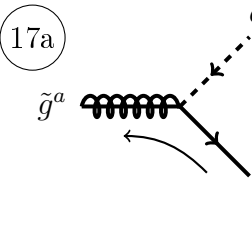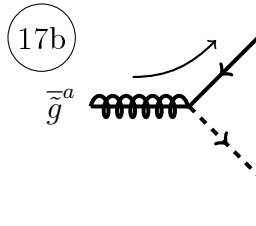$$+ f^{ade}f^{bce}(g^{\mu\nu}g^{\rho\sigma} - g^{\mu\rho}g^{\nu\sigma})]$$

⑬ $\bar{\tilde{g}}^b$ G^a_μ $\tilde{g}^c$

$$\hat{=} -g_s f_{abc}\gamma^\mu$$

⑭ $\sigma^{b\dagger}(-p_1)$ G^a_μ $\sigma^c(p_2)$

$$\hat{=} -g_s(p_1 + p_2)^\mu f_{abc}$$

⑮ G^a_μ $\sigma^{\dagger c}$ G^b_ν σ^d
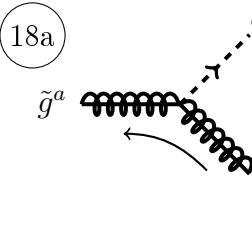
$$\hat{=} +ig_s^2 g^{\mu\nu}[f^{aec}f^{bed} + f^{bec}f^{aed}]$$
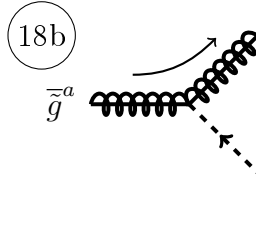
⑯a $\tilde{q}^\dagger_{Li}$ $\tilde{g}^a$ $\bar{q}^C_j$
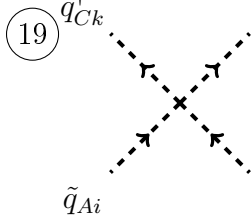
$$\hat{=} -i\sqrt{2}g_s T^a_{ij}P_L$$

⑯b q^C_i $\bar{\tilde{g}}^a$ $\tilde{q}_{Lj}$

$$\hat{=} -i\sqrt{2}g_s T^a_{ij}P_R$$

⑰a $\tilde{q}_{Rj}$ $\tilde{g}^a$ $\bar{q}_i$

$$\hat{=} +i\sqrt{2}g_s T^a_{ij}P_L$$

⑰b q_j $\bar{\tilde{g}}^a$ $\tilde{q}^\dagger_{Ri}$

$$\hat{=} +i\sqrt{2}g_s T^a_{ij}P_R$$

⑱a $\sigma^{b\dagger}$ $\tilde{g}^a$ $\bar{\tilde{g}}^c$

$$\hat{=} -\sqrt{2}g_s f^{abc}P_L$$

⑱b $\tilde{g}^b$ $\bar{\tilde{g}}^a$ σ^c

$$\hat{=} +\sqrt{2}g_s f^{abc}P_R$$

⑲ $\tilde{q}^\dagger_{Ck}$ $\tilde{q}^\dagger_{Dl}$ $\tilde{q}_{Ai}$ $\tilde{q}_{Bj}$

$$\hat{=} -ig_s^2[T^a_{ki}T^a_{lj}(\delta_{AL}\delta_{CL} - \delta_{AR}\delta_{CR})(\delta_{BL}\delta_{DL} - \delta_{BR}\delta_{DR})$$
$$T^a_{kj}T^a_{li}(\delta_{BL}\delta_{CL} - \delta_{BR}\delta_{CR})(\delta_{AL}\delta_{DL} - \delta_{AR}\delta_{DR})]$$

Figure 10.2: The curved arrows indicate the fermion flow. The Feynman rules 16b, 17b and 18b are the complex conjugates of 16a, 17a and 18a respectively. Applying a flipping rule to a vertex one has to reverse the curved arrow, i.e. the fermion flow and replace Ψ with $\bar{\Psi}^C$. In addition one has to add a minus sign for Feynman rule 13.

$$\underset{20}{\;}\; \tilde{q}^{\dagger}_{Aj} \qquad \sigma^{b\dagger}$$
$$\tilde{q}_{Ai} \qquad \sigma^{c} \qquad \hat{=}\; -g_s^2 T_{ij}^a f^{abc}(\delta_{AL}\delta_{CL} - \delta_{AR}\delta_{BR})$$

$$\underset{21}{\;}\; \sigma^a + \sigma^{a\dagger} \qquad \tilde{q}^{\dagger}_{Ai}$$
$$\tilde{q}_{Bj} \qquad \hat{=}\; -i\sqrt{2}g_s m_{\tilde{g}} T_{ij}^a (\delta_{AL}\delta_{BL} - \delta_{AR}\delta_{BR})$$

$$\underset{22}{\;}\; \sigma^{\dagger b} \qquad \sigma^{\dagger d}$$
$$\sigma^c \qquad \sigma^e \qquad \hat{=}\; -g_s^2 (f^{abc}f^{ade} + f^{abc}f^{adc})$$

10.6 Passarino-Veltman Integrals

The definition of the momenta within the Passarino-Veltman integrals in this thesis agrees with the one from `Looptools` [54] convention. The original paper [58] uses slightly different conventions. A pedagogical introduction to the evaluation of one-loop integrals can be found in [59]. A, B and C integrals are defined by:

$$\frac{i}{16\pi^2}A_0(m^2) = \int_l \frac{1}{l^2 - m^2}$$
$$\frac{i}{16\pi^2}B_{0,\mu,\mu\nu}(p^2, m_1^2, m_2^2) = \int_l \frac{\{1, l_\mu, l_\mu l_\nu\}}{[l^2 - m_1^2][(l+p)^2 - m_2^2]} \qquad (10.25)$$
$$\frac{i}{16\pi^2}C_{0,\mu,\mu\nu}(p_1^2, p_2^2, (p_1+p_2)^2, m_1^2, m_2^2, m_3^2) = \int_l \frac{\{1, l_\mu, l_\mu l_\nu\}}{[l^2 - m_1^2][(l+p_1)^2 - m_2^2][(l+p_1+p_2)^2 - m_3^2]}.$$

with the shortcut $\int_l = \mu^{2\epsilon}\int \frac{\mathrm{d}^D l}{(2\pi)^D}$. Furthermore there are supressed ε's which prescripe how the poles in the complex plane are avoided. They are hidden in the infinitesimal shift of the masses: $m_i^2 \to m_i^2 - i\varepsilon$.

The tensor integrals can be decomposed as

$$
\begin{aligned}
B_\mu &:= p_\mu B_1 \\
B_{\mu\nu} &:= g_{\mu\nu} B_{00} + p_\mu p_\nu B_{11} \\
C_\mu &= p_{1\mu} C_1 + p_{2\mu} C_2 \\
C_{\mu\nu} &:= g_{\mu\nu} C_{00} + p_{1\mu} p_{1\nu} C_{11} + p_{2\mu} p_{2\nu} C_{22} + (p_{1\mu} p_{2\nu} + p_{2\mu} p_{1\nu}) C_{12}
\end{aligned}
\tag{10.26}
$$

In the the special case of vanishing momenta the integrals take a succinct form.

$$
A_0(m^2) = m^2 \left(\Delta_\epsilon - \ln \frac{m^2}{\mu^2} + 1 \right) + \mathcal{O}(\epsilon)
\tag{10.27}
$$

where the typical UV-divergent constant $\Delta_\epsilon = \frac{1}{\epsilon} - \gamma_E + \ln 4\pi$ is defined. It comprises the Euler-Mascheroni constant γ_E.

$$
B_0(0, m_1^2, m_2^2) = \frac{A_0(m_1^2) - A_0(m_2^2)}{m_1^2 - m_2^2} = \Delta_\epsilon + 1 - \frac{m_1^2 \ln \frac{m_1^2}{\mu^2} - m_2^2 \ln \frac{m_2^2}{\mu^2}}{m_1^2 - m_2^2} + \mathcal{O}(\epsilon)
\tag{10.28}
$$

$$
B_0(0, m^2, m^2) = \frac{\partial}{\partial m^2} A_0(m^2) = \Delta_\epsilon - \ln \frac{m^2}{\mu^2} + \mathcal{O}(\epsilon)
\tag{10.29}
$$

$$
B_0(0, 0, 0) = 0
\tag{10.30}
$$

$$
B_1(0, m_1^2, m_2^2) = -\frac{\Delta_\epsilon}{2} + \frac{1}{2} \ln \frac{m_1^2}{\mu^2} + \frac{-3 + 4t - t^2 - 4t \ln t + 2t^2 \ln t}{4(t-1)^2} + \mathcal{O}(\epsilon)
\tag{10.31}
$$

$$
B_1(0, 0, 0) = 0
\tag{10.32}
$$

The scaleless integrals are defined to be zero due to their definition on how they scale in D dimensions [45]. The parameter t is given by $\frac{m_2^2}{m_1^2}$. As can be seen from 10.31 B_1 is in contrast to B_0 not symmetric in its masses but it can be shown [Romao] that

$$
B_1(p^2, m_1^2, m_2^2) = -(B_0(p^2, m_2^2, m_1^2) + B_1(p^2, m_2^2, m_1^2))
\tag{10.33}
$$

It can further be shown that

$$
C_{00}(0, 0, 0, m_1^2, m_1^2, m_2^2) = -\frac{1}{2} B_1(0, m_1^2, m_2^2)
\tag{10.34}
$$

and that $C_{00}(0, 0, 0, m_1^2, m_1^2, m_2^2)$ is a symmetric function of its masses.
From the generic ϵ-expansion of the B_0 integral [60]

$$
B_0(p^2, m_1^2, m_2^2) = \Delta_\epsilon - \int_0^1 \mathrm{d}x \, \ln \frac{-x(1-x)p^2 + xm_2^2 + (1-x)m_1^2}{\mu^2}
\tag{10.35}
$$

and Passarino-Veltman decomposition [58] one can determine the UV-divergent part of all B and C integrals. In chapter 7.7 this was necessary in order to obtain the renormalization constants in the $\overline{\text{MS}}$-scheme. Infrared and collinear singularities arise from the special case where one or multiple masses tend to zero. These poles can be regularized with a small mass cutoff Λ leading singularities of the form $\ln \Lambda$ or dimensionally which leads to ϵ-poles as in the treatment of UV-divergences. In the latter case the integral first needs to undergo the limit to zero masses and than being evaluated.

The following list shows all necessary integrals needed to determine the renormalization constants in 7.7.

$$A_0(m^2)\big|_{\text{UV-div}} = m^2 \Delta_\epsilon \tag{10.36}$$

$$B_0(p^2, m_1^2, m_2^2)\big|_{\text{UV-div}} = \Delta_\epsilon \tag{10.37}$$

$$B_1(p^2, m_1^2, m_2^2)\big|_{\text{UV-div}} = -\frac{1}{2}\Delta_\epsilon \tag{10.38}$$

$$C_{00}(p_1^2, p_2^2, (p_1 + p_2)^2, m_1^2, m_2^2, m_3^2)\big|_{\text{UV-div}} = \frac{1}{4}\Delta_\epsilon \tag{10.39}$$

The UV-divergent part of C_{11}, C_{22}, C_{12} equals zero. As can be seen already from the superficial degree of divergence also $C_i|_{\text{UV-div}} = 0$ for $i \in \{0, 1, 2\}$.

10.7 Cross section and Phase Space Integration

Once the Feynman amplitude $\mathcal{M}$ for a $2 \to N$ body scattering[26] is computed one can calculate physical observables with it. The differential cross section for $2 \to N$ scattering is given by

$$d\sigma = \frac{1}{F}d\Phi_N |\mathcal{M}|^2. \tag{10.40}$$

The flux factor is defined by $F = 4\sqrt{(k_a \cdot k_b)^2 - (m_a m_b)^2}$ which equals $F = 2s$ for massless initial state particles. The differential for the N body phase space in D dimensions is given by

$$d\Phi_N = \left(\mu^{2\epsilon}\right)^{N-1} \left(\prod_{f=1}^{N} \frac{d^{D-1}p_f}{(2\pi)^{D-1}} \frac{1}{2E_f}\right) (2\pi)^D \delta^{(D)}(k_a + k_b - \sum_{f=1}^{N} p_f). \tag{10.41}$$

The factor $\mu^{2\epsilon}$ is included to maintain the mass dimension of the cross section. As in this thesis the sum of $|\mathcal{M}|^2$ over helicities and colors $\sum |\mathcal{M}|^2$ has been calculated one can write

$$d\sigma = \frac{1}{2s}d\Phi_2 K_{ab} \sum |\mathcal{M}|^2 \tag{10.42}$$

where K_{ab} encodes the averaging over initial state helicities and colors. Specifying to the center-of-mass frame and assuming that $\sum |\mathcal{M}|^2$ is only a function of the modulus of one of

---

[26]with kinematics $k_a + k_b \to p_1 + \ldots p_N$

the final state particle's 3-momentum $|\vec{p}_i|$ and the angle θ between $\vec{k}_a$ and $\vec{p}_1$ one can write

$$
\int \mathrm{d}\Phi_2 = \mu^{2\epsilon} \int \frac{\mathrm{d}|\vec{p}_1|\mathrm{d}\Omega_1^{D-1}}{(2\pi)^{D-2}4E_1E_2}|\vec{p}_1|^{D-2}\delta\left(k_a^0 + k_b^0 - \sqrt{m_1^2 + |\vec{p}_1|^2} - \sqrt{m_2^2 + |\vec{p}_1|^2}\right)
$$

$$
= \frac{1}{(2\pi)^{D-2}}\frac{2\pi^{\frac{D}{2}-1}}{\Gamma(\frac{D}{2}-1)}\mu^{2\epsilon}\int_0^\infty \mathrm{d}|\vec{p}_1|\int_0^\pi \mathrm{d}\cos\theta \frac{1}{4E_1E_2}p_1^{D-2}\sin^{D-4}\theta
$$

$$
\delta\left(k_a^0 + k_b^0 - \sqrt{m_1^2 + |\vec{p}_1|^2} - \sqrt{m_2^2 + |\vec{p}_1|^2}\right). \tag{10.43}
$$

In the second line the integral over the D-dimensional hypersphere

$$
\int \mathrm{d}\Omega^D = \int_0^{2\pi}\mathrm{d}\phi \prod_{i=1}^{D-2}\int_0^\pi \sin^i\theta_i\mathrm{d}\theta_i = \frac{2\pi^{\frac{D}{2}}}{\Gamma(\frac{D}{2})} \tag{10.44}
$$

has been used. Because $\sum |\mathcal{M}|^2$ is calculated in terms of Mandelstam variables

$$
t = (k_a - p_1)^2
$$

$$
t = -2\left(|\vec{k}_a|\sqrt{m_1^2 + |\vec{p}_1|^2} - |\vec{k}_a||\vec{p}_1|\cos\theta\right) + m_1^2 \tag{10.45}
$$

$$
u = (k_a - p_2)^2
$$

$$
u = -2\left(|\vec{k}_a|\sqrt{m_2^2 + |\vec{p}_1|^2} + |\vec{k}_a||\vec{p}_1|\cos\theta\right) + m_2^2 \tag{10.46}
$$

it is useful to perform a change of coordinates yielding

$$
\mathrm{d}|\vec{p}_1|\,\mathrm{d}\cos\theta = -\frac{E_1E_2}{4|\vec{k}_a|^2|\vec{p}_1|^2(E_1+E_2)}\mathrm{d}u\,\mathrm{d}t. \tag{10.47}
$$

Inserting 10.47 into 10.43 and using $2|\vec{k}_a| = \sqrt{s} = E_1 + E_2$ gives

$$
\int \mathrm{d}\Phi_2 = \frac{1}{s}\frac{\pi^{-\frac{D}{2}+1}}{2^{D-3}\Gamma(\frac{D}{2}-1)}\int \mathrm{d}u\,\mathrm{d}t\left(\frac{tu - m_1^2m_2^2}{\mu^{2\epsilon}s}\right)^{\frac{D-4}{2}}
$$

$$
\frac{1}{4}\Theta(tu - 4m_1^2m_2^2)\delta\left(s + t + u - m_1^2 - m_2^2\right) \tag{10.48}
$$

where the Θ-function comes from the bounds of $|\vec{p}_1|$ and θ visible in 10.43 and the combination of 10.45 and 10.46. Working in $D = 4-2\epsilon$ dimensions and inserting $\Theta(s-4m^2)$ with $m = \frac{m_1+m_2}{2}$ to account for the production threshold one finds

$$
\frac{\mathrm{d}^2\sigma}{\mathrm{d}t\mathrm{d}u} = \frac{K_{ab}}{s^2}\frac{\pi S_\epsilon}{\Gamma(1-\epsilon)}\left[\frac{tu - m_1^2m_2^2}{\mu^2 s}\right]^{-\epsilon}\Theta(tu - m_1^2m_2^2)
$$

$$
\Theta(s - 4m^2)\delta(s + t + u - m_1^2 - m_2^2)\sum |\mathcal{M}|^2 \tag{10.49}
$$

where $S_\epsilon = (4\pi)^{-2+\epsilon}$ as defined in [31]. The averaging factors K_{ab} are given by

$$K_{qq} = \frac{1}{4N_c^2} \qquad K_{GG} = \frac{1}{4(1-\epsilon)^2(N_c^2-1)^2} \qquad K_{qG} = \frac{1}{4(1-\epsilon)N_c(N_c^2-1)}. \quad (10.50)$$

11 References

[1] M. Maggiore, *A modern introduction to quantum field theory.* Oxford master series in physics 12, Oxford University Press, 2005.

[2] M. E. Peskin and D. V. Schroeder, *An introduction to quantum field theory.* Advanced book program, Boulder (Colo.): Westview Press Reading (Mass.), 1995. Autre tirage : 1997.

[3] C. N. Yang and R. L. Mills, "Conservation of isotopic spin and isotopic gauge invariance," *Phys. Rev.*, vol. 96, pp. 191–195, Oct 1954.

[4] M. Bach, "Das anomale magnetische Moment des Myons im minimalen supersymmetrischen Standardmodell für tan $\beta = \infty$," Master's thesis, TU Dresden, 2013.

[5] P. W. Higgs, "Broken symmetries, massless particles and gauge fields," *Phys. Lett.*, vol. 12, pp. 132–133, 1964.

[6] P. W. Higgs, "Broken Symmetries and the Masses of Gauge Bosons," *Phys. Rev. Lett.*, vol. 13, pp. 508–509, 1964.

[7] P. W. Higgs, "Spontaneous Symmetry Breakdown without Massless Bosons," *Phys. Rev.*, vol. 145, pp. 1156–1163, 1966.

[8] F. Englert and R. Brout, "Broken Symmetry and the Mass of Gauge Vector Mesons," *Phys. Rev. Lett.*, vol. 13, pp. 321–323, 1964.

[9] G. S. Guralnik, C. R. Hagen, and T. W. B. Kibble, "Global Conservation Laws and Massless Particles," *Phys. Rev. Lett.*, vol. 13, pp. 585–587, 1964.

[10] T. W. B. Kibble, "Symmetry breaking in nonAbelian gauge theories," *Phys. Rev.*, vol. 155, pp. 1554–1561, 1967.

[11] J. Bernstein, "Spontaneous symmetry breaking, gauge theories, the higgs mechanism and all that," *Rev. Mod. Phys.*, vol. 46, pp. 7–48, 1974. [Erratum: Rev. Mod. Phys.46,855(1974)].

[12] A. D. H. J. Manfred Böhm, Manfred Böhm (Dr. rer. nat.), *Gauge Theories of the Strong and Electroweak Interaction.* Vieweg +Teubner, 3rd rev. ed. 2001 ed., 2001.

[13] N. Cabbibo, "Leptonic Decays in the Unitary Symmetry Scheme," in *Proceedings, International Conference on Fundamental Aspects of Weak Interactions*, pp. 299–302, 1964.

[14] M. Kobayashi and T. Maskawa, "CP Violation in the Renormalizable Theory of Weak Interaction," *Prog. Theor. Phys.*, vol. 49, pp. 652–657, 1973.

[15] C. Becchi, A. Rouet, and R. Stora, "The Abelian Higgs-Kibble Model. Unitarity of the S Operator," *Phys. Lett.*, vol. B52, pp. 344–346, 1974.

[16] C. Becchi, A. Rouet, and R. Stora, "Renormalization of the Abelian Higgs-Kibble Model," *Commun. Math. Phys.*, vol. 42, pp. 127–162, 1975.

[17] C. Becchi, A. Rouet, and R. Stora, "Renormalization of Gauge Theories," *Annals Phys.*, vol. 98, pp. 287–321, 1976.

[18] R. Adam *et al.*, "Planck 2015 results. I. Overview of products and scientific results," 2015.

[19] S. P. Martin, "A Supersymmetry primer," 1997. [Adv. Ser. Direct. High Energy Phys.18,1(1998)].

[20] S. R. Coleman and J. Mandula, "All Possible Symmetries of the S Matrix," *Phys. Rev.*, vol. 159, pp. 1251–1256, 1967.

[21] O. Pelc and L. P. Horwitz, "Generalization of the Coleman-Mandula theorem to higher dimension," *J. Math. Phys.*, vol. 38, pp. 139–172, 1997.

[22] R. Haag, J. T. Lopuszanski, and M. Sohnius, "All Possible Generators of Supersymmetries of the s Matrix," *Nucl. Phys.*, vol. B88, p. 257, 1975.

[23] G. 't Hooft, "Symmetry Breaking Through Bell-Jackiw Anomalies," *Phys. Rev. Lett.*, vol. 37, pp. 8–11, 1976.

[24] G. D. Kribs, E. Poppitz, and N. Weiner, "Flavor in supersymmetry with an extended R-symmetry," *Phys. Rev.*, vol. D78, p. 055010, 2008.

[25] A. E. Nelson, N. Rius, V. Sanz, and M. Unsal, "The Minimal supersymmetric model without a mu term," *JHEP*, vol. 08, p. 039, 2002.

[26] G. D. Kribs and A. Martin, "Supersoft Supersymmetry is Super-Safe," *Phys. Rev.*, vol. D85, p. 115014, 2012.

[27] E. Hardy, "Is Natural SUSY Natural?," *JHEP*, vol. 10, p. 133, 2013.

[28] G. D. Kribs and A. Martin, "Dirac Gauginos in Supersymmetry – Suppressed Jets + MET Signals: A Snowmass Whitepaper," 2013.

[29] P. J. Fox, A. E. Nelson, and N. Weiner, "Dirac gaugino masses and supersoft supersymmetry breaking," *JHEP*, vol. 08, p. 035, 2002.

[30] P. Diessner and W. Kotlarski, "Higgs and the electroweak precision observables in the MRSSM," *PoS*, vol. CORFU2014, p. 079, 2015.

[31] W. Beenakker, R. Hopker, M. Spira, and P. M. Zerwas, "Squark and gluino production at hadron colliders," *Nucl. Phys.*, vol. B492, pp. 51–103, 1997.

[32] L. A. Harland-Lang, A. D. Martin, P. Motylinski, and R. S. Thorne, "Parton distributions in the LHC era: MMHT 2014 PDFs," *Eur. Phys. J.*, vol. C75, no. 5, p. 204, 2015.

[33] G. Dissertori, I. Knowles, and M. Schmelling, *Quantum Chromodynamics: High Energy Experiments and Theory*. International series of monographs on physics, Clarendon Press, 2003.

[34] J. C. Collins, D. E. Soper, and G. F. Sterman, "Factorization of Hard Processes in QCD," *Adv. Ser. Direct. High Energy Phys.*, vol. 5, pp. 1–91, 1989.

[35] R. Brock *et al.*, "Handbook of perturbative QCD: Version 1.0," *Rev. Mod. Phys.*, vol. 67, pp. 157–248, 1995.

[36] A. Lahiri and P. Pal, *A First Book of Quantum Field Theory*. Alpha Science International, 2005.

[37] T. Kinoshita, "Mass Singularities of Feynman Amplitudes," *Journal of Mathematical Physics*, vol. 3, pp. 650–677, July 1962.

[38] T. D. Lee and M. Nauenberg, "Degenerate systems and mass singularities," *Phys. Rev.*, vol. 133, pp. B1549–B1562, Mar 1964.

[39] G. 't Hooft and M. J. G. Veltman, "Regularization and Renormalization of Gauge Fields," *Nucl. Phys.*, vol. B44, pp. 189–213, 1972.

[40] W. Hollik and D. Stockinger, "Regularization and supersymmetry restoring counterterms in supersymmetric QCD," *Eur. Phys. J.*, vol. C20, pp. 105–119, 2001.

[41] P. Varso, "Supersymmetrie restaurierende Counterterme in Einschleifenordnung," Master's thesis, TU Dresden, 2010.

[42] T. Hahn, "Generating Feynman diagrams and amplitudes with FeynArts 3," *Comput. Phys. Commun.*, vol. 140, pp. 418–431, 2001.

[43] B. Chokoufe Nejad, J. N. Lang, T. Hahn, and E. Mirabella, "FormCalc 8: Better Algebra and Vectorization," *Acta Phys. Polon.*, vol. B44, no. 11, pp. 2231–2239, 2013.

[44] T. Hahn and M. Perez-Victoria, "Automatized one loop calculations in four-dimensions and D-dimensions," *Comput. Phys. Commun.*, vol. 118, pp. 153–165, 1999.

[45] J. C. Collins, *Renormalization: an introduction to renormalization, the renormalization group, and the operator-product expansion*. Cambridge monographs on mathematical physics, Cambridge: Cambridge Univ. Press, 1984.

[46] T. Hahn, *FormCalc 8 User's Guide*, 2015.

[47] H. D. Politzer, "Reliable Perturbative Results for Strong Interactions?," *Phys. Rev. Lett.*, vol. 30, pp. 1346–1349, 1973.

[48] D. J. Gross and F. Wilczek, "Asymptotically Free Gauge Theories. 1," *Phys. Rev.*, vol. D8, pp. 3633–3652, 1973.

[49] F. Staub, "SARAH 4 : A tool for (not only SUSY) model builders," *Comput. Phys. Commun.*, vol. 185, pp. 1773–1790, 2014.

[50] F. Staub, "SARAH 3.2: Dirac Gauginos, UFO output, and more," *Comput. Phys. Commun.*, vol. 184, pp. 1792–1809, 2013.

[51] F. Staub, "Automatic Calculation of supersymmetric Renormalization Group Equations and Self Energies," *Comput. Phys. Commun.*, vol. 182, pp. 808–833, 2011.

[52] F. Staub, "From Superpotential to Model Files for FeynArts and CalcHep/CompHep," *Comput. Phys. Commun.*, vol. 181, pp. 1077–1086, 2010.

[53] H. Lehmann, K. Symanzik, and W. Zimmermann, "On the formulation of quantized field theories," *Nuovo Cim.*, vol. 1, pp. 205–225, 1955.

[54] T. Hahn and M. Perez-Victoria, "Automatized one loop calculations in four-dimensions and D-dimensions," *Comput. Phys. Commun.*, vol. 118, pp. 153–165, 1999.

[55] T. Hahn, "CUBA: A Library for multidimensional numerical integration," *Comput. Phys. Commun.*, vol. 168, pp. 78–95, 2005.

[56] T. Appelquist and J. Carazzone, "Infrared Singularities and Massive Fields," *Phys. Rev.*, vol. D11, p. 2856, 1975.

[57] H.-C. Cheng, J. L. Feng, and N. Polonsky, "Superoblique corrections and nondecoupling of supersymmetry breaking," *Phys. Rev.*, vol. D56, pp. 6875–6884, 1997.

[58] G. Passarino and M. J. G. Veltman, "One Loop Corrections for e+ e- Annihilation Into mu+ mu- in the Weinberg Model," *Nucl. Phys.*, vol. B160, pp. 151–207, 1979.

[59] R. K. Ellis, Z. Kunszt, K. Melnikov, and G. Zanderighi, "One-loop calculations in quantum field theory: from Feynman diagrams to unitarity cuts," *Phys. Rept.*, vol. 518, pp. 141–250, 2012.

[60] A. Denner, "Techniques for the Calculation of Electroweak Radiative Corrections at the One-Loop Level and Results forW-physics at LEP 200," *Fortschritte der Physik*, vol. 41, pp. 307–420, 1993.

Erklärung

Hiermit erkläre ich, dass ich diese Arbeit im Rahmen der Betreuung am Institut für Kern- und Teilchenphysik ohne unzulässige Hilfe Dritter verfasst und alle Quellen als solche gekennzeichnet habe. Vorname Nachname

Dresden, Juli 2016